1981

Laser excited atomic fluorescence spectrometry as a tool for chemical analysis

David Allen Goff
Iowa State University

Goff, David Allen

LASER EXCITED ATOMIC FLUORESCENCE SPECTROMETRY AS A TOOL FOR CHEMICAL ANALYSIS

Iowa State University

PH.D. 1981

PLEASE NOTE:

In all cases this material has been filmed in the best possible way from the available copy. Problems encountered with this document have been identified here with a check mark __√__.

1. Glossy photographs or pages _____
2. Colored illustrations, paper or print _____
3. Photographs with dark background __✓__
4. Illustrations are poor copy _____
5. Pages with black marks, not original copy _____
6. Print shows through as there is text on both sides of page _____
7. Indistinct, broken or small print on several pages __✓__
8. Print exceeds margin requirements _____
9. Tightly bound copy with print lost in spine _____
10. Computer printout pages with indistinct print __✓__
11. Page(s) _____ lacking when material received, and not available from school or author.
12. Page(s) _____ seem to be missing in numbering only as text follows.
13. Two pages numbered _____. Text follows.
14. Curling and wrinkled pages _____
15. Other _____

Laser excited atomic fluorescence spectrometry as a tool for chemical analysis

by

David Allen Goff

A Dissertation Submitted to the
Graduate Faculty in Partial Fulfillment of the
Requirements for the Degree of
DOCTOR OF PHILOSOPHY

Department: Chemistry
Major: Analytical Chemistry

Approved:

Signature was redacted for privacy.

In Charge of Major Work

Signature was redacted for privacy.

For the Major Department

Signature was redacted for privacy.

For the Graduate College

Iowa State University
Ames, Iowa

1981

TABLE OF CONTENTS

CHAPTER I. INTRODUCTION

Statement of the Purpose

The goal of the research presented in this dissertation is to define several problems encountered in analytical atomic fluorescence spectrometry (AFS) and to show how the application of new laser based spectroscopic techniques can contribute to the solution of these problems. This chapter is devoted to an introduction of the subject of atomic fluorescence spectrometry as a means of chemical analysis with special emphasis on the laser as a unique and superior excitation source for AFS.

Introduction to AFS

Atomic fluorescence spectrometry is a method of chemical analysis based upon the absorption of radiation by an atomic vapor, thereby producing atoms in an excited electronic state, and the measurement of the light emitted when a fraction of the excited atoms undergoes radiative deactivation. AFS is essentially a combination of the atomic absorption (AA) and atomic emission (AE) processes, combining some of the advantages of each and possessing some unique advantages and disadvantages of its own. In contrast to atomic emission spectrometry, atomic fluorescence is relatively insensitive to temperature fluctuations in the atom cell. Unlike atomic

absorption, in which the source is placed on the same optical axis, in atomic fluorescence the source is usually placed at a right angle to the atomizer-detector axis. Thus, the total noise in AAS is larger than in AFS because there is a greater light flux falling on the photodetector surface. Also, source instability near the limits of detection is less critical in atomic fluorescence than in atomic absorption. For both AAS and AFS, the spectral light source is an essential component of the instrumental arrangement and the optimization of its performance is of major importance if the capabilities of the two techniques are to be fully exploited.

Historical Background of AFS

The atomic fluorescence, as well as the atomic absorption of atomic vapors in quartz containers, has been studied by a number of physicists in the late 19th and early 20th centuries. These investigations have been summarized by Mitchell and Zemansky (1) and Pringsheim (2). In 1924, the atomic fluorescence of metal atoms in flames was observed for the first time by Nichols and Howes (3). In 1956, Boers, Alkemade and Smit (4) reported the use of atomic fluorescence to study fundamental chemical and physical processes in flames. At the International Spectroscopy Colloquium in 1962, Alkemade (5) first suggested using atomic fluorescence for analytical chemistry. However, it was Winefordner and

Vickers (6) who first experimentally demonstrated atomic fluorescence spectrometry as a means of chemical analysis.

Analytical Basis for AFS

The analytical practice of AFS, and in general all spectroscopic techniques, relies entirely upon the construction of the experimental calibration curve, which presents the plot of the blank corrected standard signal versus the volumetric concentration of the standards. It is essential that the analyst is aware of the form that the calibration curve is going to take for any analytical method chosen, otherwise, measurements may be unintentionally made under conditions which may be far from ideal. The dependence of the atomic fluorescence signal upon the type and intensity of the excitation source, experimental configuration, quantum efficiency and concentration of analyte atoms has been treated extensively in the literature (7-24). No attempt is made to go into great detail, but only to review the aspects of AFS theory applicable to this dissertation on laser excited atomic fluorescence spectrometry (LEAFS).

At low atomic concentrations (low optical densities), the integrated radiance of the fluorescence signal is linearly related to the atomic concentration, and this holds for continuum as well as line sources of excitation.

The general expression for the fluorescence radiance, B_F, is given by (12):

$$B_F = n_1 E_{\nu_{12}} \left(\frac{h\nu_{12}}{c}\right) B_{12} Y_{21} \left(\frac{\ell}{4\pi}\right)\left(1 - \frac{g_1 n_2}{g_2 n_1}\right), \ Wm^{-2}sr^{-1}$$

where:

n_1 = concentration of analyte atoms, in the lower level of the absorption transition, m^{-3}

$E_{\nu_{12}}$ = spectral radiance of exciting radiation at the absorption line, ν_{12}, $Wm^{-2}Hz^{-1}$

$h\nu$ = energy of the exciting photon, J

c = speed of light, ms^{-1}

B_{12} = Einstein coefficient of induced absorption, $m^{-3}J^{-1}s^{-1}Hz$

Y_{21} = fluorescence power (quantum) efficiency, dimensionless

ℓ = fluorescence path length in the direction of observation, m

4π = number of steradians in a sphere, sr

g_1, g_2 = statistical weights of levels 1 and 2, respectively, dimensionless

$n_1 n_2$ = concentration of states 1 and 2, respectively, m^{-3}.

The lack of detailed and precise information concerning the parameters of the experimental systems restricts knowledge of the calibration curve shape to a semiquantitative level.

However, even this information should make it less likely that ambiguous measurements will be made. In fluorescence analysis, ambiguity can be introduced due to the geometry of illumination and observation. At high atomic concentrations (high optical densities), the relationship between the fluorescence radiance and the atomic concentration becomes complex. A prefilter effect may be present because of the weakening of the excitation beam in a region that is not observed by the detector. A postfilter effect can also occur if there is a region between the illuminated volume and the detector where absorption can diminish the fluorescence intensity. The consequence of these processes is that the calibration curve can reach an intensity plateau or even take on a negative slope. This problem can be avoided by the choice of nonresonant lines or by diluting the solutions.

The merits of atomic fluorescence spectrometry in comparison to the other methods of elemental analysis (e.g., atomic absorption and atomic emission spectrometry) have been considered by many authors on the basis of theoretically calculated signal strengths and/or experimental limits of detection (11, 25-33). Before atomic absorption spectrometry could be developed, it was necessary to evolve spectral light-sources that produced lines of narrower half-width than the absorbing line in the flame. Atomic fluorescence, on the other hand, needs no such restrictive requirement on the

excitation source linewidth, and can even be generated with a continuum source (34-41).

Excitation Sources for AFS

The application of atomic fluorescence spectrometry as a widely employed tool for trace element analysis was delayed mainly by the lack of intense sources for many elements. Continuum sources radiate only a small fraction of their energy across the absorption line of an atom. Except in a few favorable cases, the excitation provided by the available atomic absorption line sources, such as hollow cathode lamps, has proven to be inadequate for obtaining good atomic fluorescence signals. Atomic fluorescence, like all forms of luminescence spectrometry, is a source intensity starved method. The major field of technological research in AFS has been the investigation of a great variety of light sources possessing among other desirable factors such as simplicity, stability, long life, low cost and high versatility the most critical of all, namely, high intensity.

Four types of excitation sources have been investigated for use in atomic fluorescence spectrometry. These can be classified as:

1) Low-intensity line sources, such as hollow cathode lamps (HCLs).

2) High-intensity line sources, such as electrodeless discharge lamps (EDLs), metal vapor lamps and some types of HCLs.

3) Continuum sources, all of which are effectively low intensity sources.

4) Extremely high-intensity sources, such as tunable dye lasers.

With the advent of the tunable dye laser (42), the application of laser sources in AFS has received considerable attention. Fraser and Winefordner (43), Kuhl and Marowsky (44) and Denton and Malmstadt (45) were among the first to report the application of lasers as an excitation source for AFS. The unique properties that distinguish lasers from other optical sources are: 1) the extremely coherent and unidirectional nature of the radiation, 2) the large amount of energy available over a small spectral region resulting in improved linearity of calibration curves to 3-5 orders of magnitude (46), 3) the extremely small area into which the light may be concentrated for use in spatial diagnostics or to saturate the absorption transition and remove the dependence of the fluorescence signal upon source stability (9,47) and the ambiguity resulting from the prefilter effect, and 4) the extended tunability over the UV-visible range.

Because the dye laser is tunable, only one source is needed per excitation region of ca. 30 nm rather than one for

each element (or group of similar elements) as is the case with conventional HCl or EDL sources. This makes it possible to do sequential multielement AFS using a tunable dye laser as the excitation source.

Not only can the dye laser be tuned to a desired wavelength, but the bandwidth of the laser can be varied from 1 nm to 10^{-4} nm or less by inserting a series of tuning elements inside the laser cavity without serious loss of laser intensity. The high degree of resolution combined with its high power makes the tunable laser source a very selective and sensitive spectroscopic probe.

In the chapters that follow, laser excited atomic fluorescence spectrometry will be applied to (1) the problem of spurious light scattering from analytical flames (48), (2) the detection of atomic species in a luminous source such as the inductively coupled plasma, and (3) the possibility of off-resonant excitation of atomic transitions.

CHAPTER II. ATOMIC FLUORESCENCE SPECTROMETRY WITH A WAVELENGTH-MODULATED CONTINUOUS WAVE DYE LASER

Introduction

Scattering is a very common phenomenon that takes place whenever light transverses any medium. The medium may be dust particles, water droplets, an aerosol, a gas, or in general, any polarizable material. The scattering of light has been recognized as a source of spectral interference in both atomic absorption and atomic fluorescence techniques because it results in a spurious absorption or emission signal which can be wrongly attributed to the analyte whose signal is being investigated. Interference effects of this type pose a particular problem, especially in the applications where the atomic fluorescence technique is potentially most valuable, that is, in the determination of trace metals in the presence of high concentrations of matrix material at concentrations below those which can be reliably determined by other methods. As one pushes for lower and lower limits of detection, and as one uses high laser powers to ensure saturation of excitation (47), light scattering from particulates and from atomic and molecular species as well as stray laser radiation will eventually become a problem.

This chapter will outline the problems of light scattering in AFS determinations, review possible ways to minimize these problems and report on the use of a wavelength modulated continuous dye laser for atomic fluorescence spectrometry (48).

Review of Literature

It was in search for an answer to the age-old question, "Why is the sky blue?" that Lord Rayleigh derived a rigorous solution, based on the electromagnetic theory, for the scattering of a parallel beam of linearly polarized radiation by small dielectric spheres (49). Twenty-seven years later, in 1908, G. Mie published the much more general, and more complex, solutions for the scattering of a plane monochromatic wave by a homogeneous sphere of any diameter and of any composition situated in a homogeneous medium (50). More recent studies (51) have shown that Mie's theory can be applied to scattering by particles of irregular shapes without serious deviation from theory. It is beyond the scope of this chapter to present an extensive treatment of the theories of light scatterings. The interested reader is referred to the above papers and to texts devoted to optics (52) and light scattering (53).

The process of light scattering can be separated into three categories, depending on the size of the scattering

particle relative to the wavelength of incident radiation. For particles very much smaller than the wavelength of radiation, Rayleigh scattering occurs. The intensity has a minimum value at right angles to the direction of incidence, is symmetrically distributed about this angle and shows the well-known λ^{-4} dependence. The scattering observed at right angles to the beam is fully plane polarized if the excitation is plane polarized. For particles very much larger than the wavelength of incident radiation, the scattering is essentially independent of wavelength.

Scattering in the region between these extremes, when the particle diameter is comparable to the wavelength of incident radiation, is also wavelength dependent but the precise analytical formulae are quite involved. The general formulations advanced by Mie are appropriate and predict that the scattered light radiance is a function of d (the ratio of the particle circumference to wavelength), m (the complex refractive index of the particle material, which accommodates absorption of the light), and θ (the angle substended between the detector and the incident path).

In a simple flame system used in AFS, the sample solution enters the flame from a spray chamber as small droplets, the solvent is evaporated to give salt particles and the particles are thermally dissociated into atoms (54). In such a system, primary radiation could be scattered by:

a) droplets (39), b) incompletely vaporized salt particles (55,56), or c) molecular aggregates of combustion products formed in the flame (39,57).

Although it is now well known that oxygenated particles of aluminum and other refractory forming elements are the most likely to cause a spurious scatter contribution to the total observed signal at the detector (58), anomalies in the literature exist regarding the extents of scattering of solutions containing various elements. The scattering problem was generally not realized in the early papers on atomic fluorescence spectrometry because most authors confined themselves to the analysis of dilute solutions of the analyte metal. However, it was not long before investigators began to publish premature claims for atomic fluorescence from Al (59) and Be, Hf, Ti, U and Zr (60) which they later attributed to light scattering.

Veillon et al. (39) were the first to demonstrate some properties of scattering which were evident in the AFS determination of Mg, Ca, Ba, Ga, In, Ni and Mn in turbulent hydrogen flames. When the wavelength dependence of the light scattered from a xenon arc continuum source by aerosol solutions was corrected for the spectral response of their system, they found that the scattered signal followed a λ^{-4} law. They also observed a high degree of polarization of the scattered light, but they made no studies into the angular distribution of the scattered light.

Omenetto et al. (61) made a comprehensive investigation into the wavelength dependence, angular distribution and polarization of light scattered from 0.1 to 1.0% Al solutions in laminar flames using both line and continuum sources of excitation. Because of the characteristic of pneumatic devices to deliver droplets of widely varying diameters to the flame, it was not possible for them to apply any rigorous scattering theory. Only with laminar flames did the wavelength dependence approximate the λ^{-4} relationship of Rayleigh scattering, but in that case, the scattering intensity was not symmetric about 90°. They found that in some cases 90° would not be the optimum viewing angle to minimize light scattering in AFS. When it came to identifying the type of scattering that they observed, they stated:

> "the only clear conclusion which can be drawn from the obtained results is that the scattering observed in flames at atmospheric pressure cannot be identified with the Rayleigh scattering"

(61). With the total consumption burners, the departure from Rayleigh behavior was even more marked due to the larger droplets introduced into the flame.

Larkins and Willis (58) estimated that solutions containing from 0.01 to 1% solids would form solid particles in their pre-mixed air-C_2H_2 flame of 0.1 to 1 μm diameter, a size comparable to the 0.2 to 0.7 μm resonance wavelengths of atomic fluorescence spectrometry. Thus, they predicted

the scattering would be of the Mie type. Their studies of the wavelength dependence of the light scattered from solutions containing high concentrations of known scattering species (Al, La and Ti) showed a complex relationship in the 200-400 nm region, a relationship that varied from one element to another, and also depended on the anions present. As an indication of the magnitude of the scattering problem, they showed that for 2% solutions of materials forming refractory oxides in the flame (Al, Zr, Ti, Ta, V, La and Ca) the scattering signal, expressed as the equivalent analyte concentration, may be several thousand times the limit of detection of the analyte in the absence of the scattering material.

Evidence shows that elements that form stable monoxides are not solely responsible for light scattering in atomic fluorescence spectrometry. Smith et al. (55) detected scattering by the comparatively readily volatized elements Cd and Pb, and Warr (56) found that solutions containing Na, Hg and Cu scattered light to extents which varied with the anions present.

Doolan and Smythe (57) have recently evaluated relative intensities of light scattered by compounds of 46 elements in H_2-air and C_2H_2-air flames. They found that the scattering intensities were dependent on the element, flame composition and temperature, and the form of the element nebulized.

Significant among their results was that Al and Si compounds, which commonly occur in sample matrices, were among the most strongly scattering particulates, and their observation of a nonlinear relationship between scattered light intensity and solution concentration. On this last point, other investigators have reported the slope of log-log plots of the intensity of scattered light *vs.* the concentration of the element to have values ranging from 0.5 (56) to 1.0 (39) to 0.8-1.4 (55) and 0.55-1.8 (58).

This next section is devoted to a review of the various ways proposed to overcome the problem of light scattering in AFS. The fact that light scattering occurs at the same time and at the same wavelength as resonance fluorescence makes it difficult to eliminate. The use of direct-line (24) rather than resonance fluorescence is a solution, but requires the presence of appropriate atomic energy levels.

In the early studies conducted by Veillon *et al.* (39), they found that the majority of the incident radiation reaching the detector was due to reflection and scattering from water droplets in the flame of the total-consumption burner and could be minimized by heating the aspirating chamber or by using organic solvents.

A problem related to light scattering is that of chemical interferences which result from the inability of the flame to volatize the analyte from matrix constituents. In

such cases, the atom population of the analyte in the flame is reduced in comparison to pure aqueous standards, resulting in a suppression of the analytical signal. Epstein et al. (62) observed a 50% suppression of the Cd fluorescence signal from bovine liver and fly ash samples. It is customary in such cases (7) to minimize chemical interferences by the addition of large amounts of strontium or lanthanum chlorides, but as noted previously, these are likely to introduce scattering errors. The use of EDTA as a releasing agent would result in a smaller scattering error because much smaller concentrations of EDTA could be used.

Haarsma et al. (63) found that the scatter signal from surface water samples could be reduced by a factor of ten when the samples were made up to a concentration of 14% perchloric acid. It was assumed that after the evaporation of the solvent, the molecular aggregates burst and the resulting particles were of a size that scattered less.

The most important factor which has been found to influence scattering values is the type of flame (57,62,64) used to carry out analysis. Total-consumption aspirator burners and turbulent hydrogen flames have been used by the early AFS investigators (39, 65-69). These burners have the advantages of being relatively inexpensive, being easily adaptable for any solvent type, and of producing large atomic concentrations of absorbers in a flame that has a low level

of background thermal emission. However, as already noted, such burners produce turbulent flames having unevaporated solvent droplets in the flame gases resulting in a large amount of scattered light. According to a comparative study conducted by Bratzel et al. (64), scatter of this nature can be reduced by going to a pre-mixed flame with a chamber-type nebulizer burner which produces finer, more uniform droplets for delivery into the flame.

Denton and Malmstadt (70) showed that by using an ultrasonic transducer to generate the aerosol, the scattering signal could be reduced by more than an order of magnitude and the atomic fluorescence signal could be increased by a comparable amount in a pre-mixed hydrogen flame.

Hydrogen flames have limited application to AFS because of their inability to provide free atoms of elements that form refractory oxides and because of the higher incidence of chemical interferences associated with these flames, especially in the analysis of complex matrices encountered in natural samples.

The higher temperature of the air-acetylene flame (2523°K compared to 2380°K for hydrogen flames) (71) significantly decreases the scatter signal intensity. This effect is more evident when dealing with less refractory matrix components. However, Epstein et al. (62) found that even with the air-acetylene flame, the scatter signal remained a substantial portion of the analytical signal.

There are several additional ways to minimize the contribution of light scattering. One method is based on the unique angular dependence of Rayleigh scattering on the orientation of the polarization vector and on the direction of scattered light (52). By using linearly polarized light for excitation and by placing the detector at right angles to the direction of propagation of the exciting light and in the same plane as the plane of polarization, one could minimize scattering while maintaining the fluorescence signal. The practical limitation of this scheme is that the cone defined by the collection optics contains light rays traveling in a range of directions rather than a unique direction. Also, scattering by larger particles cannot be similarly treated.

A modification of this scheme by Omenetto et al. (61) showed that the fluorescence-to-signal ratio could be improved from 3 to 16 times, depending on the element investigated, by using crossed polarizers, one between the source and the flame and the other between the flame and the monochromator. A significant reduction in sensitivity, however, was noted. Veillon et al. (39) noted a 20-fold reduction in the scatter signal under similar conditions, but they did not report the attenuation of the AF signal upon insertion of the polarizers.

Larkins and Willis (58) also studied the use of crossed polarizers to reduce the scattering interference and found

fluorescence-to-signal ratios to improve by factors ranging from 1.1 to 6.7 depending on the flame used, the scattering material investigated and the wavelength of excitation. The work of Shull and Winefordner (72) showed that this method will not always work, for when Ga or Cd was excited by electrodeless discharge lamps in either H_2-N_2O or H_2-air pre-mixed turbulent flames, the fluorescence signals were reduced to the same extent as the scattering signal whether the polarizers were parallel or crossed.

One can also attempt to correct for the signal due to light scattering by actually monitoring its intensity at a nonresonant wavelength. Sychra and Matousek (73) attempted to make such a correction for scattering at the 232.0 nm Ni atomic fluorescence line by using the 242.8 nm line of gold, equalizing the signals of the two lamps on the scatter signal from the aerosol droplets formed when xylene was sprayed through the burner without igniting the flame. Using an analogous technique, Larkins (74) equilized the lamp signals from a solution of pure aluminum sprayed into the flame. Such procedures depend on the debatable assumption that all matrices will scatter these two lines to the same extent. A major disadvantage of these systems is that the lamps must be changed from analyte to reference for each correction causing both inconveniences and possible misalignment of optics.

Rains et al. (75) employed a xenon arc continuum source whose intensity was optically balanced with the line source of an electrodeless discharge lamp (EDL) used to excite the analyte. The radiation from each source was alternately passed through the flame by a mirror chopper, and the signal from the flame during the incidence of continuum radiation was subtracted from the signal during the incidence of line radiation by means of a lock-in amplifier. The correction was based on the assumption that the continuum radiation source would induce negligible fluorescence, from either the analyte or matrix constituents which have fluorescing lines or bands within the spectral bandpass of the monochromator. They found that the atomic fluorescence signal from the xenon arc continuum source was 4 orders of magnitude smaller than that excited by the EDL and, therefore, did not interfere. One disadvantage of the method is that such a large spectral window is necessary to admit equal irradiance from the continuum and line sources that the detector receives an unnecessarily large background emission signal.

A system based entirely on a xenon arc continuum source, with the capability to compensate for scattering, has been proposed by Fowler et al. (36). The radiation coming from the flame is modulated by a quartz-refractor plate inside the detector monochromator, allowing the spectrum to be repetitively scanned and the resulting modulated signal to

be extracted by a lock-in amplifier. Compared to the spectral radiance of the line sources, the continuum source has a low spectral radiance; therefore, the detection limits obtained were inferior to those obtained with line sources. The system did render the scatter signal from a 1000 μg mL^{-1} zirconium solution indistinguishable from the blank.

The scheme of Chester and Winefordner (76) using two electrodesless discharge lamps amplitude modulated at different frequencies seems readily adaptable to provide scatter corrected measurements if the wavelength dependence of the scattered light is properly accounted for and if the sample matrix is free of components that would fluoresce when irradiated by the reference lamp. Otherwise, an over-compensation for scatter would result.

Haarsma et al. (63) used an externally heated nitrogen stream to adjust the temperature of an EDL independent of the microwave power applied. They found that the fluorescence signal had a pronounced maximum with increasing temperature, whereas the intensity of the light source remained essentially constant. They attributed this behavior to self-reversal. A simple formula based on measurements at two temperatures and on the method of standard additions was used to correct for scattered light. The major disadvantage of this method is that one cannot do "real time" correction

for light scattering as the sample matrix or flame conditions change.

The recent work by Doolan and Smythe (57,77) is based on a system employing two monochromators and identical detector-readout channels positioned symmetrically about the irradiation axis. To correct for light scatter, one monochromator was tuned to a nonfluorescing line emitted by the electrode discharge lamp and the other monochromator was tuned to the resonant fluorescence line of the analyte. The success of this system depends on the existence of an intense nonabsorbing line as close as possible, within the limits imposed by the spectral bandpass of the monochromators, to the analyte line to minimize the complexities of wavelength dependence with different scattering species.

Another possibility is to use a magnetically tuned EDL for excitation whenever the atom of interest shows a favorable Zeeman affect (78), but this method of correction is susceptible to errors because the analyte and reference lines are of opposite polarization and may be scattered to varying amounts as the sample matrix changes.

Background correction by wavelength-modulated atomic fluorescence spectrometry (WMAFS) can be compared in theory and practice to background correction in atomic absorption by the application of the Zeeman effect (79-83). Both methods utilize one light source and are thus freed from the

strict requirement of good optical alignment of two separate sources. In Zeeman AAS, background correction is based on the splitting of a resonant wavelength into its Zeeman components when the radiation source is subjected to a magnetic field. If the magnetic field is large enough, the $\sigma\pm$ components will be outside the absorption profile. Absorption by the analyte will occur only at the π component while the background absorption, of broadband nature, will occur at all components. Since the π and $\sigma\pm$ components are perpendicularly polarized, it is possible to monitor them separately and obtain an analyte absorption signal that is freed from the broad background absorption of the sample matrix.

A wavelength-modulated CW dye laser has several unique advantages in minimizing the problem of scattered light in atomic fluorescence spectrometry. For AFS, the background spectrum due to light scattering is also broadband in nature. One can effectively extract an atomic fluorescence signal from a relatively large light scattering background by the applications of a wavelength modulated laser excitation source. The need for wavelength modulation has already been pointed out in earlier work (84). However, the modulation frequency of 1.5 Hz used in that work is too slow to be useful in practical atomizers such as the flame. The recent availability of an electro-optical tuner for the CW dye

laser (85) has made it possible to provide rapid wavelength modulation of the laser radiation (86,87).

When the tuner is driven by a square wave of frequency ω, the output waveform of such a laser can be described as:

$$\lambda_1 = \lambda_0 \qquad \text{for } \omega = 0 \text{ to } \pi$$

$$\lambda_2 = \lambda_0 + \Delta\lambda \qquad \text{for } \omega = \pi \text{ to } 2\pi$$

If such a laser is used as the excitation source for atomic fluorescence spectrometry and is tuned such that λ_0 is in resonance with the atomic transition and $\lambda_0 + \Delta\lambda$ is shifted off of the atomic transition, then the resulting signals falling on the detector can be given by:

$$I_{\lambda_1} = I_{T.E.} + I_{Scatt.} + I_{A.F.}$$

$$I_{\lambda_2} = I_{T.E.} + I_{Scatt.}$$

where:

$I_{T.E.}$ = thermal emission signal from the flame

$I_{Scatt.}$ = light scattering signal

$I_{A.F.}$ = atomic fluorescence signal.

These two signals can be subtracted electronically with a lock-in amplifier to give a net signal,

$$I_{net} = I_2 - I_1 = I_{A.F.}$$

which is independent of the light scattering problem.

The evaluation of such a scheme based on an electro-optically tuned dye laser for atomic fluorescence spectrometry has been performed using a pre-mixed air-acetylene

flame for the determination of barium (48) and is described here.

Experimental

A schematic of the experimental arrangement for this work is shown in Figure 2.1. The individual components and the most important experimental conditions are listed in Table 2.1. The argon ion laser is operated at 5-W all-lines output. Rhodamine 110 dye from Exciton Chemical Co., Dayton, OH, is used in the dye laser to give about 50 mW of tuned output. The laser bandwidth is estimated to be about 0.5 Å. Distilled water is deionized by passing through a mixed-bed ion-exchange resin and used for all solutions. The barium solutions were prepared by serial dilutions (2-fold, 5-fold, 10-fold, 20-fold, etc.) from a 1000-ppm barium stock solution prepared from Certified ACS grade $BaCl_2$. The solutions were stored in polyethylene bottles and run the same day as prepared.

With no tuning element inside the cavity of the dye laser, it runs freely in a 50-100 Å band depending on the concentration of the dye. The addition of an etalon decreases this lasing range somewhat because of the losses introduced. What is more important is that the laser output is restricted to 0.5 Å bands separated by 10 Å each, corresponding to the free spectral range (FSR) of the etalon.

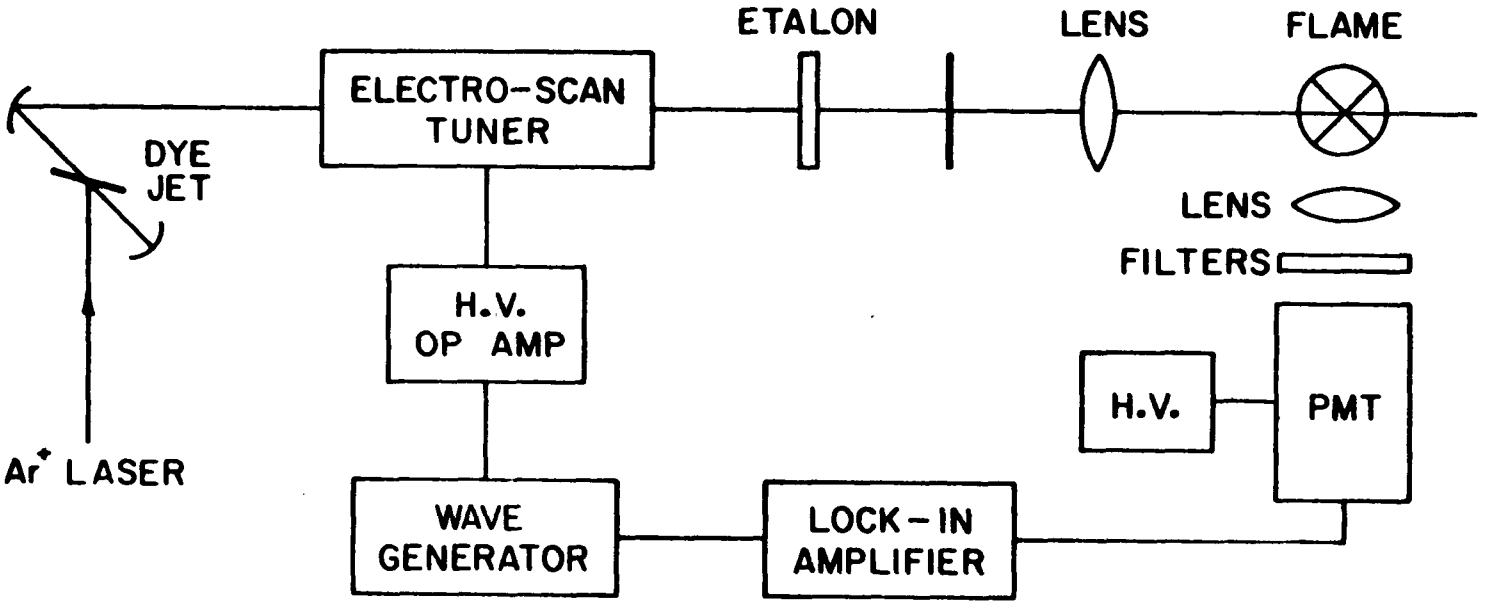

Figure 2.1. Block diagram of an atomic fluorescence spectrometer based on a wavelength-modulated CW dye laser

Table 2.1. Components for atomic fluorescence spectrometry based on a wavelength-modulated CW dye laser

Item	Manufacturer
Ar ion laser	Model 553, Control Laser Corp., Orlando, FL
CW dye laser	Model 375, Spectra-Physics Inc., Mountain View, CA
Electro-scan tuner	Model LS-14, Ithaca Research Corp., Ithaca, NY
Lens (source)	40-mm diameter, 94-mm focal length achromatic fused silica lens
Lens (detector)	67-mm diameter, 76-mm focal length achromatic fused silica lens
Filters	Model 7155 variable interference filter, Oriel Corp., Stamford, CT 600-nm short pass filter Corning glass filters 4-45, 3-67, 3-69, Corning Glass Works, Corning, NY
Photomultiplier tube	56 TVP, Amperex Electronic Corp., Slatersville, RI
Photomultiplier housing	Model 3378, Pacific Photometric Instruments, Emeryville, CA
Photomultiplier power supply (set at -1600 V)	Model 242, Keithley Instruments Inc., Cleveland, OH
Lock-in amplifier	Model 9503/5002, Ortec, Inc., Oakridge, TN (10^{-14} A full-scale)
Wave generator	Model 162, Wavetek, San Diego, CA
H.V. op amp	Model PZ-70, Burleigh Instruments Inc., E. Rochester, NY
Burner-nebulizer (C_2H_2, 0.8 L/min; air, 3.8 L/min; solution, 0.7 mL/min)	Premix slot burner with pneumatic nebulization, Varian Associates, San Carlos, CA
Power meter	Model 210, Coherent Radiation, Palo Alto, CA
Oscilloscope	Model 7904 with 7A16 Plug-ins, Tektronix Inc., Beaverton, OR
Photodiode	Model PVS-010, Infrared Industries, Waltham, MA
Monochromator	Double Grating Monochromator, Bausch & Lomb, Rochester, NY
Mechanical Chopper (1 KHz)	Model 125A, Princeton Applied Research, Princeton, NJ

The electro-scan tuner can pass vertically polarized photons of wavelengths that are separated by its FSR of 600 Å. It should be noted that vertically polarized photons pass through the dye laser's cavity with the least loss due to the Brewster angle configuration of the dye jet stream. The consequence of these facts is that the electro-scan tuner limits the laser output to only one of the etalon bands. The wavelength that is transmitted by the electro-scan tuner is a function of both the geometrical orientations of the crystal with respect to the laser axis and of the D.C. voltage applied to the crystal. Under normal operation, the position of the crystal is fixed. In this way, a square-wave modulation of the applied voltage results in alternate lasing between two wavelengths separated by a multiple of 10 Å. In practice, the laser is first tuned without the square-wave modulation to the atomic resonance by adjusting the tune angle and the D.C. bias voltage of the electro-scan tuner until the laser output is near the desired wavelength. Then the etalon is inserted and the laser is tuned by the etalon to the atomic transition. A 50-ppm solution of Ba in the flame gives a clearly visible fluorescence output and is used to optimize the laser wavelength. The modulation is then superimposed on the D.C. bias so that lasing alternates between two wavelengths 10 Å apart. This is found to be optimum since any larger separation of the two wavelengths

will require larger applied voltages, which in turn demands a faster slew rate of the high voltage op amp. Also, for such small separations, the wavelength dependence of light scattering can be neglected. Finally, by readjusting the D.C. bias voltage, one can shift the dye laser gain curve to obtain equal intensities at the two wavelengths. This last step is necessary to ensure that light scattering is not modulated, so that it will not be detected.

In Figure 2.2, we can see the course of events as displayed on an oscilloscope. The top trace (ground = 2 divisions from top) represents the square-wave modulation applied to the electro-scan tuner. Slight curvatures in the vertical segments are results of the limited slew rate of the op amp. The second trace (ground = 2 divisions from top) is the negative-going signal from a photodiode monitoring the laser output through a monochromator set at the barium resonance frequency of 5535 Å. The third trace (ground = 4 divisions from top) is the same as the second trace, except that the monochromator is set at 5545 Å. The curvature on the falling edges of the photodiode signal simply refects the characteristic fall times of these diodes. In fact, the spectral output is quite close to being 100% modulated. The bottom trace (ground = 6 divisions from top) shows the total output of the laser, with no detectable modulation of the amplitude.

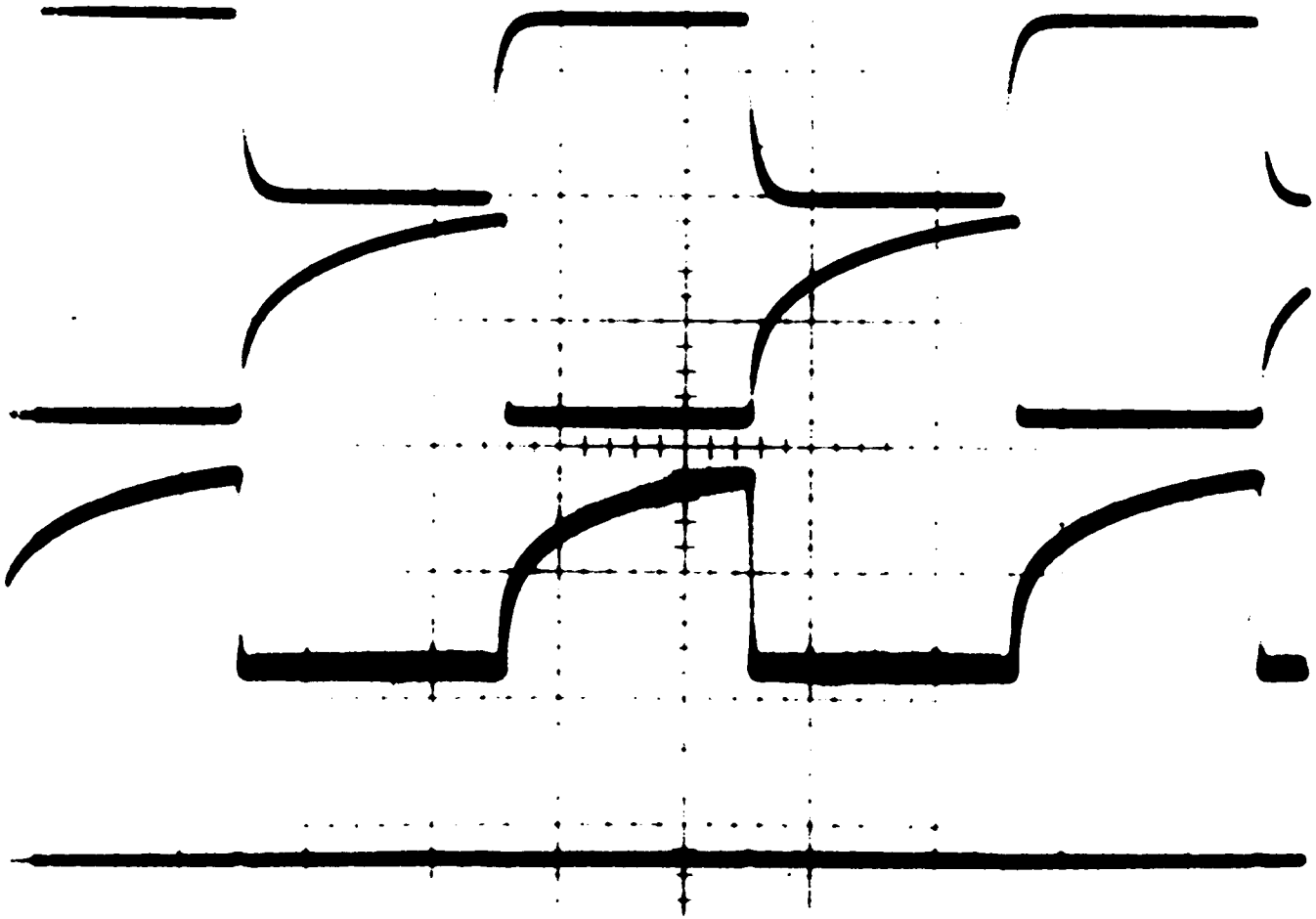

Figure 2.2. Oscilloscope display of modulation of the laser wavelength (see text for details). The horizontal scale is 0.25 msec/div

Electro-scan tuners that replace the function of the etalon are also commercially available. It seems at first sight that using such tuners will produce equivalent results. In practice, however, it requires a very reliable wave generator and a very stable high voltage op amp to reproducibly center on the atomic resonance line using these other tuners. In contrast, this present scheme relies only on the etalon to properly center on the atomic line. Slight imperfections in the modulation electronics will lead only to incomplete modulation between the two fixed wavelengths, but it will not change these two wavelengths.

Results and Discussion

The sensitivity and the ultimate limit of detection for a given atomic fluorescence spectrometer depend on many experimental variables. The most obvious ones are the flow rate of the solution, flame stoichiometry, exciting photon flux, laser bandwidth, efficiency of the collection optics and the stability of the detection electronics. For the purpose of demonstrating the usefulness of this scheme of wavelength modulation, it is most appropriate to compare it with an amplitude modulation scheme while fixing all of these other experimental variables. Therefore, two parallel sets of measurements on the atomic fluorometric determination of barium using the 5535 Å resonance line have been performed.

The first set is based on amplitude modulation using a mechanical chopper for a fixed-wavelength laser and is shown in Figure 2.3. The second set is based on the wavelength modulated laser described above and is shown in Figure 2.4. The modulation frequency is 1 KHz in both cases. Data points for higher barium concentrations are not shown but extrapolate quite well for at least two orders of magnitude.

It can be seen that for the case of amplitude modulation, contributions from light scatter set in at about 300 ppb Ba so that lower concentrations cannot be detected, even though the photomultiplier tube has no difficulties in registering much smaller signals. For the case of wavelength modulation, one can extend the limit of detection to the 10-ppb Ba range. The ultimate limit here is determined by the overload capacity of the particular lock-in amplifier used. By using a monochromator rather than a set of filters, as is done in Ref. 88, one should be able to reduce the D.C. signal from flame background emission further, so that still lower limits of detection can be achieved. Increasing laser power is another alternative. Furthermore, the modulation frequency in this work was chosen to coincide with the available mechanical chopper so that a proper comparison could be made. For actual applications, the modulation frequency should be chosen to minimize the effects of fluctuations in the flame (89) and other electronic noise in the system. These

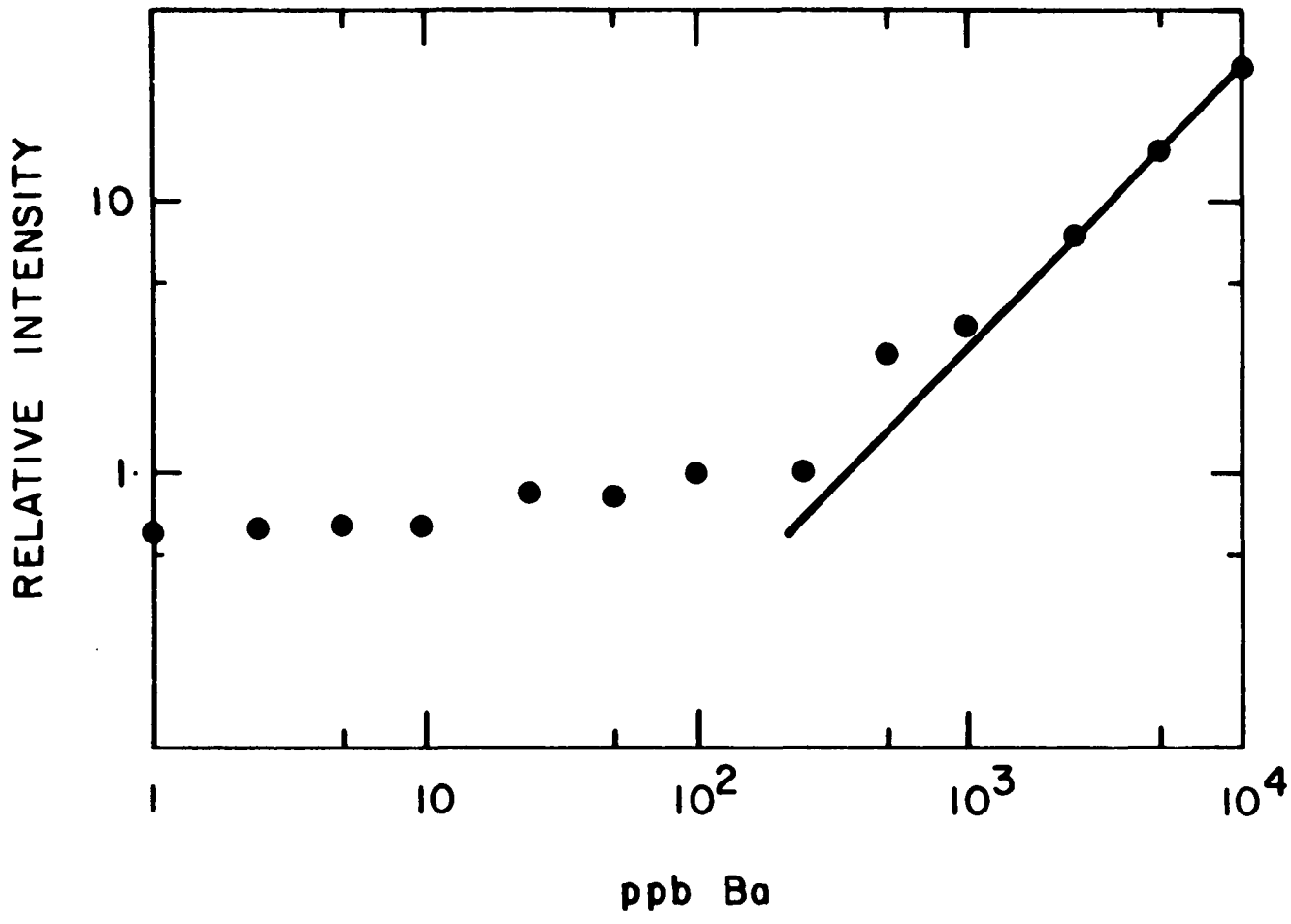

Figure 2.3. Analytical calibration curve for atomic fluorescence of barium (553.5 nm) using amplitude modulation of 1 KHz. The curve is linear to above 10^6 ppb Ba. The limit of detection is 300 ppb Ba

Figure 2.4. Analytical calibration curve for atomic fluorescence of barium (553.5 nm) using wavelength modulation at 1 KHz. The curve is linear to above 10^6 ppb Ba. The limit of detection is 20 ppb Ba

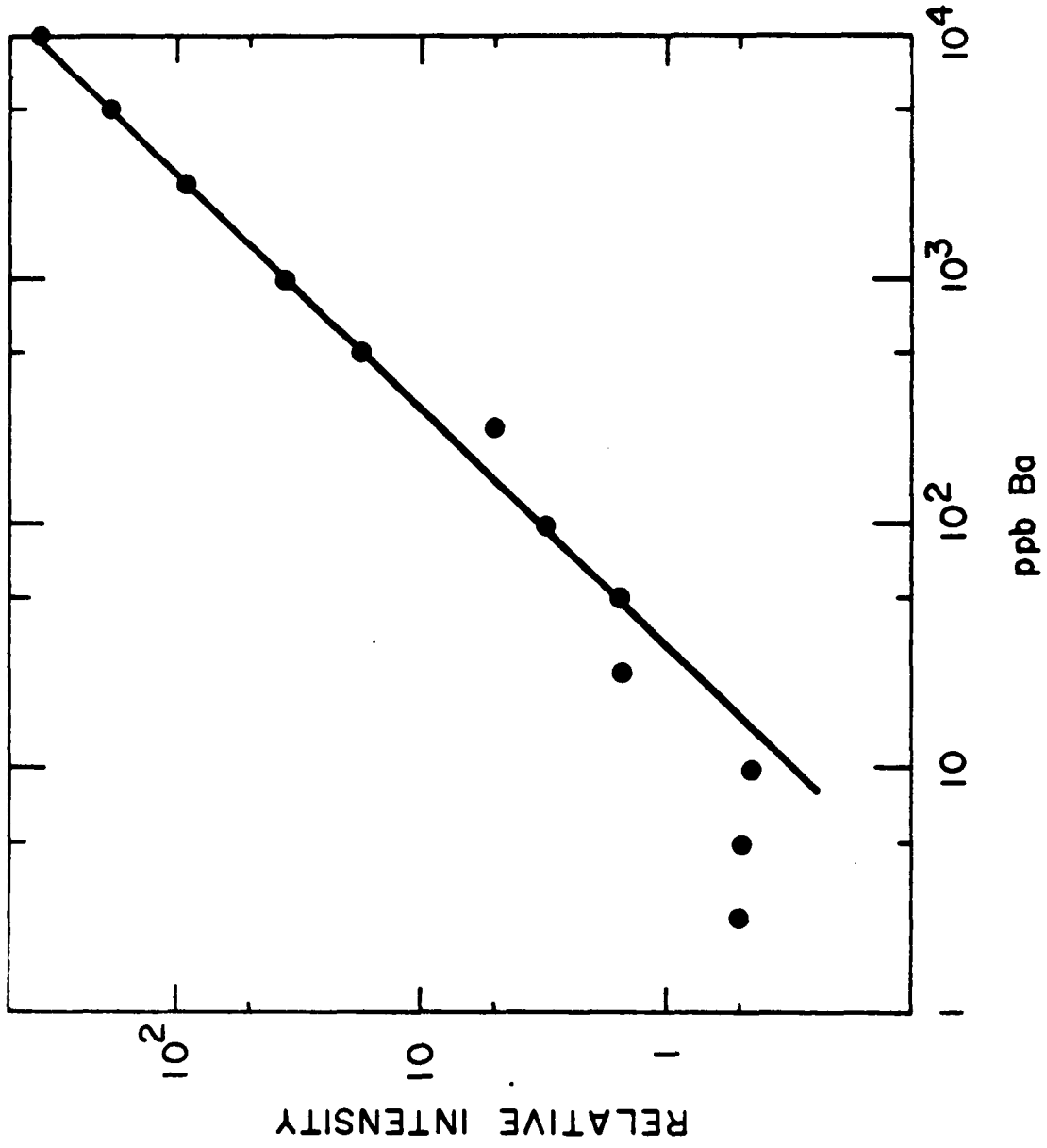
RELATIVE INTENSITY
10^2
10
1
1
10
10^2
10^3
10^4
ppb Ba

electro-scan tuners can be effectively used even in the MHz range (86,87). It is interesting to note that by using a combination of electro-scan tuners, one can in principle rapidly step from one atomic line to another (within the gain curve of the dye) by properly controlling the voltages on the electro-scan tuners. This opens up the possibility of sequential multi-element analysis using laser-excited atomic fluorescence spectrometry, free from the limitation of conventional mechanical scanning devices.

One possible way to increase the laser excitation power and thus improve the limit of detection is to place the atomizer inside the laser cavity. For a typical dye laser with an output coupler of 1% transmission, the ratio of intensity inside the cavity to outside the cavity is 100 to 1.

There are several problems associated with putting a flame inside the laser cavity. For example, disturbances of the optical path of the laser by the thermal gradients associated with a flame can introduce undesirable angular modulation to the electro-optical tuner resulting in amplitude and spectral noise and degradation of the limit of detection. To evaluate the potential of intra-cavity wavelength modulated LEAFS, the experimental arrangement of Figure 2.4 was modified to allow a pre-mixed 13 hole air-C_2H_2 Denton burner (90) to be placed inside the cavity between the

electro-scan tuner and the folding mirror. The sample was introduced as an aerosol into the flame by means of an ultrasonic nebulizer (Model UNS-1, Plasma-Therm. Inc., Kresson, NJ). This nebulizer-burner combination was found to be more stable than the commercial pneumatic nebulizer pre-mixed slot burner used in the previous work.

The limit of detection for barium by this method was found to be 400 ppb, a value comparable to the one obtained by conventional amplitude modulation LEAFS outside the cavity. Although the improvement hoped for was not obtained, these studies do show that it is possible to do sub-μgmL^{-1} determinations by intra-cavity wavelength modulated LEAFS. The full potential of this method could be more nearly realized by designing a system that would take such factors into consideration as improving the laminar flow of the flame gases to decrease the tendency of the electro-optic tuning crystal to move the laser off of the analytical wavelength due to slight shifts in the optical path introduced by the intra-cavity flame.

The experimental arrangement of Figure 2.1 was used to test the practical application of wavelength modulated laser excited atomic fluorescence spectrometry (WMLEAFS) to the determination of barium in standard sample No. 89 lead-barium glass supplied by the National Bureau of Standards, Washington, D. C.

After drying the powdered glass for one hour at 110°C to remove surface moisture, a 1.6117 g portion was placed in a 100-ml platinum dish. To it was added 4 ml of H_2O, 40 ml of 48% HF and 10 ml of concentrated HNO_3 (91). The solution was allowed to stand for two hours and then 6 ml of 70% $HClO_4$ was added and fumed on a hot plate until no more white fumes came off. The inside of the dish was washed with a small amount of water and taken to dryness. Then, 25 ml of concentrated HCl was added and the solution brought to a boil. When all was dissolved, 25 ml of H_2O was added slowly while boiling. The solution was boiled until clear, then cooled, transferred to a 250-ml volumetric flask and brought to volume with deionized water. To each of five 500-ml volumetric flasks was added 10 ml of the sample solution and varying amounts of a 50-ppm Ba stock solution. Beginning with the first flask, the amounts added were 0, 10, 20, 30 and 40 ml.

Figure 2.5 presents the WMLEAFS signals obtained from these solutions. The regression line for these points is extrapolated to its intersection with the concentration axis giving an estimation of the analyte concentration responsible for the signal from the unspiked sample solution. When the sample weight and the dilution factors are accounted for, the barium concentration in the original sample can be determined and compared to the NBS Certified value.

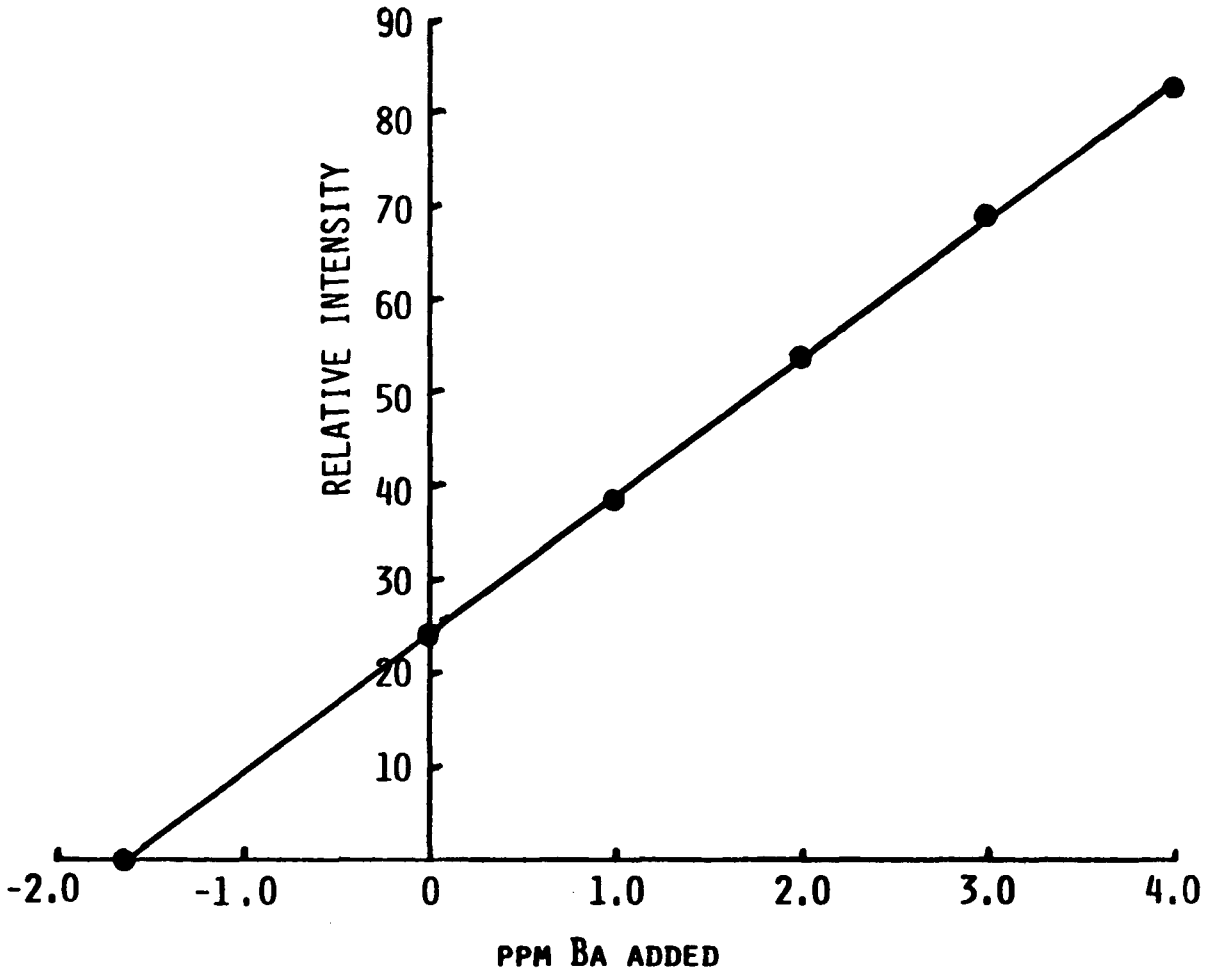

Figure 2.5. Standard addition curve based on wavelength modulation for the determination of the barium content of NBS sample No. 89. Intensity measurements are ± 1 unit

Figure 2.6 presents the determination of barium in the same solutions, under the same conditions, with the exception that the laser wavelength is fixed on resonance and the signal is obtained by amplitude modulation of the dye laser with a mechanical chopper. In the amplitude modulation mode, the lock-in amplifier cannot discriminate against light scattering which occurs at the same time and the same wavelength as the atomic fluorescence signal; therefore, a higher value for the sample concentration of barium is obtained. Scatter from instrumental components is indistinguishable from the H_2O blank in both modes of operation.

The results of these determinations are presented in Table 2.2. The difference in the barium concentration determined by the two methods is a measure of the extent of light scattering in laser excited atomic fluorescence spectrometry using an air-C_2H_2 pre-mixed slot burner. It should be noted that the light scattered from the sample matrix has an equivalent analyte concentration of 0.98 ppm which is appreciable when compared to the true analyte concentration of 1.62 ppm. This spurious signal renders the experimental error of the conventional method unacceptable. These experiments show that wavelength modulation of the laser is a convenient and reliable way to overcome the problem of light scattering in the determination of trace elements in complex sample matrices.

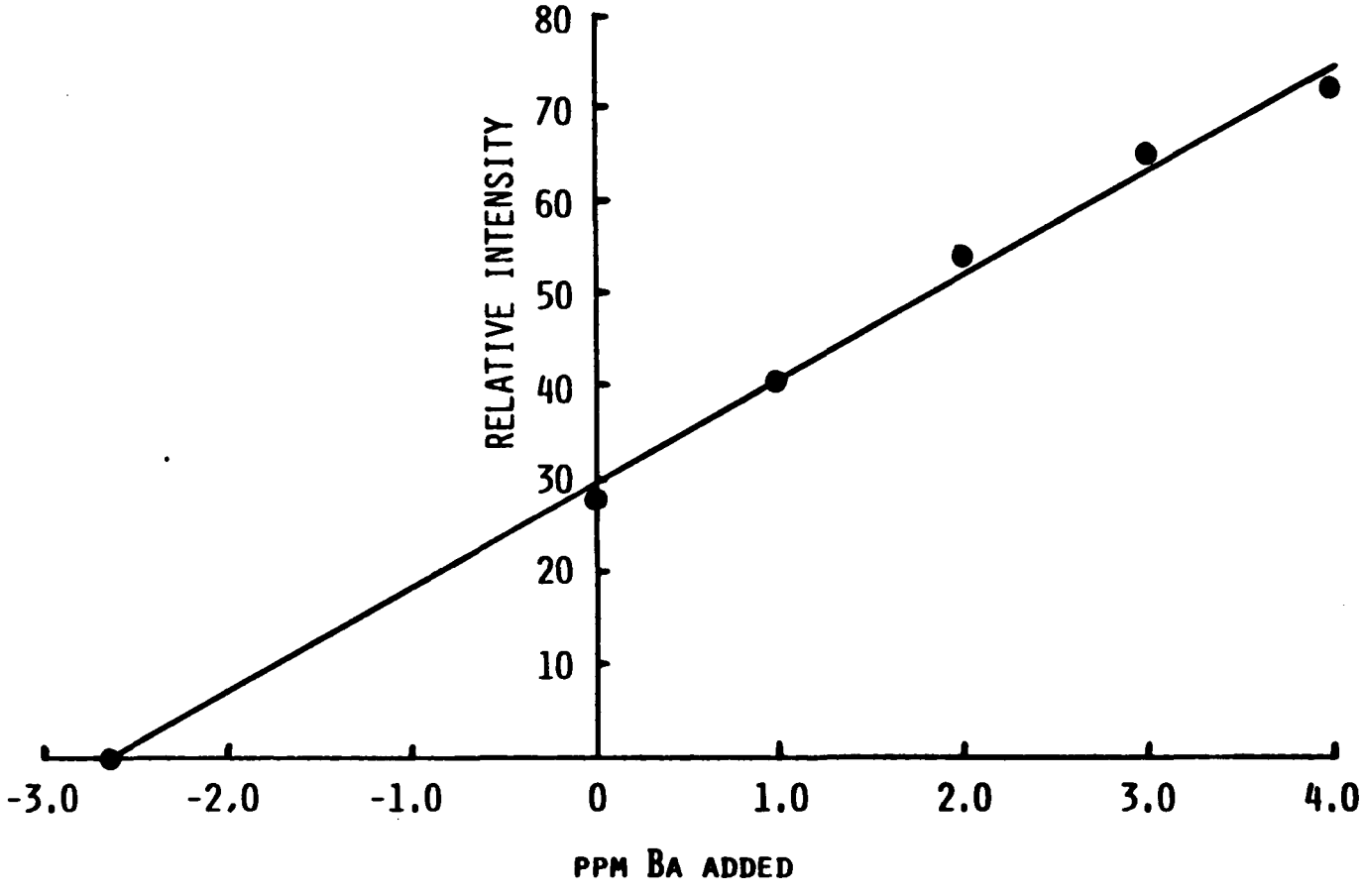

Figure 2.6. Standard addition curve based on amplitude modulation for the determination of the barium content of NBS sample No. 89. Intensity measurements are ± 3 units

Table 2.2. Comparison of amplitude modulated (AM) and wavelength modulated (WM) laser excited atomic fluorescence spectrometry (LEAFS) for the determination of barium in NBS standard sample No. 89, certificate value: 1.40% BaO

Method of determination	Correlation coefficient	Negative x intercept	Experimental % BaO	% error
AMLEAFS	0.9939	2.61 ppm Ba	2.26	61.7
WMLEAFS	0.9998	1.63 ppm Ba	1.41	0.7

Conclusions

The use of an electro-optically tuned CW dye laser in atomic fluorescence spectrometry offers several advantages: (1) wavelength modulation becomes feasible so that problems associated with light scattering can be minimized and the limits of detection can be improved; (2) the frequency of modulation can be extended to the MHz range so that optimization of this frequency to eliminate inherent fluctuations is possible; and (3) reliable and rapid tuning can be accomplished, leading to the possibility of multi-element analysis.

CHAPTER III. EVALUATION OF THE INDUCTIVELY COUPLED ARGON PLASMA AS AN ATOM SOURCE FOR LASER EXCITED ATOMIC FLUORESCENCE SPECTROMETRY

Introduction

One of the major problems that remains to be solved in laser excited atomic fluorescence spectrometry is the inadequacy of conventional atomic reservoirs to provide reliable atom formation from real samples in typical analytical situations while retaining the good optical properties that are essential to LEAFS. Despite their popularity, chemical flames have serious limitations when applied to the production of free atomic vapor. The attainable atomic concentration is limited by the high dilution effect of the sample by the flame gases. Combustion restraints prohibit precise control over the chemical environment of the sample. The flames that are the most efficient atomizers and give the greatest freedom from interelement effects (e.g., fuel-rich air-acetylene or nitrous oxide-acetylene flames) unfortunately contain effective quenchers (CO, N_2, CO_2) which lower fluorescence yields. The use of fuel-rich conditions to enhance dissociation of oxides is not desirable in LEAFS because of the high background emission that results. Nonflame atomizers need to be investigated in search of improvements in the above-mentioned areas.

The main requirements of an atomic reservoir for LEAFS can be enumerated as follows: ease of handling, good stability and high reproducibility, the ability to produce a high concentration of analyte atoms in an environment that is relatively free from quenchers and high background radiance, and a high volatization efficiency to minimize light scattering.

In the early 1960s, Reed (92-95) called attention to three attractive properties possessed by inductively coupled plasmas (ICP) that should contribute to their usefulness as vaporization cells and free atom reservoirs for analytical atomic emission spectrometry (AES). These properties also have significance in atomic fluorescence spectrometry (AFS). They are: high gas temperatures (to aid in volatilization), the capability of being sustained in noble gas environments (important in free atom considerations) and freedom from electrode contaminations (no electrodes are used in an ICP). It is in these respects that the ICP should be a superior fluorescence cell compared to conventional analytical flames. The higher temperature and longer interaction time leads to a higher degree of volatilization and atomization and, consequently, an increase in freedom from the physical and chemical interferences which are well documented in flame cells (7). The ICP is expected to minimize the scattering effect as a consequence of its high volatilization

efficiency. The noble gases (usually Ar) used to sustain the ICP contributes to a smaller quenching cross-section and thus increased fluorescence quantum yields. Svoboda et al. (22) showed that in hot Ar gas the fluorescent yields of atoms ranged from 0.95-1.0, whereas in common flame mixtures, the values were in the range of 0.014-0.75.

Review of Literature

Professor V. A. Fassel has published an excellent review (96) of the history of the ICP as a source for atomic emission spectrometry. Those interested in a detailed description of the theory and operation of the ICP are referred to the references in Eckert's review (97). The inductively coupled plasma receives its name because a time varying RF field is inductively coupled to a gas medium which is highly ionized (thus, the name plasma). The ICP discharge is able to sustain itself when the support gas flows through the induction coil. Temperatures in the range of 8000°K are produced. Samples are introduced into the plasma in the form of aerosols and pass through the plasma excitation region. By the time the sample species reach a height of 15-20 mm above the coil, they have had a residence time of ca. 2 milliseconds at temperatures ranging from 5500-8000°K. These residence times and temperatures are approximately twice those found in even nitrous

oxide-acetylene flames. The combination of high temperature and relatively long residence time leads to an unusually high degree of atomization of the analyte species. It is when the atomization is essentially complete that dissociation equilibria play a less significant role and vaporization-atomization effects are unlikely to be serious problems.

Montaser and Fassel (98) introduced the ICP as an atomization cell for AFS, using microwave electrodeless discharge lamps as excitation sources. They conducted preliminary investigations into the spatial dependence of the fluorescence signal in the plasma tail plume and into the dependence of the fluorescence signal on varying gas flow rates through the torch. Their results showed that under their optimum conditions, the AFS detection limits in the ICP were inferior to those obtained in conventional flames.

More recently, Pollard et al. (99) studied atomic fluorescence spectrometry in the ICP with a CW dye laser excitation source. They concluded that lower RF powers gave better detection limits because of the resulting reduction in background emission from the plasma. The use of these lower powers (0.5-1 KW) in the ICP is possibly undesirable due to the unknown effect of lower power upon the desolvation and vaporization processes for complex sample matrices.

The limited wavelength range of the CW dye laser and the necessity of lowering the RF power to reduce background

radiation could be overcome through the use of a pulsed laser with gated detection. Gated operation results in a significant improvement in S/N ratio if the system under study is background noise (not molecular fluorescence or light scatter) limited. The detector is "on" only during the laser "on" time, so that background noise (shot and fluctuation), which is also measured only during this short time interval will be greatly diminished. For a complete theoretical treatment, consult references 100 and 101. A dye laser has the significant advantage over other sources of being able to run with a very low duty cycle (ratio of "on" time to "off" time), while maintaining a high average power.

It is difficult to find a highly efficient laser dye for wavelengths in the UV region of the spectrum because of the strong absorption of the fluorescence emission by due molecules in the excited state. Kuhl and Spitschan (102) were among the first to point out that frequency mixing in nonlinear crystals could be used to overcome the difficulties of obtaining a laser dye in the UV region where most atoms of interest have their strongest transitions. Because of this, experiments requiring UV excitation take advantage of the properties of nonlinear crystals such as ADP and KDP to generate the second harmonic when visible laser radiation impinges on these crystals.

Experimental

A schematic of the experimental setup used to study the ICP as an atomization source for laser excited atomic fluorescence spectroscopy is shown in Figure 3.1. The individual components and the most important experimental conditions are given in Table 3.1. A CMX-4 (Chromatix, Sunnyvale, CA) flashlamp pumped dye laser operating in the frequency doubling mode was used in these studies as the source of tunable UV radiation of narrow bandwidth.

Generation of ultraviolet output from the CMX-4 is accomplished by utilizing the preferred intracavity doubling technique, taking advantage of the higher intracavity power compared to that available for doubling outside the cavity. Spectral narrowing of the laser output is possible by insertion of etalons inside the laser cavity.

Tuning of the laser is possible by simultaneously rotating the birefringent tuning element, the frequency doubling crystal and the intracavity Fabry-Perot etalon. Both high and low finesse etalons (ca. 0.2 cm^{-1} and ca. 0.5 cm^{-1} bandwidths, respectively) were available in the system used. The laser bandwidth without an etalon is ca. 3 cm^{-1}.

The lasing medium was made by dissolving 0.285 g of rhodamine 6G perchlorate dye (Exciton Chemical Co. Inc.,

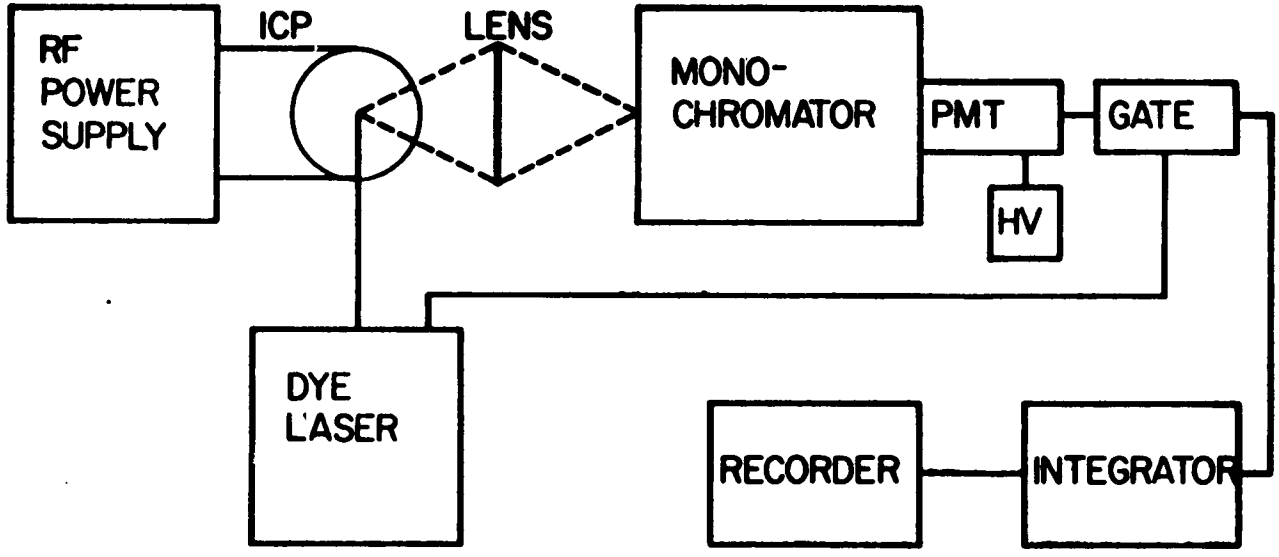

Figure 3.1. Block diagram of the ICP-pulsed laser atomic fluorescence spectrometer

Table 3.1. Components for laser excited atomic fluorescence in an inductively coupled argon plasma

Item	Manufacturer
Flashlamp Pumped Dye Laser with Frequency Doubling Crystal (30 Hz, 1 μsec, 3 mW)	Chromatix Model CMX-4 Sunnyvale, CA
Inductively Coupled Plasma	Plasma Therm, Inc. Model HFS-2500D Kresson, NJ
Stepping Motor Drive	Denco Research, Inc. Model Sm-2A Tucson, AZ
Stepping Motors	Computer Devices Model 34H-509A Santa Fe Springs, CA
Monochromator (250 mm, f/3.5, 3.3 nm/mm)	Jarrell-Ash Co. Model 82-410 Waltham, MA
Photomultiplier Tube	Amperex Electronic Corp. Model 56DVP Slatersville, RI
H.V. Power Supply (set at -2000 V)	Hammer Electronics Co., Inc. Model NV-13-P Princeton, NJ
Charge Transfer Gate	Laboratory constructed (103)
Integrator	Modified Model 417 Picoammeter Keithley Instruments, Inc. Cleveland, OH
Strip Chart Recorder (1"/min)	Leeds & Northrup Co. Philadelphia, PA
Pulse Shaper	Wavetek Model 162 San Diego, CA

Table 3.1. (Continued)

Item	Manufacturer
Lens	60 mm diameter, 70 mm focal length aspherical biconvex
Nebulizer	Cross flow nebulizer Laboratory constructed (104)

Dayton, OH) in 4 liters of 1:1 methanol:water. The flash lamp was run at 15 J/pulse giving a fundamental output of 175 mW in the visible and a frequency doubled output of 3 mW in the UV.

The laser was tuned to the 302.0 nm a^5D_4 to $y^5D_4^0$ transition of FeI and the transition corresponding to $y^5D_4^0$ to a^5F_5 at 382.0 nm was monitored in emission and fluorescence. The etalon position was fine tuned to maximize the fluorescence signal. This transition pair was chosen because it represents a Stokes direct-line fluorescence system with good oscillator strengths and because it was at a wavelength easily accessible with a frequency-doubled dye laser like the CMX-4. In previously published work (46), the a^5D_4 to $y^5F_5^0$ transition at 296.7 nm and the $y^5F_5^0$ to a^5F_5 transition

at 373.5 nm and a nitrogen pumped dye laser were used. The corresponding gA values for the two sets of transitions make these essentially equivalent systems for LEAFS, except that atomic emission at 382.0 nm is less intense and, therefore, a slightly favorable case for study.

The ICP unit was driven at 27.1 MHz by the RF generator operated at 1.25 KW. Reflected power was kept to a minimum by the automatic matching network in the power supply. The argon plasma gas flow, which sustained the plasma and provided thermal isolation and stabilization of the plasma, was set to 20 $Lmin^{-1}$. The sample was introduced with a cross flow pneumatic nebulizer (104). The aerosol flow rate was set to 1.45 $Lmin^{-1}$. An extended torch, AFS-1 in reference 98, was used to keep the atomic vapor in a constricted volume for these studies.

The ICP was mounted on an adjustable (X-Y-Z) mount to allow the laser to illuminate any part of the plasma without disturbing the alignment of the laser and the collection optics of the detection system.

A 1:1 image of the torch plume was focused onto the entrance slit of the monochromator (0.25 m, f/3.5, 3.3 nm/mm). This monochromator was chosen because of its high throughput. A monochromator of high dispersion was not necessary because of the 80 nm Stokes shift of the atomic fluorescence wavelength from the laser excitation wavelength. The

monochromator was rotated 90° about its optical axis to place its slits in the same horizontal plane as the laser beam and thus more effectively collect the atomic fluorescence signal. A slit width of 2 mm was used to match the image of the fluorescence signal, giving a spectral bandpass of 6.6 nm.

An Amperex 56 DVP photomultiplier tube was operated at -2000 Volts D.C. to convert the atomic fluorescence signal to an electrical signal. Because the laser output was made up of 1 μsec pulses at a rate of 30 Hz, a laboratory constructed detection system based on an inexpensive charge transfer gate (103) and a modified picoammeter was used to integrate the PMT signal and drive the strip chart recorder. The CMX-4 laser has a 0 to 10 Volt D.C. sync output pulse that precedes the actual laser pulse by 4 μsec. This synch output pulse was used to trigger a Wavetek Model 162 signal generator whose output is shown on the bottom trace of Figure 3.2. The output of this signal generator was used to open and close the charge transfer gate as shown in the top trace. The switching transients (the spikes at the opening and closing of the gate) were adjusted with the trim pots in the gate to give a signal of zero when the PMT was blocked. The resulting 2 μsec window of signal that occurs when the laser is "on" is all that goes to the picoammeter which has been modified (103) to provide a 1 sec RC time constant to smooth the resulting pulses and provide a D.C. signal to drive the strip chart

Figure 3.2. Oscilloscope display of gate operation. Bottom trace: pulse applied to the gate (vertical, 2V/div; horizontal, 0.5 μsec/div). Top trace: output from the gate showing laser pulses (vertical, 5 mV/div; horizontal, 0.5 μsec/div)

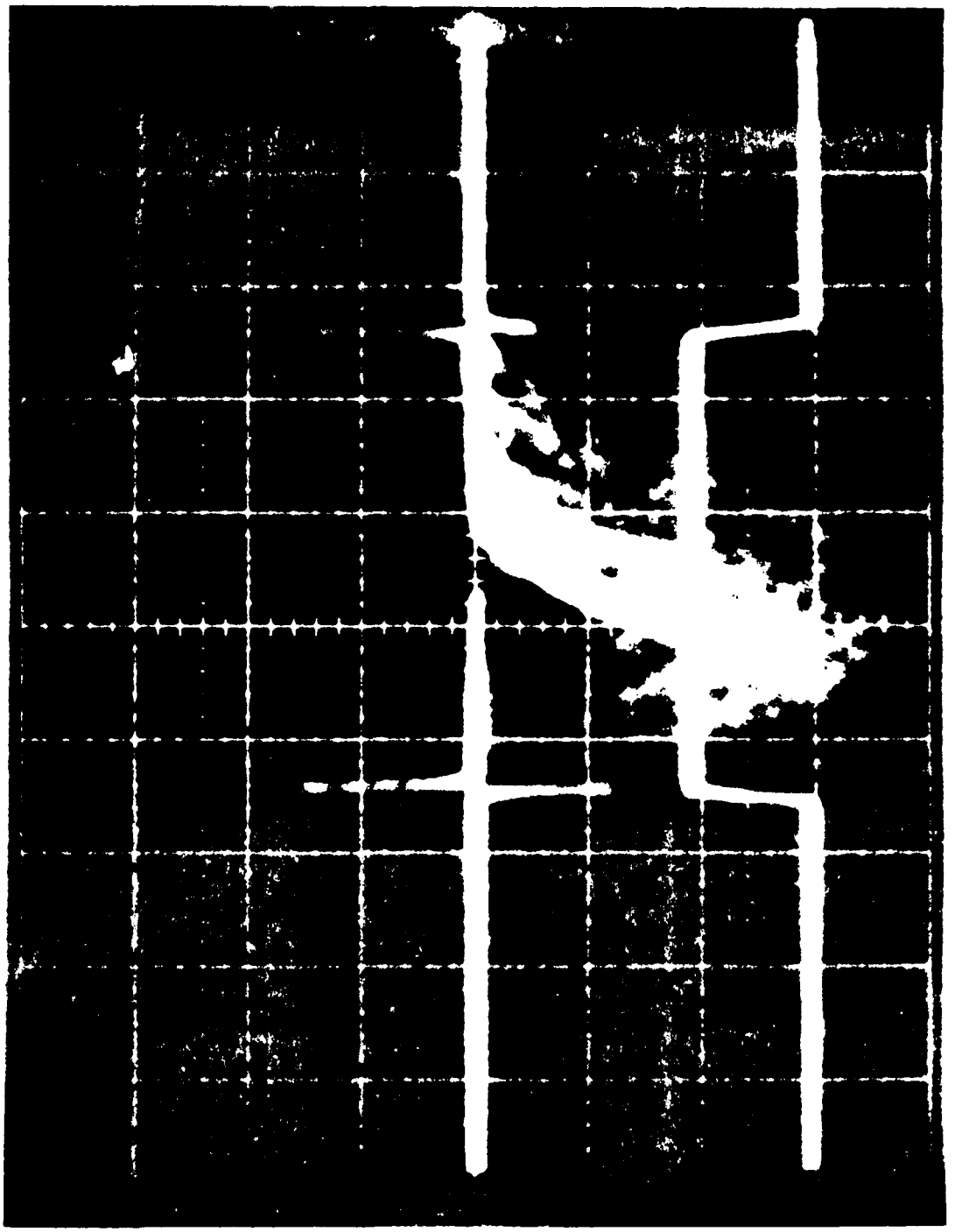

recorder. The detection system has a duty cycle of 2 μsec x 30 sec^{-1} = 3 x 10^{-5} which allows the plasma background emission signal to be reduced by over 4 orders of magnitude while registering the entire laser-excited atomic fluorescence signal.

Results and Discussion

Studies into the effect that narrowing the spectral output of laser had on the resulting fluorescence signal were conducted with the following results:

Table 3.2. Effect of etalon choice on the net AFS signal

Etalon No.	Description	Power (mW)	Net AFS Signal (Arbitrary Units)
1	High Finesse	1	20
2	Low Finesse	3	50
3	Blank	4	27

The above table demonstrates the trade-off that exists between narrowing of the laser and decreasing the output power. The laser was used with the low finesse etalon for the remainder of the studies. In this mode of operation, the laser gave 3 mW average power with a bandwidth of 0.5 cm^{-1}.

By moving the ICP torch with the aid of stepping motors, it was possible to obtain spatial profiles of the atomic fluorescence, atomic emission and background plasma emission signals with a spatial resolution of 2 mm as defined by the unfocused laser beam and the entrance slit of the detection system. This resolution could be improved to the range of 10-100 μm by focusing the laser beam and using narrower slits on the monochromator.

To obtain the degree of spectral interference due to plasma and atomic emission at the Fe wavelength, the spatial variation of the emission was measured by vertically scanning the torch while blocking the laser output. This is shown in Figure 3.3. The emission signal is shown to fall off rapidly from the top of the extended torch (ca. 4 cm) to nearly zero by 8 cm. It should be noted here that most of the analytical emission work done in ICP-AES is done at 1.5 cm above the load coil. The advantage of doing ICP-AFS higher in the tail plume is shown in Figures 3.4 and 3.5 where we see that the fluorescence signal increases with height to a maximum at 6.5 cm above the load coil and then decreases at larger distances. The fall in intensity can be attributed to diffusion and recombination of the Fe atoms at large distances, and to increased fluorescence quenching as air is entrained.

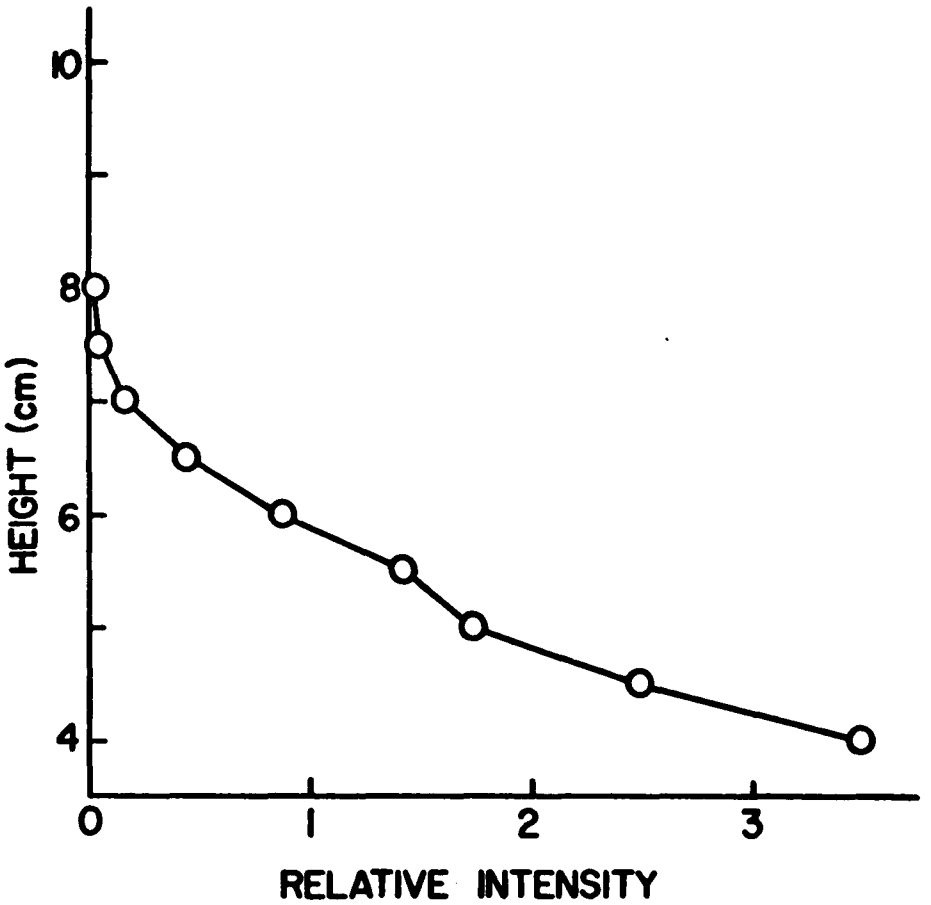

Figure 3.3. Height profile (cm above the load coil) for atomic emission of iron (382.0 nm, 100 ppm Fe). Intensity measurements are ± 5%

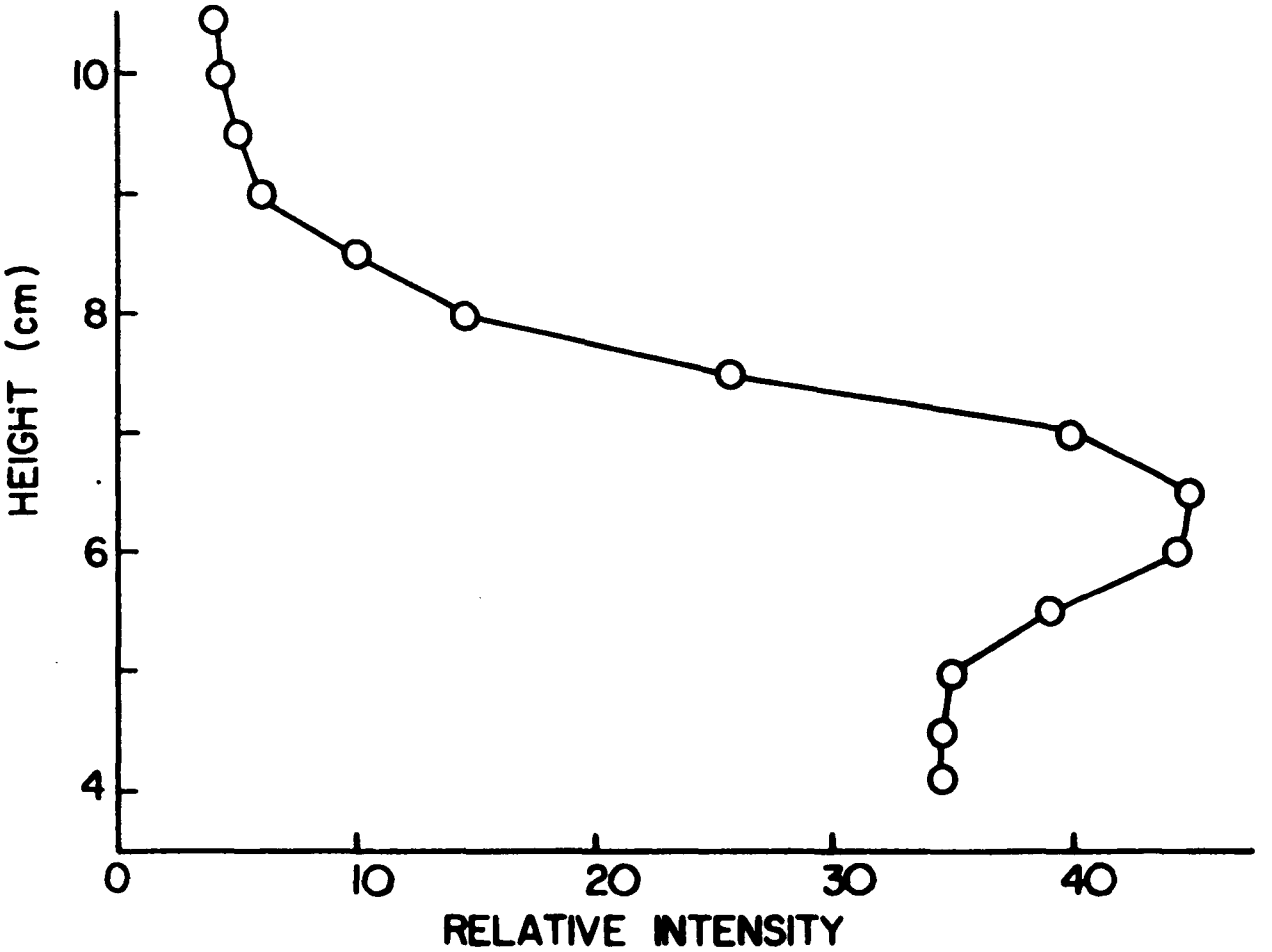

Figure 3.4. Height profile (cm above the load coil) for atomic fluorescence of iron (382.0 nm, 100 ppm Fe) with dye laser excitation (302.0 nm, 3 mW). Intensity measurements are ± 5%

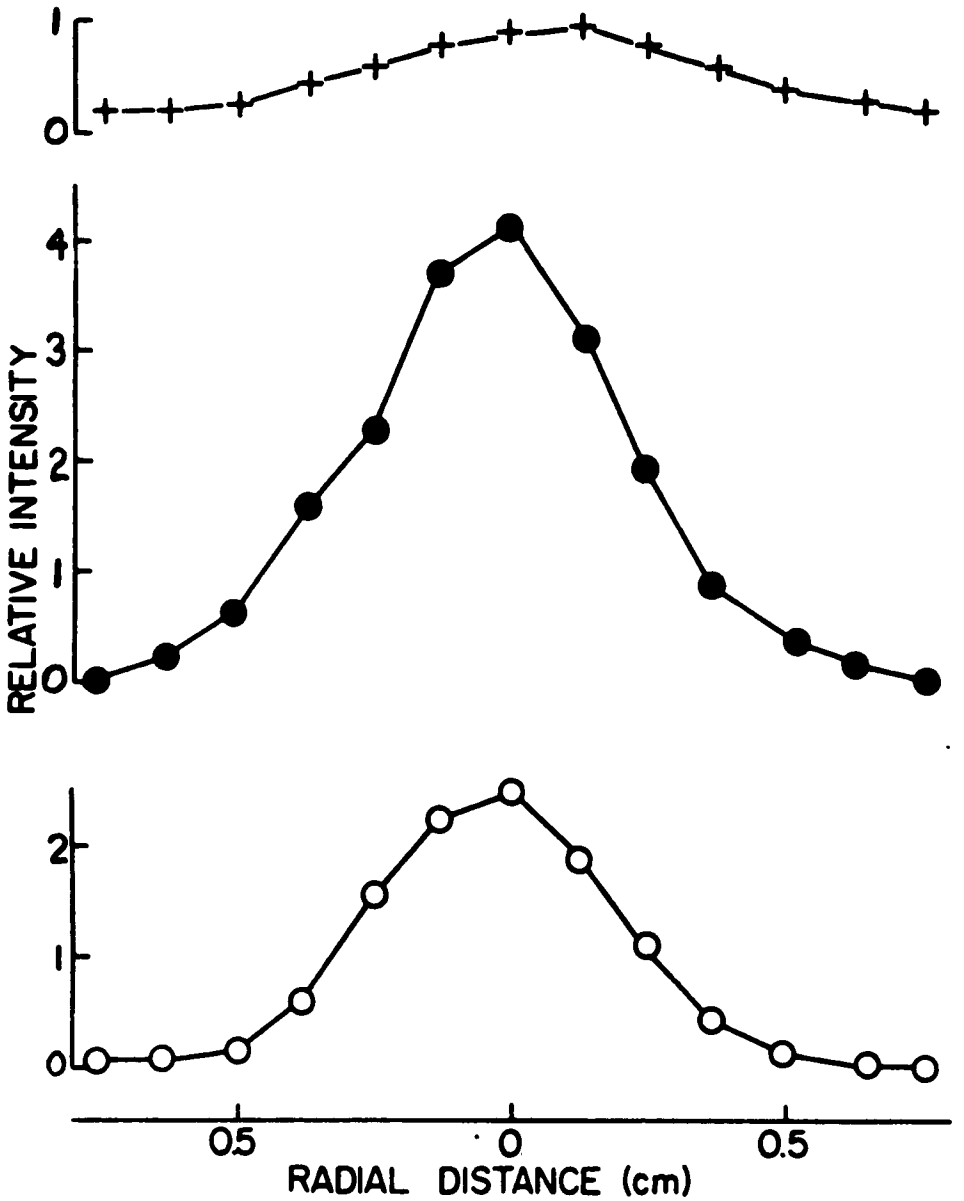

Figure 3.5. Lateral profiles for atomic fluorescence of iron (382.0 nm, 100 ppm Fe); 0, 4.5 cm above the load coil; •, 6.5 cm above the load coil; +, 8.5 cm above the load coil. Intensity measurements are ± 5%

The behavior of the fluorescence signal at low concentrations of Fe was investigated at the optimum observation region determined above. This is shown in Figure 3.6 together with the atomic emission signal from the same 382.0 nm line. The limit of detection (LOD) at the point where S/N = 3 was found to be 30 $ngmL^{-1}$. This is comparable to values obtained for Fe in flames (46) using roughly the same average power. The LOD here is more promising than that obtained using cw lasers to excite ICP-AFS (99), taking into account that the laser power used here is more than a factor of 100 lower.

Conclusions

From these studies, several criteria for using the ICP as an atom source for LEAFS can be enumerated:

1) The choice of neutral atomic lines or ionic lines for LEAFS depends on the particular local ionic equilibria. It is obvious that the conventional torch design and viewing region which are maximized for atomic and ionic emission are not best for LEAFS. More extensive studies into torch designs must be pursued before the ultimate potential of the ICP as an atom source for LEAFS is realized.

2) It is clear that LEAFS can compete with AES only for atomic transitions towards the UV region of the spectrum. There, thermal and other excitation mechanisms in AES become

Figure 3.6. Analytical calibration curve for atomic fluorescence, ●, and atomic emission, O, of iron with the ICP-pulsed dye laser system at an observation height of 6.5 cm above the load coil. The three sigma limit of detection for the LEAFS determination of iron is 30 ppb Fe

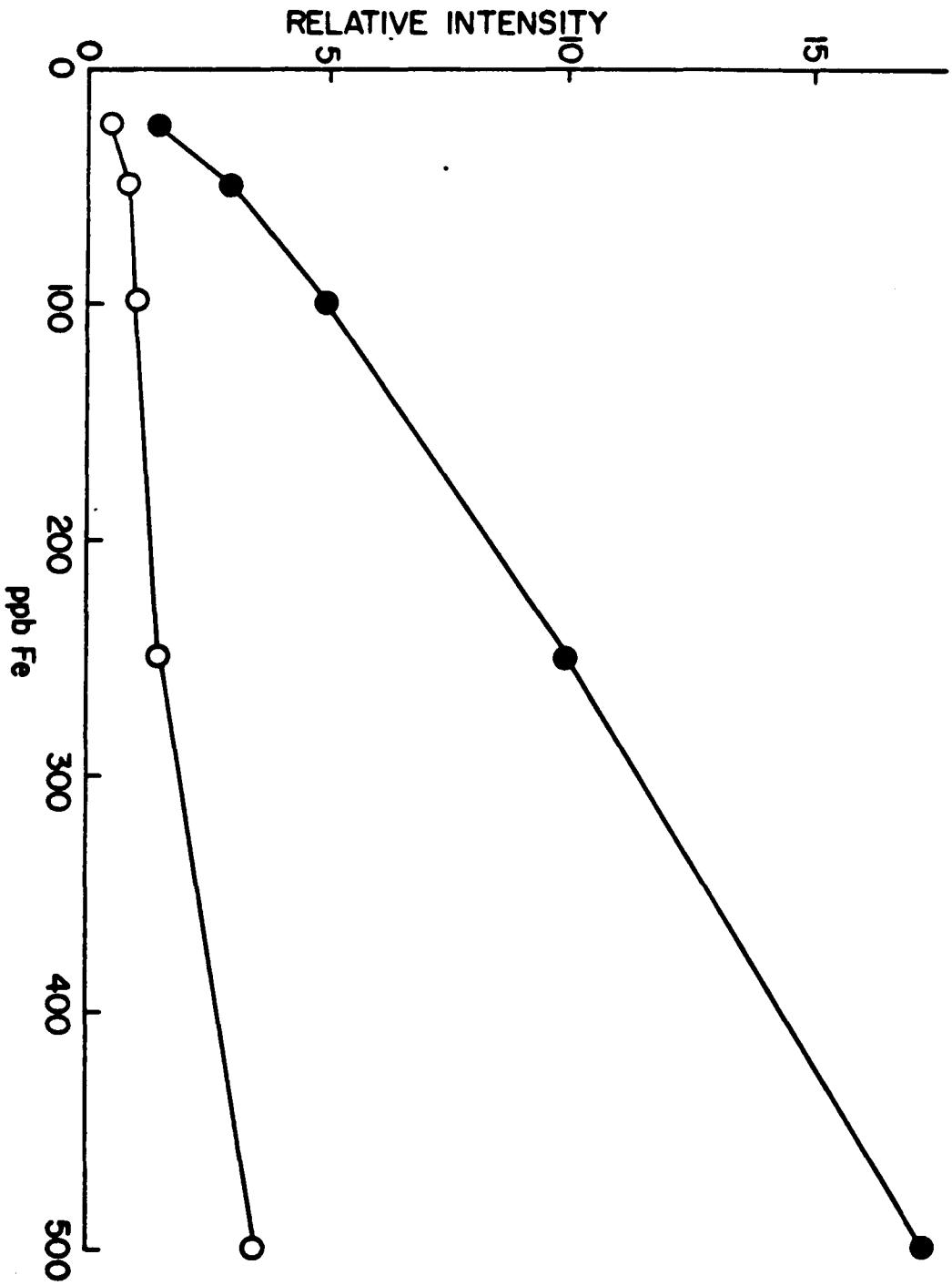
RELATIVE INTENSITY
0
5
10
15
0
100
200
300
400
500
ppb Fe

less efficient according to the factor $e^{-\Delta E/kT}$, where T is the temperature (electronic or translational), k is the Boltzman constant and ΔE is the energy of the excited state. This competition between AES and LEAFS is more important in the ICP compared to flames, because of the generally higher temperature of the former.

3) Lasers matching atomic transitions, particularly in the UV, with high average powers are needed. The LOD in this work is determined by fluctuations in the background. Therefore, the signal-to-noise ratio can be improved with higher excitation power. Frequency-doubled output from commercial ring dye lasers has been achieved in the 50 mW range, and may provide some improvement in LOD's.

The aforementioned technical problems must be solved before one can benefit from the real advantages of the ICP as an atom source for AFS, e.g., the freedom from interferences from a wide range of sample compositions. Meanwhile, LEAFS is a convenient tool for probing local atomic and ionic concentrations for plasma diagnosis, particularly when using low analyte concentrations to avoid disturbing the local equilibria.

CHAPTER IV. OFF-RESONANT LASER EXCITATION OF ATOMIC FLUORESCENCE

Introduction

During experiments conducted to investigate the analytical application of the two-photon excitation (105) and the thermally assisted fluorescence (106) processes of sodium in an intracavity hydrogen-oxygen flame, we made some very interesting observations. While the laser was operating in the red-orange region of the spectrum (ca. 610 nm), what appeared to be the yellow D lines of sodium (589.0 and 589.6 nm) were visually observed from the region where the laser beam passed through the flame. The following study was designed to investigate these observations and to demonstrate the application of off-resonant LEAFS.

Wavelength Dependence

Experimental

A schematic of the experimental arrangement for this work is shown in Figure 4.1. The individual components and the most important experimental conditions are listed in Table 4.1. The entire experiment was placed under the control of a PDP-11 computer. The dye laser was modified to allow the flame to be placed inside the laser cavity. The normal output coupler was replaced with a total reflector

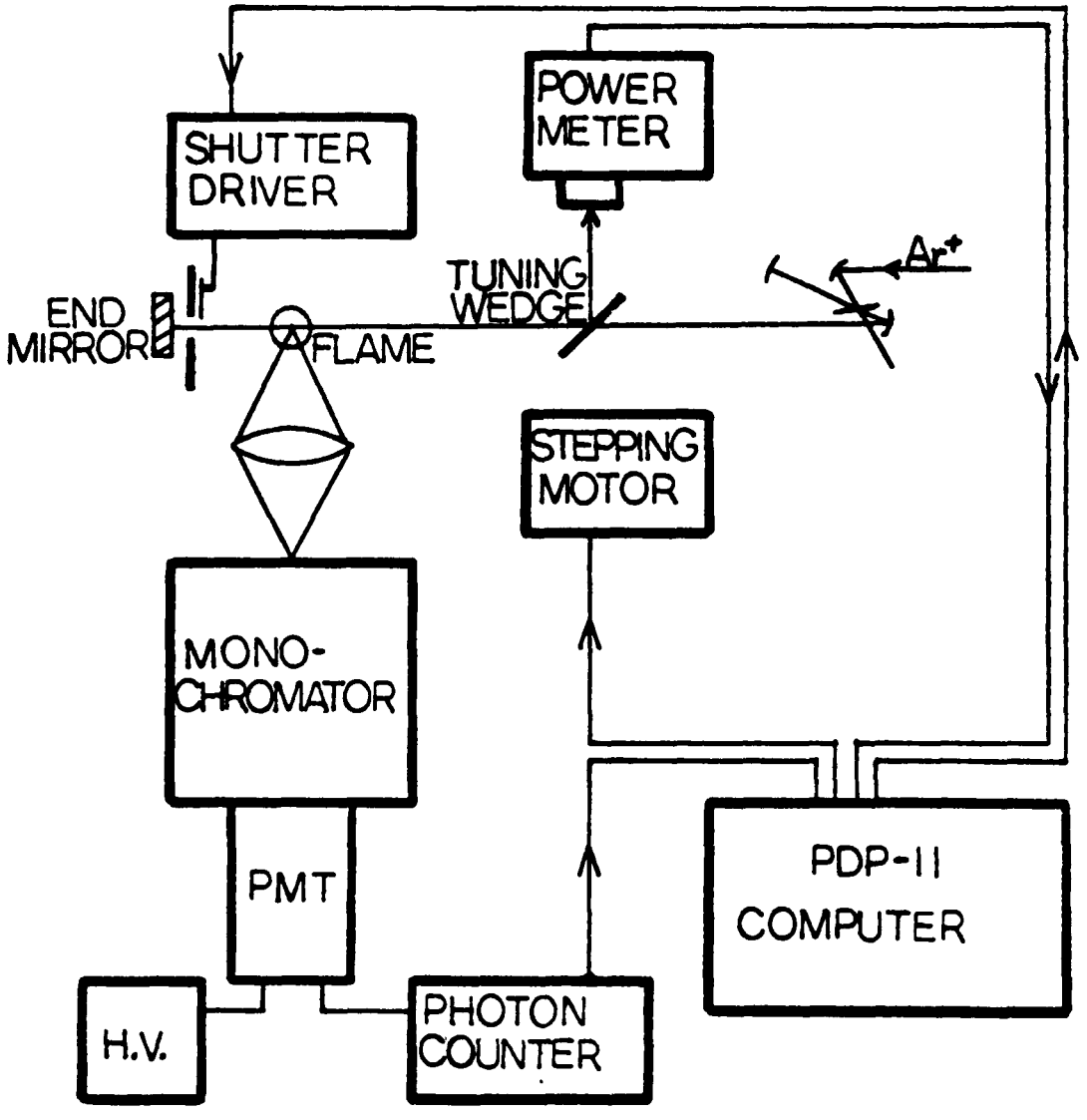

Figure 4.1. Block diagram of modified dye laser fluorescence spectrometer used for intra-cavity off-resonant excitation of sodium

Table 4.1. Components for intra-cavity off-resonant laser excitation of sodium fluorescence

Item	Manufacturer
Ar Ion Laser (5 W, all line)	Model 553 Control Laser Corp. Orlando, FL
CW Dye Laser	Model 375 Spectra-Physics Inc. Mountain View, CA
Shutter	Model UniBlitz 23X Vincent Associates Inc. Rochester, NY
Shutter Driver	Model UniBlitz 100-2 Vincent Associates Inc. Rochester, NY
Monochromator (250 mm, f/10, 1.5 nm/mm)	Double Grating Monochromator No. 33-86-66 Bausch and Lomb Rochester, NY
Photomultiplier Tube	56TVP Amperex Electronic Corp. Slatersville, RI
Photon Counting System	Current Pre-Amp: Model 9301 Ortec Inc. Oakridge, TN Scaler Timer: Model 5201L Hewlett Packard Co. Corvallis, OR
Computer	PDP-11 with RT-11 Operating System and LPS-11 Lab Peripheral System Digital Equipment Corp. Maynard, MA
Collection Lens	67 mm diameter, 76 mm focal length achromatic fused silica lens

Table 4.1. (Continued)

Item	Manufacturer
Stepping Motor	Model HS-50 Superior Electronics Co. Bristol, CT
Power Monitor	Model 2800 Digital Voltmeter Keithley Instruments Inc. Cleveland, OH and Thermopile from Model 210 Powermeter, Coherent Radiation Palo Alto, CA
Burner	Model 4020 Total Consumption Burner Beckman Instruments Fullerton, CA
Photomultiplier Power Supply (set at -2000 V)	Model 242 Keithley Instruments Inc. Cleveland, OH

to increase the intra-cavity power. Computer controlled scanning of the dye laser was accomplished by coupling the tuning wedge to the stepping motor with a screw drive. Data were taken at every half revolution (100 steps) of the stepping motor, corresponding to wavelength steps of ca. 1.0 nm. The bandwidth of the laser, defined by the tuning wedge, is estimated to be 0.3 nm. The excitation wavelength of the system was calibrated by determining the wavelength of

the laser (obtained at the Rayleigh scatter wavelength) at each stepper motor position. These values were stored in a computer file and used later in the data interpretation routines (see Appendix A).

Both the red and blue wings of each of the Na D lines were studied. Ten second integrations were obtained both with the dye laser beam passing through the flame and with it blocked by the computer controlled optical shutter. The net signal was thus obtained and normalized with respect to the dye laser power measured relative to the constant fraction which was reflected out of the cavity by the surface of the tuning wedge.

The laser excited fluorescence signal from the sodium flame was focused by the collection lens onto the slits of the double grating monochromator having a bandpass of 0.2 nm. The signal was converted to electronic form by the high gain photomultiplier tube and the resulting signal was digitized by the photon counting system. This allowed the experiment to be monitored in real time. At the same time, the data were transferred to the computer for data processing and storage.

The atomization cell, shown in Figure 4.2, was constructed out of brass and utilized a conventional Beckman total consumption burner to allow mixing of the flame gases with the pneumatically aspirated sample. The lens system,

Figure 4.2. Cut away view of separated flame used to generate sodium vapor. Excitation zone was 1.6 cm above the chimney

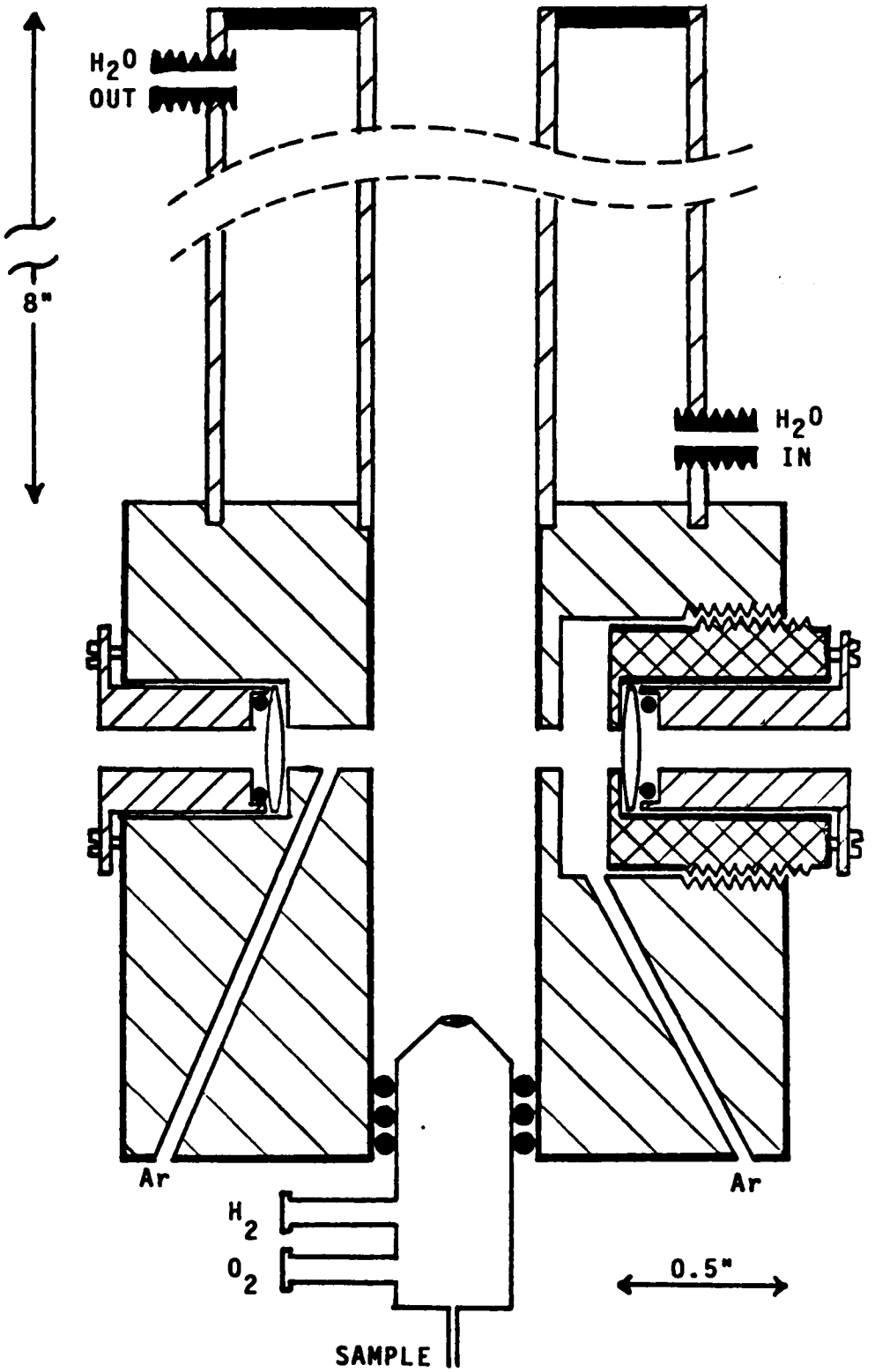
H_2O
OUT
8"
H_2O
IN
Ar
Ar
H_2
O_2
0.5"
SAMPLE

although not employed in these experiments, was designed to increase the power density by allowing the intracavity laser beam to be focused and recollimated. A cooling water flow of 0.75 $Lmin^{-1}$ allowed the flame cell to be operated for hours without any damage. For this work, the region of observation was 16 mm above the top of the 8 inch chimney. This flame reservoir was used because of its ability to produce Na atoms in an environment which was relatively low in flame background and atomic emission. In this configuration, the flame cell could be compared to the separated flame of Hingle et al. (107). Attempts to study the off-resonant excitation of Na in the unseparated flame of the Beckman burner were prohibited by the high levels of atomic emission and by the laser quenching caused by unevaporated solvent particles interrupting the beam.

The spectra of the red and blue wings of the Na D lines were obtained using 1 x 10^{-3} M solutions of rhodamine 6G and rhodamine 110 dyes from Exciton Chemical Co., Dayton, OH. A 10 ppm Na solution was aspirated at a rate of 3 mL min^{-1} into the Beckman total consumption burner. The O_2 and H_2 flow rates were set to 5.8 and 7.9 $Lmin^{-1}$, respectively. An Ar flow of ca. 0.5 $Lmin^{-1}$ was passed over the focusing lenses in the base of the brass cell to protect them from the hot flame gases.

The flame was placed inside the laser cavity to take advantage of the higher energy density and increased effective absorption pathlength through the sample. Experiments conducted with the atom cell placed outside the laser cavity confirmed that the observed signal was not peculiar to the particular experimental configuration used.

Results and discussion

The dependence of the off-resonant laser-excited signal on intracavity laser power at a fixed wavelength of 603.2 nm is shown in Figure 4.3. The intracavity dye laser power was decreased by lowering the pump power from the argon ion laser. The linear dependence obtained is of significance when one tests such theories as the "three-photon" scattering explanation given by Carlsten et al. (108). Their studies were conducted on a mixture of Sr vapor and argon buffer gas in a 500°C oven using a nitrogen pumped pulsed dye laser tuned near the 460.73 nm resonance line of Sr as the excitation source. They detected not only atomic fluorescence at line center, ω_0, but also a third photon at ω_3 corresponding to two photons absorbed at the laser frequency, ω_L (predicting a quadratic dependence on laser power), and the third photon being emitted such that $2\omega_L - \omega_3 = \omega_0$. This process is shown in Figure 4.4(a). Not only did our experiments show a linear dependence on laser power, but the ω_3

Figure 4.3. Dependence of fluorescence signal on intra-cavity power. Laser wavelength is 6032 Å, monochromator wavelength is 5890 Å

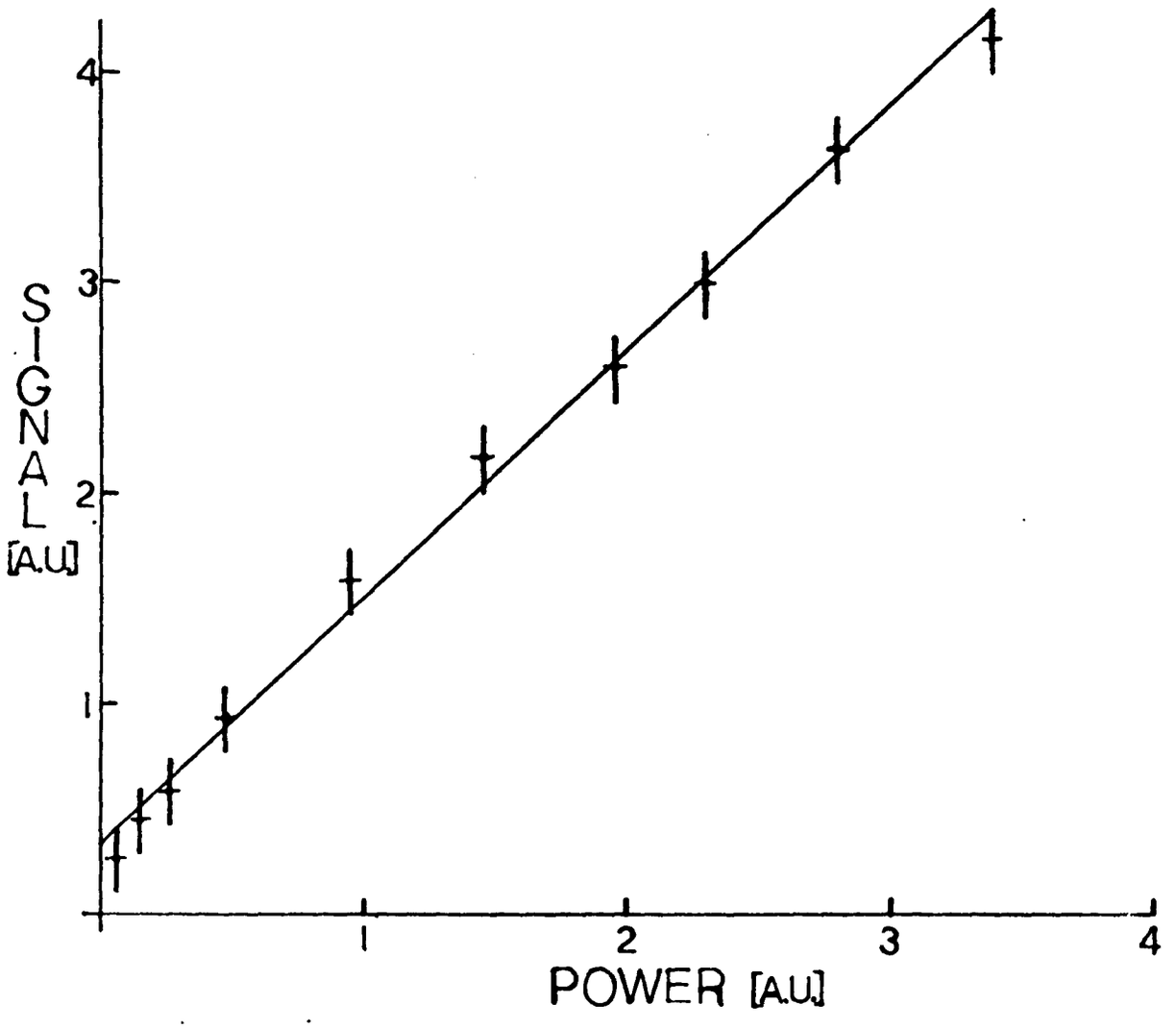
SIGNAL [A.U]
4
3
2
1
1
2
3
4
POWER [A.U]

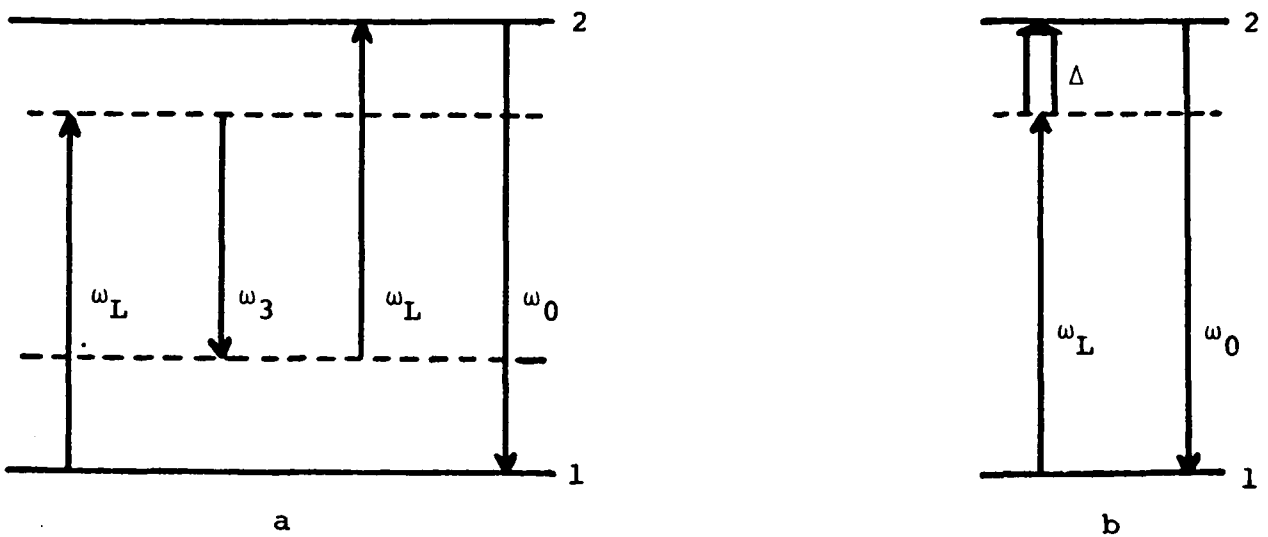

Figure 4.4 Energy level diagrams representing a) the three photon scattering and b) the collision induced fluorescence theories for off-resonant laser excitation of atomic fluorescence. See text for a discussion of the symbols

component (predicted to be equal in intensity to the fluorescent signal) was not detected when the region at $\lambda_3 = (\frac{2}{603.2} - \frac{1}{589.0})^{-1} = 618.1$ nm was scanned.

Scattering of high intensity light and the effect of collisions have been studied using several theoretical approaches including those by Mollow (109,110) and by Carlsten, Szöke and Raymer (108). No attempt is made here to go into an involved theoretical discussion, but only to glean from the appropriate theories an explanation of our observations and some principles to guide us in the analytical application of this phenomena.

Let us begin by defining the following terms. The detuning, Δ, is defined by $\Delta = \omega_0 - \omega_L$, where ω_0 is the atomic resonance frequency and ω_L is the incident laser frequency as shown in Figure 4.4(b). Let us define the damping rate of the upper state to be given by $\gamma = \gamma_N + \gamma_E + \gamma_I$, where the rate γ_N is due to the natural radiative decay of the excited state (the Einstein A coefficient), while γ_E and γ_I result from elastic and inelastic collisions, respectively. The Rabi frequency on resonance (111) is given by

$$\Omega = \mu E/\hbar \tag{3}$$

where $\mu = e\langle 1|\hat{\varepsilon}_L \cdot \vec{r}|2\rangle$ is the electric dipole matrix element between the two relevant atomic states. It should be noted

that the square of the Rabi frequency is proportional to the laser intensity, $I_L \propto \Omega^2$.

When the laser is tuned far off atomic resonance, $|\Delta| >> \gamma$, the collisionally induced fluorescence can be expressed as

$$I_F = N\left(\frac{\gamma_E}{\gamma_N + \gamma_I}\right) \frac{(\gamma_N/2)\Omega^2}{\Delta^2} , \qquad (4)$$

where N is the number density of analyte atoms. Mihalas (112) has pointed out that there is a frequency beyond which this impact approximation fails.

Theories for the redistribution function outside the impact region have not been conveniently developed. It should be pointed out that the fluorescence component depends heavily on the collision dynamics, for the collisions must supply (or absorb) the energy difference between the laser photon and the fluorescence photon.

When the above theory is modified to account for the effect of high laser intensity when collisions are also present, the integrated collisionally induced fluorescent intensity is then given by

$$I_F = \frac{N(\gamma_N/4)\Omega^2(\Omega' + \Delta)[\eta(\Omega' + \Delta) - \Delta]}{(\Delta^2 + \Omega^2)(\Delta^2 + \eta\,\Omega^2)} \qquad (5)$$

where the parameter η is defined as

$$\eta = \frac{\gamma_N + \gamma_I + \gamma_E}{2(\gamma_N + \gamma_I)} \tag{6}$$

and Ω' is the detuning parameter defined as

$$\Omega' = \Delta + \delta \tag{7}$$

where δ is the Stark shift given by

$$\delta = \Delta\{[1 + (\Omega/\Delta)^2]^{1/2} - 1\} . \tag{8}$$

It should be noted that the fluorescence intensity given in equation (5) is no longer related to laser wavelength by the simple $1/\Delta^2$ relationship given in equation (4). The dependence of I_F on Δ is not easily seen since γ_E (and therefore η) is usually a function of Δ (108).

Figures 4.5 and 4.6 show the experimentally determined dependence of the fluorescent signal on the degree of detuning of the laser from the D_2 (589.0 nm, 16,973 cm^{-1}) and D_1 (589.6 nm, 16,956 cm^{-1}) lines of sodium. These curves represent the 611.8 nm - 639.8 nm region on the red side and the 552.3 nm - 583.8 nm region on the blue side of the Na-doublet. As an indication of the magnitude of the laser induced fluorescence signal, at a laser wavelength of 617.9 nm, the net induced fluorescence signal was 9,750 cps compared to an atomic emission signal of 3,500 cps. Thus, the fluorescence signal is over 2.5 times the emission signal though the laser was over 380 Å away from resonance.

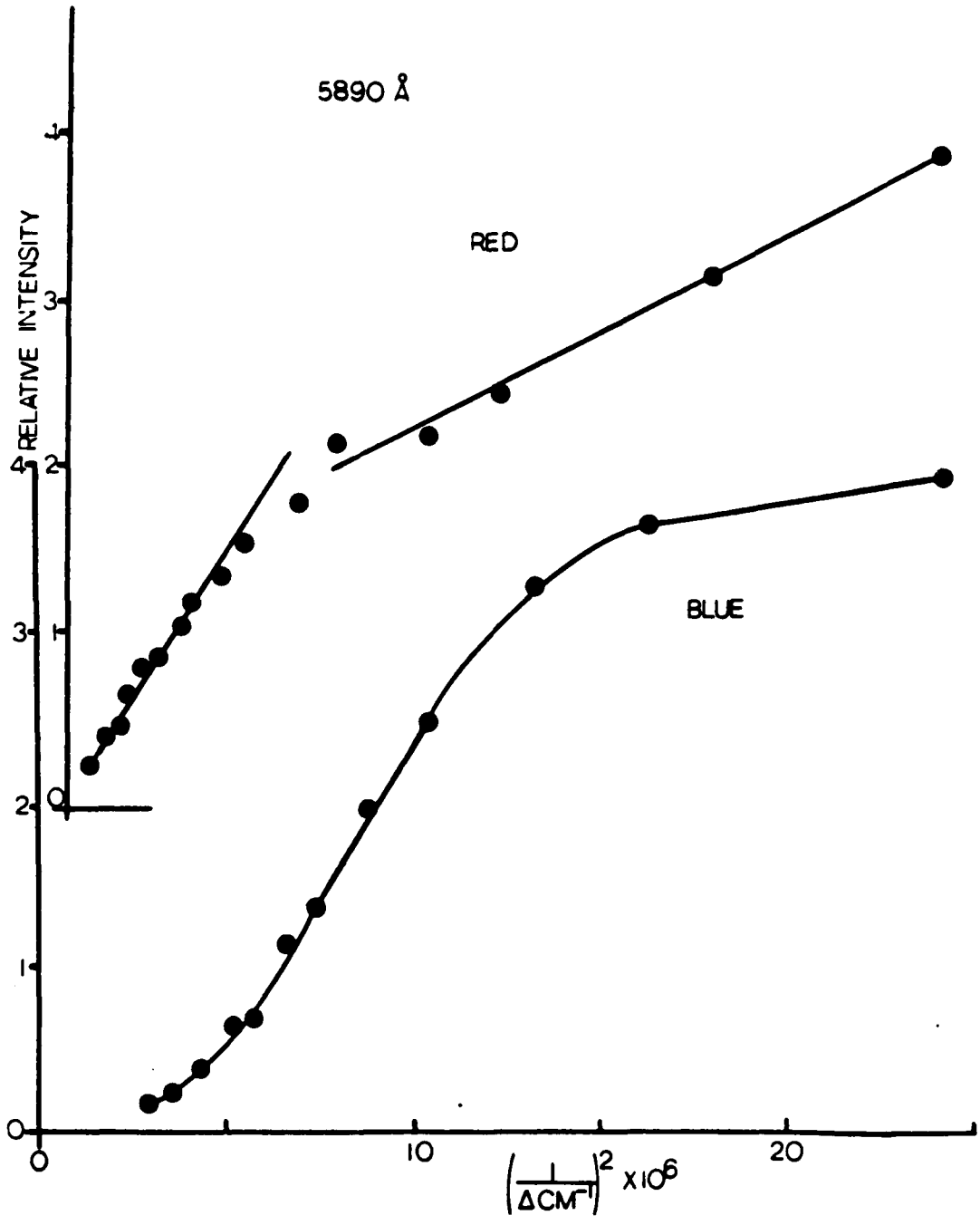

Figure 4.5. Fluorescence intensity of the red and blue wings of the 5890 Å line of sodium (10 ppm Na) plotted against the squared reciprocal of the laser detuning from line center. Intensity measurements are ± 3%

Figure 4.6. Fluorescence intensity of the red and blue wings of the 5896 Å line of sodium (10 ppm Na) plotted against the squared reciprocal of the laser detuning from line center. Intensity measurements are ±3%

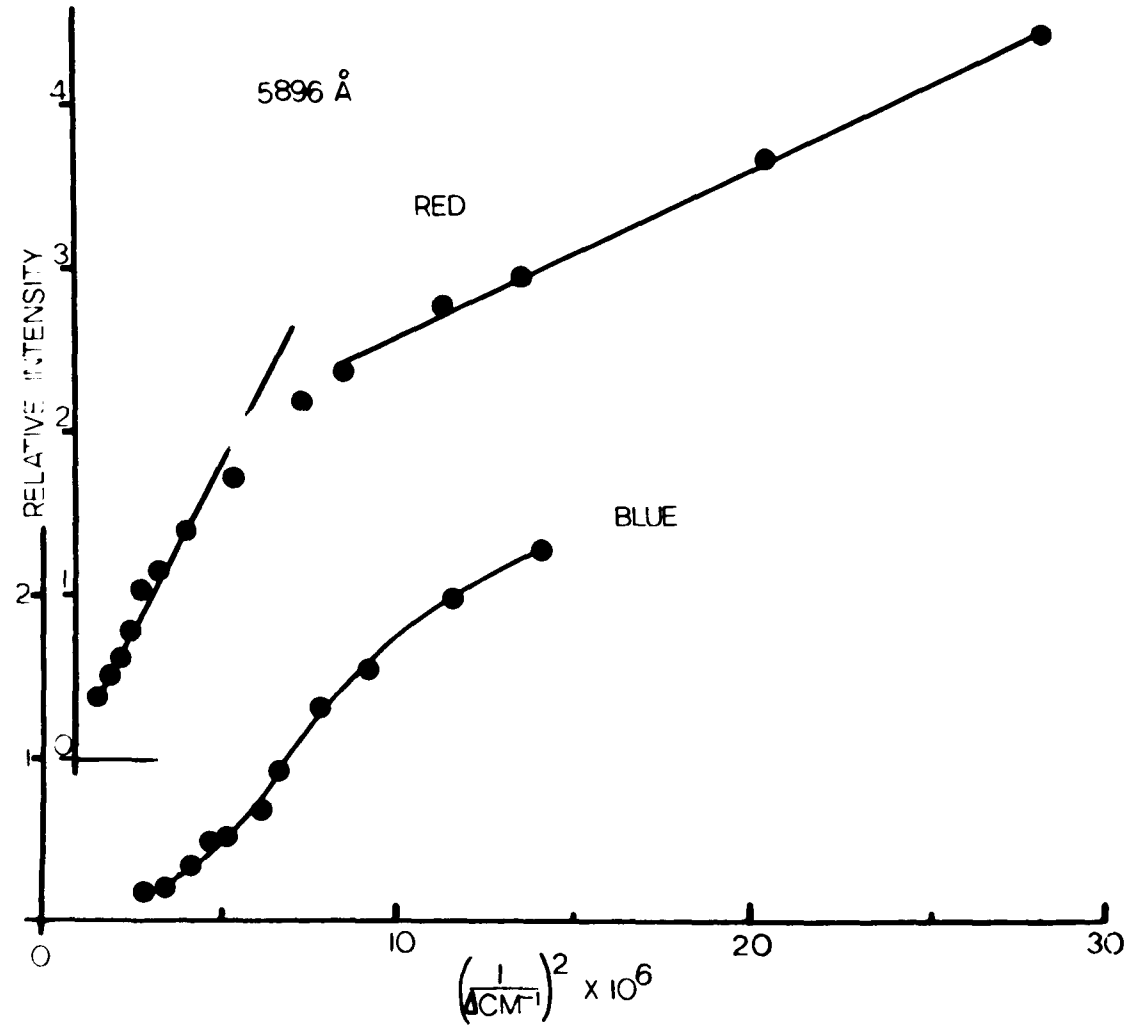
5896 Å
RED
BLUE
RELATIVE INTENSITY
4
3
2
1
0
2
1
0
10
20
30
$\left(\frac{1}{\lambda CM^{-1}}\right)^2 \times 10^6$

All signals went to zero when deionized water was aspirated instead of the 10 ppm Na solution.

The analytical implications of these findings is that atomic fluorescence analysis can be done with lasers that are not exactly in atomic resonance. Also, this off-resonant collisionally induced signal represents a new kind of spectral interference in atomic fluorescence that cannot be eliminated even with wavelength modulation.

Application of Off-Resonant Excitation

Experimental

The following experiment was conducted to demonstrate the practicality of using off-resonant lasers to excite the fluorescence of atomic species in an analytical flame. A commercial atomic absorption spectrometer (Model 1200, Varian Associates, Palo Alto, CA) with a Ni hollow cathode lamp was used to profile the Ni ground state population in the air-acetylene flame of a 13 hole pre-mixed Denton burner (90). A maximum absorbance at the 336.9 nm line of 0.025 was found at a height of 16 mm above the burner head when a 100 ppm Ni solution was aspirated into the flame by the ultrasonic nebulizer.

The 337.1 nm output of a nitrogen laser (113) was then used to excite this 336.9 nm (0 - 29,669 cm^{-1}) absorption line of Ni. The resulting Stokes direct-line fluorescence

at 347.2 nm (880 - 29,669 cm^{-1}) was monitored through the double grating monochromator (2.0 nm bandpass). A schematic of the experimental arrangement is given in Figure 4.7. The individual components and the most important conditions are given in Table 4.2.

The detection system is similar to that used in Chapter III. The nitrogen laser was triggered at 30 Hz by the sync output pulse (0 to +5 V) from the trigger generator. The variable delay pulse (0 to +3 V) of the trigger generator was used to open the gate 0.9 μsec after the sync output pulse to allow the ca. 20 nsec nitrogen laser pulse to be centered in the 0.25 μsec window of the gate. The signal was gated from the photomultiplier tube to the picoammeter which was modified (as in Chapter III) to serve as an integrator and amplifier. A strip chart recorder was connected to the amplifier output to give a permanent record of the experiment.

Results and discussion

According to the atomic absorption studies performed at the 336.9 nm line with this flame-nebulizer system, a 10 ppm Ni solution would have an absorbance of only 0.0025 at line center, a value that is below the sensitivity value (0.0044 absorbance) quoted (33) for AAS determinations.

Figure 4.7. Block diagram of the nitrogen laser based spectrometer for off-resonant excitation of nickel atomic fluorescence

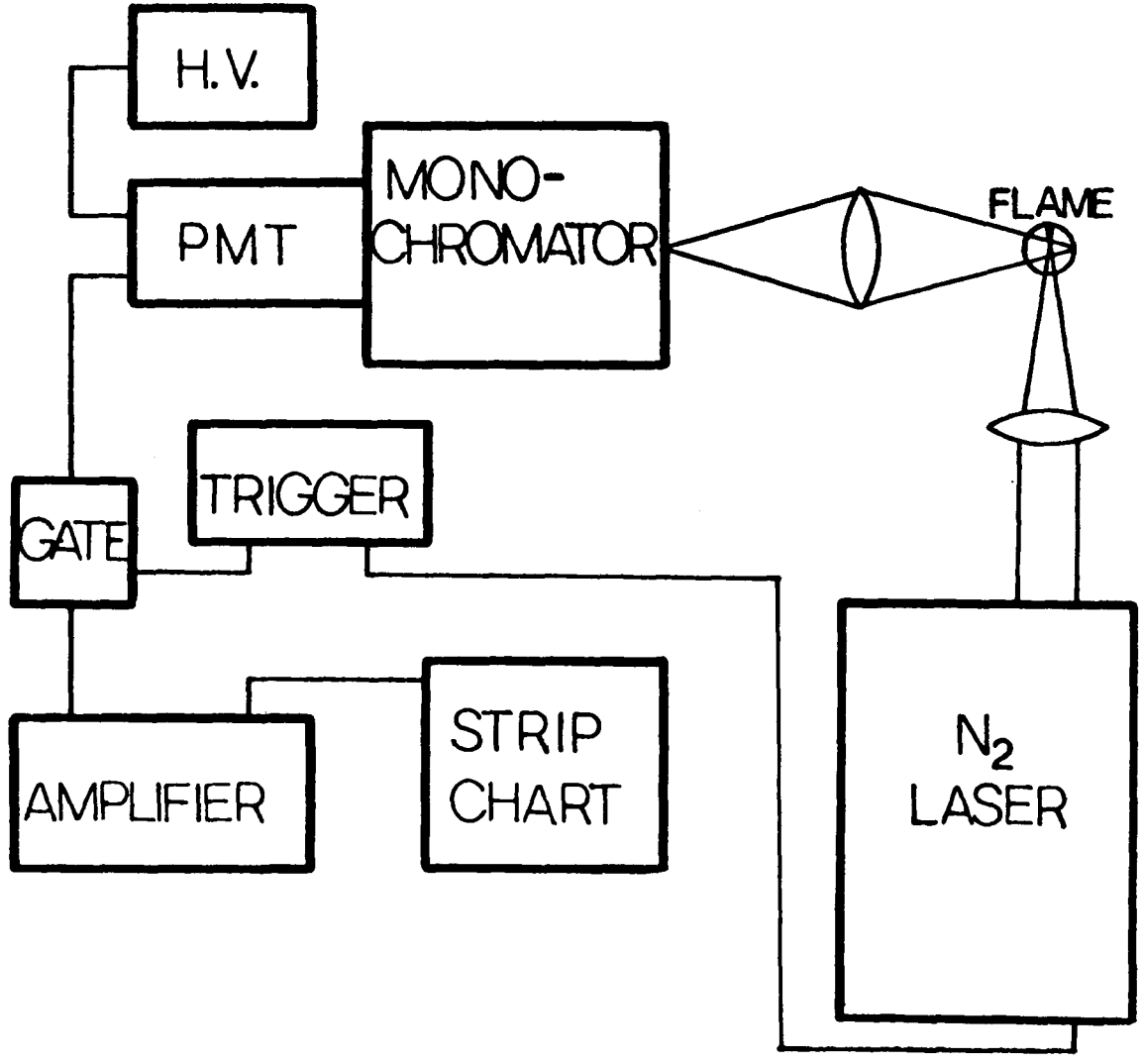
H.V.
PMT
MONO-
CHROMATOR
FLAME
TRIGGER
GATE
AMPLIFIER
STRIP
CHART
N_2
LASER

Table 4.2. Components for off-resonant laser excitation of atomic fluorescence

Item	Manufacturer
Nitrogen Laser (25 mW, 20 nsec)	Molectron Corp. Model UV 12 or 14 Sunnyvale, CA
Trigger (30 Hz)	Wavetek Model 162 San Diego, CA
Gate	Laboratory constructed (103)
Amplifier	Keithley Instruments Inc. Model 417 Picoammeter Cleveland, OH
Photomultiplier Tube	Amperex Electronic Corp. 56 DVP Slatersville, RI
Photomultiplier Power Supply (-2000 V)	Hammer Electronics Co. Inc. Model NV-13-P Princeton, NJ
Monochromator (250 mm, f/10, 1.5 nm/mm)	Bausch & Lomb Inc. Double Gating Monochromator No. 33-86-66 Rochester, NY
Lens (source)	50 mm diameter, 500 mm focal length biconvex quartz
Lens (detector)	67 mm diameter, 76 mm focal length achromatic quartz
Recorder (1"/min)	Houston Instruments Model 5120-2 Bellaire, TX
Burner (air-acetylene)	13 hole Denton burner (90) Laboratory constructed
Ultrasonic Nebulizer (50 Watt forward power)	Plasma Therm, Inc. Model UNS-1 Kresson, NJ

When the 337.1 nm output of the commercial nitrogen laser was focused onto the flame, the off-resonant excited fluorescence signals shown in Figure 4.8 were obtained from 10 ppm Ni and blank solutions.

The noise in this experiment could be reduced by designing a detection system that would compensate for pulse to pulse variations in laser power and be less susceptible to the electromagnetic interference (EMI) from the laser.

It was the purpose of this study to demonstrate that a laser can be used to excite the fluorescence of atomic species in an analytical flame by absorption into the collisionally broadened wings of the atomic transition.

The recently developed excimer lasers (114,115) with their high power and short wavelengths (see Appendix B) hold much promise as radiation sources for this mode of laser excited atomic fluorescence analysis. Indeed, it should be possible to do simultaneous multielement atomic fluorescence using one such intense excitation source.

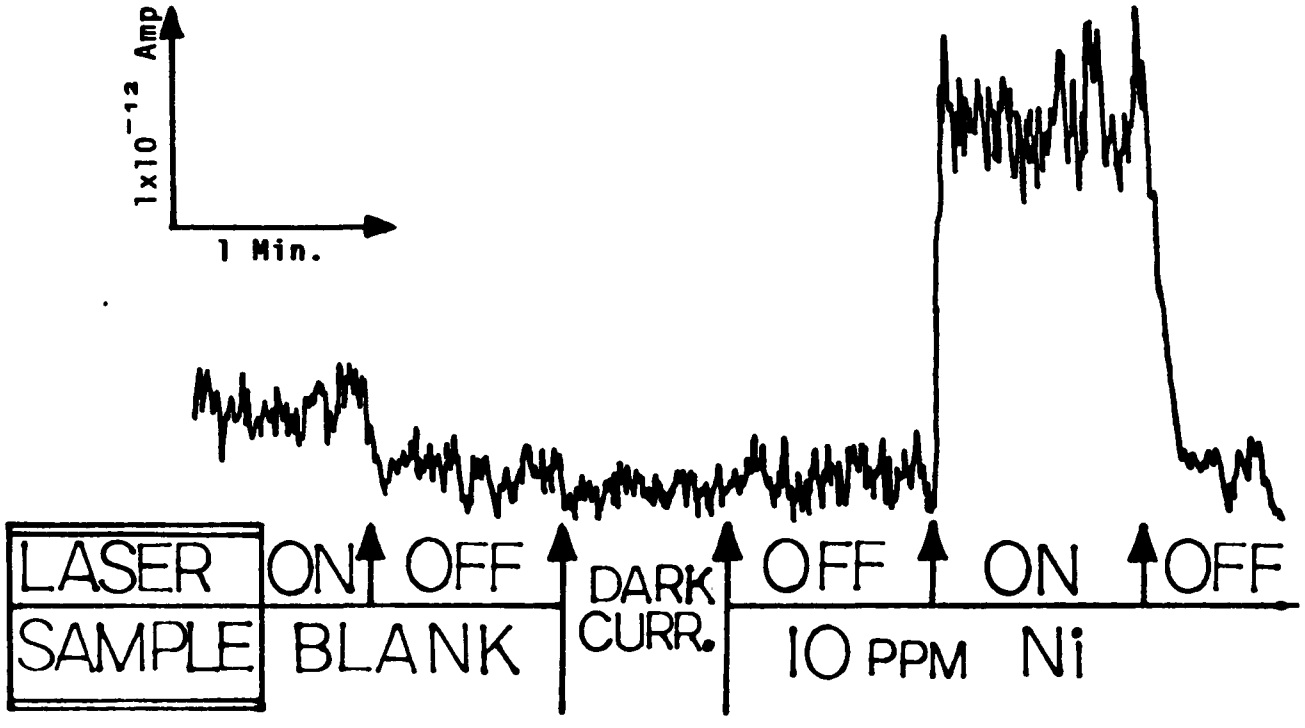

Figure 4.8. Strip chart recording of nickel atomic fluorescence (347.2 nm) by off-resonant nitrogen laser excitation (337.1 nm, 25 mW). A 6×10^{10} Amp bucking current was used to suppress the PMT dark current

REFERENCES

1. Mitchell, A. C. C.; Zemansky, M. W. "Resonance Radiation and Excited Atoms"; University Press: Cambridge, 1961.

2. Pringsheim, P. "Fluorescence and Phosphorescence"; Interscience: New York, 1949.

3. Nichols, E. L.; Howes, H. L. Phys. Rev. 1924, 23, 472.

4. Boers, A. L.; Alkemade, C. T. J.; Smit, J. A. Physica 1956, 22, 358.

5. Alkemade, C. T. J. "Excitation and Related Phenomena in Flames"; Proceedings of the 10th Colloquium Spectroscopicum Internationale, Spartan Books: Washington, D.C., 1963, p. 143.

6. Winefordner, J. D.; Vickers, T. J. Anal. Chem. 1964, 36, 161.

7. Sychra, V.; Svoboda, V.; Rubeska, I. "Atomic Fluorescence Spectroscopy"; Van Nostrand Reinhold Co.: New York, 1975.

8. Winefordner, J. D.; Schulman, S. G.; O'Haver, T. C. "Luminescence Spectrometry in Analytical Chemistry"; Wiley Interscience: New York, 1972; Vol. 38.

9. Omenetto, N.; Benetti, F.; Hart, L. P.; Winefordner, J. D.; Alkemade, C. T. J. Spect. Acta 1973, 28B, 289.

10. "New Applications of Lasers to Chemistry"; Hieftje, G. M., Ed.; American Chemical Society Symposium Series No. 52, American Chemical Society: Washington, D.C., 1978.

11. Alkemade, C. T. J. Pure Appl. Chem. 1970, 23, 73.

12. Boutilier, G. D.; Blackburn, M. B.; Mermet, J. M.; Weeks, S. J.; Haragushi, H.; Winefordner, J. D.; Omenetto, N. Appl. Opt. 1978, 17, 2291.

13. Daily, J. W. Appl. Opt. 1976, 15, 955.

14. Hooymayers, H. P. Spect. Acta 1968, 23B, 567.

15. Jansen, B. J.; Hollander, T. Spect. Acta 1977, 32B, 165.

16. Measures, R. M. J. Appl. Phys. 1968, 39, 5232.

17. Olivares, D. R.; Hieftje, G. M. Spect. Acta 1978, 33B, 79.

18. "Analytical Laser Spectroscopy"; Omenetto, N., Ed.; J. Wiley & Sons Ltd.: New York, 1979.

19. Omenetto, N.; Hart, L. P.; Benetti, P.; Winefordner, J. D. Spect. Acta 1973, 28B, 301.

20. Omenetto, N.; Omenetto, P.; Hart, L. P.; Winefordner, J. D.; Alkemade, C. T. J. Spect. Acta 1973, 28B, 289.

21. Omenetto, N.; Winefordner, J. D.; Alkemade, C. T. J. Spect. Acta 1975, 30B, 335.

22. Svoboda, V.; Browner, R. F.; Winefordner, J. D. Appl. Spect. 1972, 26, 505.

23. Winefordner, J. D. J. Chem. Ed. 1978, 55, 72.

24. Winefordner, J. D.; Parsons, M. L.; Mansfield, J. M.; McCarthy, W. J. Spect. Acta 1967, 23B, 37.

25. Winefordner, J. D.; Svoboda, V.; Cline, L. J. CRC Critical Reviews in Analytical Chemistry 1970, 1, 233.

26. Winefordner, J. D.; Parsons, M. L.; Mansfield, J. M.; McCarthy, W. J. Anal. Chem. 1967, 39, 436.

27. Coleman, R. F. Anal. Chem. 1974, 46, 989A.

28. Barnett, W. B.; Kahn, H. L. Anal. Chem. 1972, 44, 935.

29. Dagnall, R. M.; West, T. S.; Young, P. Talanta 1966, 13, 803.

30. Alkemade, C. T. J. Proc. Soc. Anal. Chem. 1973, 10, 130-143.

31. Green, J. H. S. Proc. Soc. Anal. Chem. 1974, 11, 49.

32. McHard, J. A.; Foulk, S. J.; Nikdel, S.; Ullman, A. H.; Pollard, B. D.; Winefordner, J. D. Anal. Chem. 1979, 51, 1613.

33. Kirkbright, C. F.; Sargent, M. "Atomic Absorption and Fluorescence Spectroscopy"; Academic Press: New York, 1974.

34. Johnson, D. J.; Fowler, W. K.; Winefordner, J. D. Talanta 1977, 24, 227.

35. Johnson, D. J.; Palankey, F. W.; Winefordner, J. D. Anal. Chem. 1974, 46, 1898.

36. Fowler, W. K.; Knapp, D. O.; Winefordner, J. D. Anal. Chem. 1974, 46, 601.

37. Gustausson, A.; Ingman, F. Spect. Acta 1979, 34B, 31.

38. Cresser, M. S.; West, T. S. Spect. Acta 1970, 25B, 61.

39. Veillon, C.; Mansfield, J. M.; Parsons, M. L.; Winefordner, J. D. Anal. Chem. 1966, 38, 204.

40. Ellis, D. W.; Demers, D. R. Anal. Chem. 1966, 38, 1943.

41. Bratzel, M. P.; Dagnall, R. M.; Winefordner, J. D. Anal. Chim. Acta 1970, 52, 157.

42. Sorokin, P. P.; Lonkard, J. R. IBM J. Res. Dev. 1966, 10, 162.

43. Fraser, L. M.; Winefordner, J. D. Anal. Chem. 1971, 43, 1693.

44. Kuhl, J.; Marowsky, G. Opt. Comm. 1971, 4, 125.

45. Denton, M. B.; Malmstadt, H. V. Appl. Phys. Lett. 1971, 18, 485.

46. Weeks, S. J.; Haraguchi, I.; Winefordner, J. D. Anal. Chem. 1978, 50, 360.

47. Piepmeier, E. H. Spect. Acta 1972, 27B, 431.

48. Goff, D. A.; Yeung, E. S. Anal. Chem. 1978, 50, 625.

49. Rayleigh, Lord Phil. Mag. 1881, 12, 81.

50. Mie, G. Ann. d. Physik 1908, 25, 377.

51. Plass, G. N. Appl. Optics 1964, 3, 867.

52. Born, M.; Wolf, E. "Principles of Optics"; Pergamon: New York, 1975.

53. Kerker, M. "The Scattering of Light and Other Electromagnetic Radiation"; Academic Press: New York, 1969.

54. Hieftje, G. M.; Malmstadt, H. V. Anal. Chem. 1968, 40, 1860.

55. Smith, R.; Elser, R. C.; Winefordner, J. D. Anal. Chim. Acta 1969, 48, 35.

56. Warr, P. D. Talanta 1971, 18, 234.

57. Doolan, K. J.; Smythe, L. E. Spect. Acta 1979, 34B, 187.

58. Larkins, P. L.; Willis, J. B. Spect. Acta 1974, 29B, 319.

59. Dinnin, J. I. Anal. Chem. 1967, 39, 1491; 1968, 40, 1825.

60. Zacha, K. E.; Bratzel, M. P.; Winefordner, J. D.; Mansfield, J. M. Anal. Chem. 1968, 40, 1733; 1969, 41, 1315.

61. Omenetto, N.; Hart, L. P.; Winefordner, J. D. Appl. Spect. 1972, 26, 612.

62. Epstein, M. S.; Rains, T. C.; Menis, O. Can. J. Spectrosc. 1975, 20, 22.

63. Haarsma, J. P. S.; Vlogtman, J.; Agterdenbos, J. Spect. Acta 1976, 31B, 129.

64. Bratzel, Jr., M. P.; Dagnall, R. M.; Winefordner, J. D. Anal. Chem. 1969, 41, 713.

65. Winefordner, J. D.; Staab, R. A. Anal. Chem. 1964, 36, 165.

66. Winefordner, J. D.; Staab, R. A. Anal. Chem. 1964, 36, 1367.

67. Mansfield, J. M.; Winefordner, J. D.; Veillon, C. Anal. Chem. 1965, 37, 1049.

68. Armentrout, D. N. Anal. Chem. 1966, 38, 1235.

69. Goodfellow, G. I. Anal. Chim. Acta 1966, 35, 132.

70. Denton, M. B.; Malmstadt, H. V. Anal. Chem. 1972, 44, 1813.

71. Gaydon, A. G.; Wolfhard, H. G. "Flames; Their Structure, Radiation and Temperature"; J. Wiley and Sons: New York.

72. Shull, M.; Winefordner, J. D. Appl. Spectrosc. 1971, 25, 97.

73. Sychra, V.; Matousek, J. Anal. Chim. Acta 1970, 52, 376.

74. Larkins, P. L. Spectrochim. Acta 1971, 26B, 477.

75. Rains, T. C.; Epstein, M. S.; Menis, O. Anal. Chem. 1974, 46, 207.

76. Chester, T. L.; Winefordner, J. D. Spect. Acta 1976, 31B, 21.

77. Doolan, K. J.; Smythe, L. E. Spect. Acta 1977, 32B, 115.

78. Koizumi, H.; Yasuda, K. Spect. Acta 1976, 31B, 237.

79. Fernandez, F. J.; Myers, S. A.; Slavin, W. Anal. Chem. 1980, 52, 741.

80. Koizumi, H.; Yasuda, K. Spect. Acta 1976, 31B, 523.

81. de Loos-Vollebregt, M. T. C.; de Galan, L. Spect. Acta 1978, 33B, 495.

82. Koizumi, H.; Yasuda, K. Anal. Chem. 1978, 48, 1178.

83. Koizumi, H.; Yasuda, K. Anal. Chem. 1975, 47, 1679.

84. Fairbank, W. M.; Hansch, T. W.; Schawlow, A. L. J. Opt. Soc. Amer. 1975, 65, 199.

85. Telle, J. M.; Tang, C. L. Appl. Phys. Lett. 1974, 24, 85.

86. Telle, J. M.; Tang, C. L. Appl. Phys. Lett. 1975, 26, 572.

87. Blit, S.; Olsson, A.; Tang, C. L. Opt. Lett. 1979, 4, 245.

88. Green, R. B.; Travis, J. G.; Keller, R. A. Anal. Chem. 1976, 48, 1954.

89. Hubbard, D. P.; Michel, R. G. Anal. Chem. 1973, 67, 55.

90. Gutzler, D. E.; Denton, M. B. Anal. Chem. 1975, 47, 830.

91. Belt, Jr., C. B. Anal. Chem. 1967, 39, 676.

92. Reed, T. B. Int. Sci. Technol. 1962, 6, 42.

93. Reed, T. B. Appl. Phys. 1961, 32, 821.

94. Reed, T. B. Appl. Phys. 1961, 31, 2534.

95. Reed, T. B. Appl. Phys. 1963, 34, 2266.

96. Fassel, V. A. Anal. Chem. 1979, 51, 1290A.

97. Eckert, H. V. High Temp. Sci. 1974, 6, 99.

98. Montaser, A.; Fassel, V. A. Anal. Chem. 1976, 48, 1490.

99. Pollard, B. D.; Blackburn, M. B.; Nikdel, S.; Massoumi, A.; Winefordner, J. D. Appl. Spect. 1979, 33, 5.

100. Boutilier, G. D.; Bradshaw, J. D.; Weeks, S. J.; Winefordner, J. D. Appl. Spect. 1977, 31, 307.

101. Omenetto, N. Anal. Chem. 1976, 48, 75A.

102. Kuhl, J.; Spitschan, H. Opt. Comm. 1973, 7, 256.

103. Iles, M. K. Ames Laboratory, Iowa State University, Ames, Iowa, private communication.

104. Kniseley, R. N.; Amenson, A.; Butler, C. C.; Fassel, V. A. Appl. Spect. 1974, 28, 285.

105. Van Dijk, C. A.; Zeegers, P. J. T.; Nienhuis, G.; Alkemade, C. T. J. JQSRT 1978, 20, 55.

106. Omenetto, N.; Rossi, G. Spect. Acta 1969, 24B, 95.

107. Hingle, D. N.; Kirkbright, G. R.; West, T. S. Analyst 1968, 93, 522.

108. Carlsten, J. L.; Szöke, A.; Raymer, M. G. Phys. Rev. A 1977, 15, 1029.

109. Mollow, B. R. Phys. Rev. A 1976, 13, 758.

110. Mollow, B. R. Phys. Rev. A 1970, 2, 76.

111. Huber, D. L. Phys. Rev. 1969, 178, 93.

112. Mihalas, D. "Stellar Atmospheres"; Freeman: San Francisco, CA, 1970.

113. Kasuya, T.; Lide, Jr., D. R. Appl. Optics 1967, 6, 69.

114. Shaw, M. J. Prog. Quant. Electr. 1979, 6, 3.

115. Huestis, D. L. Opt. Spect. 1979, 13, 51.

116. Corliss, C. H.; Bozman, W. R. "Experimental Transition Probabilities for Spectral Lines of Seventy Elements"; National Bureau of Standards Monograph 53, U. S. Government Printing Office: Washington, D.C., 1962.

ACKNOWLEDGEMENTS

I wish to thank my major professor, Dr. Ed Yeung, for the support and guidance he gave me during my graduate career.

I also wish to express my appreciation to all of the professors, staff and fellow students at Iowa State University and Ames Laboratory who contributed to that challenging and very rewarding segment of my life.

Finally, I sincerely thank my parents, my wife, Jocelynn, and my two daughters, Michelle and Jennifer, for the encouragement and love that they showed me during my research and writing.

APPENDIX A. COMPUTER PROGRAMS USED

This Appendix contains listings of the computer programs used to collect and process data from the off-resonant laser excited atomic fluorescence experiments of Chapter 4. The programs are summarized in the following table.

Table A.1. Summary of the computer programs used to collect and process the off-resonant LEAFS data

Program	Function
NRAFS	Master program to control the scanning LEAFS spectrometer, receive and store the raw data
JOG	Subroutine used by NRAFS to step scan the wavelength drive on the dye laser
DATFIN	Puts data into final form for plotting
XYPLOT	Creates an (x,y) file from DATFIN and allows this to be output on an x-y recorder.

```
TT:=NRAFS.FOR
      DIMENSION JSTEP(1001),COUNT(1001),POWER(1001)
      DIMENSION BCOUNT(1001),BPOWER(1001),NORMCT(1001)
      REAL NORMCT
      EXTERNAL IADC
      WRITE (5,150)
150   FORMAT(' FILE# ?. . .11<=IFILE<=99. .CC BACKGROUND = IFILE - 111')
      READ (5,175)IFILE
175   FORMAT (I2)
      JFILE=IFILE-1
      DEFINE FILE IFILE(1,8010,U,NREC)
      DEFINE FILE JFILE(1,8010,U,NREC)
      WRITE (5,325)
325   FORMAT (' INITIAL STEP, #WAVELENGTHS, #STEPS (PER HALF CYCLE)')
      READ (5,350)ISTEP,NWAVE,NSTEP
350   FORMAT (I5,I5,I4)
      WRITE (5,352)
352   FORMAT(' #COUNT CYCLES--FOREGROUND, BACKGROUND')
      READ (5,354)NUMCT,NUMBK
354   FORMAT(I3,I3)
      N=1
      IREVSL=0
360   IF (NWAVE) 365,750,370
365   IDIR= -1
      GO TO 375
370   IDIR= +1
375   NPTS = IDIR*NWAVE
      NJOG=IDIR*NSTEP
      JSTEP(0)=ISTEP-2*NJOG
380   IX=IADC(0)
      IF (IX.LT.3000) GO TO 400
      GO TO 380
```

```
400     DO 500 J=N,N+NPTS-1
        JSTEP(J)=JSTEP(J-1)+(2+IREVSL)*NJOG
        IREVSL=0
        CALL LED(JSTEP(J), 'I6')
        SUMCT=0
        SUMPWR=0
        DO 410 KCT=1,NUMCT
        PWR=FLOAT(IADC(2)-"4000)/2048.
        SUMPWR=SUMPWR+PWR
        CT=FLOAT(IADC(1)-"4000)/2048.
        SUMCT=SUMCT+CT
        IF (NUMCT-KCT.LE.0) GO TO 415
        ICMF=0
        CALL SETR(4,0,200.,ICMF)
        CALL LWAIT(ICMF,0)
405     IX=IADC(0)
        IF (IX.LT.3000) GO TO 410
        GO TO 405
410     CONTINUE
415     CALL REL(1,1)
        CALL JOG(NJOG)
        POWER(J)=SUMPWR/NUMCT
        COUNT(J)=SUMCT/NUMCT
        SUMBCT=0
        SUMBPR=0
        ICMF=0
        CALL SETR(4,0,200.,ICMF)
        CALL LWAIT(ICMF,0)
420     IX=IADC(0)
        IF (IX.LT.3000) GO TO 430
        GO TO 420
430     DO 440 KBK=1,NUMBK
        BPR=FLOAT(IADC(2)-"4000)/2048.
```

```
      SUMBPR=SUMBPR+BPR
      BCT=FLOAT(IADC(1)-'4000)/2048.
      SUMBCT=SUMBCT+BCT
      IF (NUMBK-KBK.LE.0) GO TO 450
      ICMF=0
      CALL SETR(4,0,200.,ICMF)
      CALL LWAIT(ICMF,0)
435   IX=IADC(0)
      IF (IX.LT.3000) GO TO 440
      GO TO 435
440   CONTINUE
450   CALL JOG(NJOG)
      CALL REL(1,0)
      BPOWER(J)=SUMBPR/NUMBK
      BCOUNT(J)=SUMBCT/NUMBK
      IF (POWER(J).NE.BPOWER(J)) GO TO 460
      NORMCT(J)=0.0
      WRITE(5,455)
455   FORMAT(' THE POWER IS NOT BEING MODULATED')
      GO TO 470
460   NORMCT(J)=(COUNT(J)-BCOUNT(J))/(POWER(J)-BPOWER(J))
470   ICMF=0
      CALL SETR(4,0,200.,ICMF)
      CALL LWAIT(ICMF,0)
480   IX=IADC(0)
      IF (IX.LT.3000) GO TO 500
      GO TO 480
500   CONTINUE
      KPOSN=JSTEP(J-1)+2*NJOG
      CALL LED(KPOSN, 'I6')
      WRITE(5,510)
510   FORMAT(' DO YOU WISH TO CONTINUE (0)NO,(1)YES')
      READ (5,520) ICONT
520   FORMAT (I1)
```

```
      IF (ICONT) 750,750,540
540   N=J
      WRITE (5,550)
550   FORMAT (' #WAVELENGTHS?')
      READ (5,560)NWAVE
560   FORMAT(I5)
      IF (NWAVE) 600,750,620
600   IDRFLG=-1
      GO TO 630
620   IDRFLG=1
630   IF (IDIR.EQ.IDRFLG) GO TO 360
      IREVSL=-2
      NRESET=-2*NJOG
      CALL JOG(NRESET)
650   IX=IADC(0)
      IF (IX.LT.3000) GO TO 360
      GO TO 650
      GO TO 360
750   WRITE (5,760)
760   FORMAT(' THE SCAN IS OVER --- FILES ARE BEING CREATED')
      J=J-1
      WRITE(IFILE'1)J,(JSTEP(K),COUNT(K),POWER(K),NORMCT(K),K=1,J)
      WRITE(JFILE'1)J,(JSTEP(K),BCOUNT(K),BPOWER(K),
     1NORMCT(K),K=1,J)
      STOP
      END
*
```

```
TT:=0X1:JOG.FOR
      SUBROUTINE JOG (N)
      EXTERNAL IDOR
      IF(N.GE.0)GO TO 5
      IF(N.LT.0)GO TO 10
5     DO 6 I=1,IABS(N)
      IX=IDOR (0,0,"3,"3)
      IX=IDOR (0,0,"3,"0)
      ICMF=0
      CALL SETR(4,0,1.,ICMF)
6     CALL LWAIT(ICMF,0)
      GO TO 20
10    DO 11 I=1,IABS(N)
      IX=IDOR (0,0,"3,"1)
      IX=IDOR (0,0,"3,"0)
      ICMF=0
      CALL SETR(4,0,1.,ICMF)
11    CALL LWAIT (ICMF,0)
20    RETURN
      END
*
```

```
C I:=DX1:DATA IN.FOR

      REAL NORMCT, NRMCTL
      DIMENSION JSTEP(1001),COUNT(1001),POWER(1001),NORMCT(1001)
      DIMENSION MSTEP(101),ANGS(101),DLCMHI(101),DLCMLO(101)
      DIMENSION LSTEP(601),IANGST(601),DELCM(601),CMSQ(601),NRMCTL(601)
      WRITE(5,50)
50    FORMAT(' THIS PROGRAM TAKES RAW DATA FROM IFILE, WAVELENGTHS
     1 FROM MFILE AND CREATES LFILE CONTAINING:')
      WRITE(5,51)
51    FORMAT(' NL, IANGST(NL), DELCM(NL), CMSQ(NL), NRMCT(NL)')
      WRITE (5,150)
150   FORMAT(' FILE NUMBER?. . . 10<=IFILE<=99')
      READ(5,165) IFILE
      DEFINE FILE IFILE(1,8010,U,NREC)
      READ (IFILE'1) N,(JSTEP(K),COUNT(K),POWER(K),NORMCT(K),K=1,N)
      WRITE (5,155)
155   FORMAT(' WHICH FILE CONTAINS THE WAVELENGTHS??')
      READ (5,165) MFILE
      DEFINE FILE MFILE(1,3508,U,NREC)
      READ (MFILE'1) M,(MSTEP(MK),ANGS(MK),DLCMHI(MK),DLCMLO(MK),MK=1,M)
      WRITE (5,160)
160   FORMAT(' WHAT DO YOU WANT THE FINAL FILE NUMBER TO BE??')
      READ(5,165) LFILE
165   FORMAT (I2)
      NL=1
180   NPTS=NL-1
      WRITE (5,200)N,NPTS
200   FORMAT(' IBEGIN=??(0 EXITS)   IEND=??    N=',I4,'  NPTS=',I4)
      READ(5,210)IBEGIN,IEND
210   FORMAT(I4,I4)
      IF (IBEGIN.EQ.0) GO TO 600
      IFLAG=1
      INDEX=IBEGIN
      IF (IBEGIN.LT.IEND) GO TO 240
```

```
      IFLAG=-1
      ITEMP=IEND
      IEND=IBEGIN
      IBEGIN=ITEMP
240   WRITE(5,250)
250   FORMAT(' WHICH D-LINE??  5890=(0),....,5896=(1)')
      READ(5,165)IDLINE
300   DO 500 J=IBEGIN,IEND
      LSTEP(NL)=JSTEP(INDEX)
      DO 450 MWAV=1,M
      IF (MSTEP(MWAV).EQ.JSTEP(INDEX)) GO TO 475
450   CONTINUE
      IANGST(NL)=5000
470   DELCM(NL)=0.0
      CMSQ(NL)=0.0
      NRMCTL(NL)=0.0
      GO TO 480
475   IANGST(NL)=ANGS(MWAV)
      IF (IANGST(NL).EQ.5000) GO TO 470
      DELCM(NL)=ABS(DLCMHI(MWAV)+IDLINE*17.)
      CMSQ(NL)=(DELCM(NL))**2
      NRMCTL(NL)=NORMCT(INDEX)
480   INDEX=INDEX+IFLAG
      NL=NL+1
500   CONTINUE
      GO TO 180
600   NL=NL-1
      LSIZE=NL*7+1
      DEFINE FILE LFILE(1,LSIZE,U,NREC)
      WRITE(LFILE'1)NL,(IANGST(L),DELCM(L),CMSQ(L),NRMCTL(L),L=1,NL
      WRITE (5,700)
700   FORMAT(' IT IS FINISHED')
950   STOP
      END
*
```

```
TT:=DX1:XYPLOT.FOR


      DIMENSION X(1001),Y(1001),XF(1001),YF(1001)
      DIMENSION INTB(1001),REALC(1001),REALD(1001),REALE(1001)
      WRITE(5,50)
50    FORMAT(' THIS PROGRAM WILL CREATE AN X-Y FILE FROM ANY TWO
     1 COLUMNS OF ANY FILE, AND THEN PLOT THEM ON AN X-Y RECORDER')
      WRITE(5,51)
51    FORMAT(' IT ALSO ALLOWS EDITING OF POINTS (BY OMISSION)')
      WRITE(5,100)
100   FORMAT(' FILE NUMBER?...10<=IFILE>=99')
      READ(5,200) IFILE
200   FORMAT (I2)

      WRITE(5,220)
220   FORMAT(' IS THIS AN X-Y FILE??... YES(1)...NO(0)')
      READ(5,200)ISXY
      WRITE(5,230)
230   FORMAT(' DO YOU WANT LOG10(X)??,...LOG10(Y)??')
      READ(5,240)IFLOGX,IFLOGY
240   FORMAT(I2,I2)

      IF (ISXY.NE.1) GO TO 250

      DEFINE FILE IFILE(1,2401,U,NREC)
      READ (IFILE'1) N,(XF(K),YF(K),K=1,N)
      GO TO 260
```

```
250     DEFINE FILE IFILE(1,8010,U,NREC)
        READ(IFILE'1)N,(INTB(K),REALC(K),REALD(K),REALE(K),K=1,N)
260     NX=1
        NY=1

265     NPTS=NX-1
        WRITE(5,270)N,NPTS
270     FORMAT(' NBEGIN=?...NEND=?    N=',I4,'    SO FAR NPTS=',I4)
        READ(5,280)NBEGIN,NEND
280     FORMAT(I4,I4)
        IF (NBEGIN.EQ.0) GO TO 600
        IFLAG=1
        INDEX=NBEGIN
        NDXRST=NBEGIN
        IF (NBEGIN.LT.NEND) GO TO 300
        IFLAG=-1
        NTEMP=NEND
        NEND=NBEGIN
        NBEGIN=NTEMP
300     IF (ISXY.NE.1) GO TO 365
350     DO 360 I=NBEGIN,NEND
        X(NX)=XF(INDEX)
        IF (IFLOGX.EQ.0) GO TO 352
        IF (X(NX).LE.0) GO TO 352
        X(NX)=ALOG10(X(NX))
352     Y(NY)=YF(INDEX)
        IF (IFLOGY.EQ.0) GO TO 354
        IF (Y(NY).LE.0) GO TO 354
        Y(NY)=ALOG10(Y(NY))
354     INDEX=INDEX+IFLAG
        NX=NX+1
360     NY=NY+1
        GO TO 265
```

```
365     WRITE(5,370)
370     FORMAT(' X-AXIS IS??...N(-1)...INTB(0)...SOMETHING ELSE(1)')
        READ(5,200)IABSC
        IF (IABSC) 400,420,440
400     DO 410 I=NBEGIN,NEND
        X(NX)=INDEX
        IF (IFLOGX.EQ.0) GO TO 405
        IF (X(NX).LE.0) GO TO 405
        X(NX)=ALOG10(X(NX))
405     INDEX=INDEX+IFLAG
410     NX=NX+1
        GO TO 498
420     DO 430 I=NBEGIN,NEND
        X(NX)=INTB(INDEX)
        IF (IFLOGX.EQ.0) GO TO 425
        IF (X(NX).LE.0) GO TO 425
        X(NX)=ALOG10(X(NX))
425     INDEX=INDEX+IFLAG
430     NX=NX+1
        GO TO 498
440     WRITE(5,445)
445     FORMAT(' X-AXIS IS??...REALC(-1)...REALD(0)...REALE(1)')

        READ(5,200)IABSC
        IF (IABSC) 450,470,490
450     DO 460 I=NBEGIN,NEND
        X(NX)=REALC(INDEX)
        IF (IFLOGX.EQ.0) GO TO 455
        IF (X(NX).LE.0) GO TO 455
        X(NX)=ALOG10(X(NX))
455     INDEX=INDEX+IFLAG
460     NX=NX+1
        GO TO 498
470     WRITE(5,472)
```

```
472     FORMAT(' DO YOU WANT:      X=1/CMSQ??      YES(1),,,NO(0)')
        READ(5,200) IRECP
        DO 480 I=NBEGIN,NEND
        IF (IRECP.EQ.0) GO TO 473
        IF (REALD(INDEX).EQ.0.0) GO TO 473
        X(NX)=1.0/REALD(INDEX)
        GO TO 474
473     X(NX)=REALD(INDEX)
474     IF (IFLOGX.EQ.0) GO TO 475
        IF (X(NX).LE.0) GO TO 475
        X(NX)=ALOG10(X(NX))
475     INDEX=INDEX+IFLAG
480     NX=NX+1
        GO TO 498
490     DO 495 I=NBEGIN,NEND
        X(NX)=REALE(INDEX)
        IF (IFLOGX.EQ.0) GO TO 492
        IF (X(NX).LE.0) GO TO 492
        X(NX)=ALOG10(X(NX))
492     INDEX=INDEX+IFLAG
495     NX=NX+1

498     WRITE(5,499)
499     FORMAT(' Y-AXIS IS??,,,N(-1),,,INTB(0),,,SOMETHING ELSE(1)')
        READ(5,200)IORD
        INDEX=NBXRST
        IF (IORD) 500,520,540
500     DO 510 I=NBEGIN,NEND
        Y(NY)=INDEX
        IF (IFLOGY.EQ.0) GO TO 405
        IF (Y(NY).LE.0) GO TO 405
        Y(NY)=ALOG10(Y(NY))
505     INDEX=INDEX+IFLAG
510     NY=NY+1
        GO TO 265
```

```
520     DO 530 I=NBEGIN,NEND
        Y(NY)=INTR(INDEX)
        INDEX=INDEX+IFLAG
530     NY=NY+1
        GO TO 265
540     WRITE(5,545)
545     FORMAT(' Y-AXIS IS??...REALC(-1)...REALD(0)...REALE(1)')

        READ(5,200)IORD
        IF (IORD) 550,570,590
550     DO 560 I=NBEGIN,NEND
        Y(NY)=REALC(INDEX)
        IF (IFLOGY.EQ.0) GO TO 555
        IF (Y(NY).LE.0) GO TO 555
        Y(NY)=ALOG10(Y(NY))
555     INDEX=INDEX+IFLAG
560     NY=NY+1
        GO TO 265
570     DO 580 I=NBEGIN,NEND
        Y(NY)=REALD(INDEX)
        IF (IFLOGY.EQ.0) GO TO 575
        IF (Y(NY).LE.0) GO TO 575
        Y(NY)=ALOG10(Y(NY))
575     INDEX=INDEX+IFLAG
580     NY=NY+1
        GO TO 265
590     DO 595 I=NBEGIN,NEND
        Y(NY)=REALE(INDEX)
        IF (IFLOGY.EQ.0) GO TO 592
        IF (Y(NY).LE.0) GO TO 592
        Y(NY)=ALOG10(Y(NY))
592     INDEX=INDEX+IFLAG
595     NY=NY+1
        GO TO 265
```

```
600     NX=NX-1
        NY=NY-1
610     WRITE(5,620)
620     FORMAT(' DIGITAL (-1), GRAPH (0), OR BOTH (1)')
        READ(5,200)JOB
        IF (JOB) 800,900,800
800     WRITE(5,850) (J,X(J),Y(J),J=1,NX)
850     FORMAT(1X,I4,2G15.5)
        IF (JOB.EQ.-1) GO TO 905
900     CALL GRAPH(X,Y,NX)

905     WRITE(5,910)
910     FORMAT(' CREATE AN X-Y FILE??...YES(FILE NUMBER??= )....NO(0)')
        READ(5,200)MFILE
        IF (MFILE.EQ.0) GO TO 915
        MSIZE=1+NX*4
        DEFINE FILE MFILE(1,MSIZE,U,NREC)
        WRITE(MFILE'1)NX,(X(J),Y(J),J=1,NX)

915     WRITE(5,920)
920     FORMAT(' REGRAPH??(-1)...EXIT??(0)...NEW X-Y??(1)')
        READ(5,200)NRENTR
        IF (NRENTR) 610,950,260

950     CONTINUE
        STOP
        END
```

APPENDIX B. WAVELENGTHS AND ATOMIC TRANSITIONS

Table B.1 gives the wavelengths of the excimer and nitrogen laser lines for use in the off-resonant excitation of the atomic transitions given in Table B.2.

Table B.1. Wavelengths of excimer lasers

Laser	Medium	Wavelength (114)
a)	ArF	193 nm
b)	KrCl	222 nm
c)	KrF	249 nm
d)	XeBr	282 nm
e)	XeCl	305 nm
f)	N_2	337 nm
g)	XeF	351 nm

Table B.2 gives a listing of all atomic transitions (116) within 1000 cm^{-1} of ground state that are within 100 Å of one of the above laser lines.

Table B.2. Atomic transitions near laser lines from Table B.1

Element	Wavelength (Å)	Lower Level (cm^{-1})	gA (10^8 sec^{-1})	Laser (See Table B.1)
Ag I	3382.89	0	1.3	f
Al I	2367.06	112	1.2	b
	2567.99	0	1.0	c
	3082.16	0	2.7	e
	3092.71	112	5.5	e
As I	1936.96	0	3.5	a
	1971.97	0	5.0	a
Au I	2427.95	0	1.8	c
B I	2088.93	0	1.5	a
	2089.59	16	2.4	a
	2496.78	0	7.0	c
	2497.73	16	14.0	c
Ba I	3071.58	0	1.8	e
	3501.11	0	1.8	g
Be II	3130.42	0	68.0	e
	3131.07	0	45.0	e
Bi I	1953.89	0	2.9	a
	1959.48	0	0.58	a
	2021.21	0	1.0	a
	2228.25	0	0.14	b
	2230.61	0	0.63	b
	2276.58	0	0.18	b
	3067.72	0	7.0	e
Ca I	2398.56	0	0.35	c
	2721.64	0	0.074	d
Cd I	2288.02	0	12.0	b
Cd II	2144.38	0	106.0	b
	2265.02	0	99.0	b

Table B.2. (Continued)

Element	Wavelength (Å)	Lower Level (cm^{-1})	gA (10^8 sec^{-1})	Laser (See Table B.1)
Ce II	2519.02	988	2.0	c
	2862.76	0	0.61	d
	2761.42	0	2.5	d
	2781.89	988	0.78	d
	2861.35	988	0.36	d
	2871.08	988	0.61	d
	2871.63	0	0.30	d
	2956.71	0	0.29	e
	3130.87	0	1.6	e
	3142.31	988	0.83	e
	3314.04	0	0.42	f
	3333.04	0	0.40	f
	3364.35	988	0.49	f
	3416.86	988	0.63	f,g
	3426.21	988	1.7	f,g
	3456.67	988	0.18	f,g
	3468.89	988	0.31	f,g
	3470.41	988	0.17	g
	3479.61	0	0.29	g
	3480.27	0	0.42	g
	3485.05	0	2.1	g
	3513.79	988	0.44	g
	3527.85	0	0.32	g
	3532.88	0	0.23	g
	3594.61	0	0.15	g
	3604.20	988	0.47	g
Co I	2174.60	0	1.1	b
	2268.17	0	0.54	b
	2284.85	816	0.64	b
	2295.23	0	0.61	b
	2304.18	816	0.91	b
	2305.18	816	1.1	b
	2309.02	0	6.8	b
	2402.06	816	6.5	c
	2407.25	0	25.0	c
	2411.62	816	31.0	c
	2424.93	0	22.0	c
	2429.23	816	0.72	c
	2432.21	816	24.0	c
	2435.83	0	4.0	c
	2473.90	816	0.85	c
	2521.36	0	20.0	c

Table B.2. (Continued)

Element	Wavelength (Å)	Lower Level (cm^{-1})	gA (10^8 sec^{-1})	Laser (See Table B.1)
Co I	2528.97	816	16.0	c
	2574.35	816	5.7	c
	2886.44	816	0.39	d
	2987.16	0	0.83	e
	2989.59	0	0.82	e
	3000.55	816	0.17	e
	3013.60	0	0.36	e
	3017.55	816	0.96	e
	3042.48	816	0.27	e
	3044.00	0	3.1	e
	3061.82	816	2.1	e
	3062.20	816	0.059	e
	3064.37	816	0.082	e
	3082.62	0	0.60	e
	3089.60	816	0.38	e
	3121.42	0	0.27	e
	3121.57	816	0.12	e
	3139.94	816	0.33	e
	3412.63	0	1.1	f,g
	3431.58	816	1.6	f,g
	3456.93	816	0.065	f,g
	3465.80	0	2.3	f,g
	3474.02	0	3.6	g
	3510.43	816	0.75	g
	3513.48	816	2.0	g
	3520.08	816	0.16	g
	3526.85	0	2.6	g
	3575.36	816	1.2	g
Cr I	3351.97	0	0.038	f,g
	3578.69	0	8.3	f,g
	3593.49	0	7.0	f,g
	3605.33	0	5.2	f,g
Cu I	2024.34	0	0.17	a
	2165.09	0	0.26	b
	2178.94	0	0.31	b
	2181.72	0	0.23	b
	2225.70	0	0.10	b
	2441.64	0	0.064	c
	2492.15	0	0.31	c
	3273.96	0	1.9	f

Table B.2. (Continued)

Element	Wavelength (Å)	Lower Level (cm^{-1})	gA (10^8 sec^{-1})	Laser (See Table B.1)
Dy II	3003.76	0	0.27	e
	3141.12	0	0.82	e
	3280.08	828	1.6	f
	3319.88	0	1.3	f
	3393.59	828	5.4	f
	3396.17	0	1.5	f
	3407.79	0	5.9	f
	3413.78	828	1.8	f,g
	3434.37	0	2.0	f,g
	3441.45	828	1.7	f,g
	3445.58	0	3.8	f,g
	3460.97	0	4.4	g
	3494.49	828	5.2	g
	3506.81	828	1.5	g
	3531.70	0	19.0	g
	3534.96	828	4.8	g
	3538.50	0	3.7	g
	3546.84	828	1.5	g
	3563.14	828	2.2	g
	3585.08	0	2.6	g
Eu I	2723.96	0	2.5	d
	2731.37	0	1.7	d
	2732.61	0	1.4	d
	2735.25	0	2.8	d
	2743.28	0	2.3	d
	2745.61	0	1.3	d
	2747.83	0	2.6	d
	2878.87	0	2.2	d
	2892.54	0	4.2	d
	2893.03	0	2.9	d
	2908.99	0	3.2	d
	2958.91	0	0.51	e
	3058.98	0	1.6	e
	3106.18	0	3.7	e
	3111.43	0	11.0	e
	3322.26	0	0.61	f
	3334.33	0	6.6	f
	3350.40	0	0.76	f
	3457.05	0	0.46	f,g
	3467.88	0	0.45	f,g
	3589.27	0	0.31	g
	4594.03	0	6.7	g

Table B.2. (Continued)

Element	Wavelength (Å)	Lower Level (cm^{-1})	gA (10^8 sec^{-1})	Laser (See Table B.1)
Eu II	2727.78	0	8.1	d
	2729.33	0	0.37	d
	2744.26	0	0.22	d
	2813.94	0	4.9	d
	2820.78	0	2.8	d
	2862.57	0	0.35	d
	2887.85	0	0.092	d
	2906.68	0	3.5	d
	2957.47	0	0.033	e
	2991.33	0	0.26	e
	3077.36	0	0.15	e
Fe I	2166.77	0	8.5	b
	2178.09	416	4.2	b
	2191.84	704	2.1	b
	2196.04	888	2.2	b
	2297.79	416	1.3	b
	2447.71	0	0.98	c
	2462.18	416	1.6	c
	2462.64	0	9.2	c
	2472.88	704	14.0	c
	2479.78	704	15.0	c
	2483.27	0	34.0	c
	2484.19	888	14.0	c
	2486.37	0	1.1	c
	2487.37	704	0.51	c
	2488.15	416	35.0	c
	2489.75	978	28.0	c
	2490.64	704	26.0	c
	2491.16	888	21.0	c
	2498.89	416	1.3	c
	2501.13	0	10.0	c
	2510.83	416	11.0	c
	2512.36	416	0.84	c
	2518.10	704	8.9	c
	2522.85	0	29.0	c
	2524.29	888	6.6	c
	2527.43	416	16.0	c
	2529.13	704	6.1	c
	2529.83	888	2.1	c
	2530.69	704	0.85	c
	2535.60	978	9.0	c

Table B.2. (Continued)

Element	Wavelength (Å)	Lower Level (cm^{-1})	gA (10^8 sec^{-1})	Laser (See Table B.1)
Fe I	2540.98	888	9.8	c
	2545.98	704	9.1	c
	2549.61	416	6.7	c
	2720.90	416	6.6	d
	2723.58	704	4.2	d
	2737.31	888	4.2	d
	2742.41	704	3.1	d
	2744.07	978	1.8	d
	2750.14	416	3.5	d
	2756.26	416	1.2	d
	2795.01	0	0.077	d
	2825.69	0	0.10	d
	2835.46	0	0.084	d
	2840.42	416	0.093	d
	2863.86	704	0.15	d
	2869.31	416	0.27	d
	2874.17	0	0.30	d
	2912.16	0	0.53	d
	2953.94	704	1.7	e
	2957.36	888	0.96	e
	2965.26	978	0.54	e
	2966.90	0	3.9	e
	2969.36	888	0.12	e
	2970.10	888	0.98	e
	2973.13	704	1.6	e
	2973.24	416	3.0	e
	2981.45	416	0.68	e
	2983.57	0	3.0	e
	2986.46	888	0.033	e
	2994.43	416	2.8	e
	3000.95	704	2.8	e
	3007.28	704	0.25	e
	3008.14	888	2.3	e
	3017.63	888	0.50	e
	3020.49	704	1.4	e
	3020.64	0	5.5	e
	3021.07	416	3.5	e
	3024.03	888	0.64	e
	3025.84	978	0.96	e
	3037.39	888	2.3	e
	3047.60	704	2.9	e
	3059.09	416	2.0	e

Table B.2. (Continued)

Element	Wavelength (Å)	Lower Level (cm^{-1})	gA (10^8 sec^{-1})	Laser (See Table B.1)
Fe I	3440.61	0	2.8	f,g
	3440.99	416	0.64	f,g
	3443.88	704	0.34	f,g
	3465.86	888	0.52	f,g
	3475.45	704	0.64	g
	3476.70	978	0.28	g
	3490.58	416	0.58	g
	3497.84	888	0.19	g
	3526.04	704	0.13	g
Fe II	2395.62	385	96.0	c
	2399.24	668	34.0	c
	2404.43	863	7.0	c
	2404.88	668	100.0	c
	2406.66	863	33.0	c
	2410.52	863	33.0	c
	2411.07	977	25.0	c
	2413.31	977	26.0	c
	2585.88	0	42.0	c
Ga I	2294.20	0	0.067	b
	2418.70	826	0.63	c
	2450.07	0	4.1	c
	2500.17	826	7.3	c
	2500.70	826	0.67	c
	2874.24	0	5.9	d
Gd I	2778.76	215	2.2	d
	2787.68	533	3.6	d
	3043.01	999	3.5	e
	3046.48	533	3.8	e
	3059.92	215	2.2	e
	3069.42	215	1.4	e
	3087.05	0	1.7	e
	3119.01	533	2.3	e
	3127.25	999	2.0	e
	3136.93	0	3.0	e
	3137.30	0	3.0	e
	3138.71	533	2.2	e
	3282.25	999	4.5	f
	3294.08	533	6.5	f
	3357.61	533	2.8	f

Table B.2. (Continued)

Element	Wavelength (Å)	Lower Level (cm^{-1})	gA (10^8 sec^{-1})	Laser (See Table B.1)
Gd I	3373.84	0	1.1	f
	3406.92	533	2.3	f
	3411.02	999	2.9	f,g
	3423.90	999	14.0	f,g
	3486.20	533	2.2	g
	3497.09	533	0.86	g
	3513.65	999	9.0	g
	3525.15	999	1.1	g
	3583.65	215	0.74	g
	3588.21	0	0.55	g
	3596.84	999	0.99	g
Gd II	2770.98	633	0.19	d
	2980.15	633	2.7	e
	2999.04	262	4.8	e
	3010.13	0	7.7	e
	3032.84	633	8.7	e
	3034.05	262	6.1	e
	3068.64	633	3.9	e
	3076.92	0	2.0	e
	3083.35	262	0.3	e
	3098.64	0	1.4	e
	3098.90	0	0.54	e
	3101.91	262	0.72	e
	3119.94	262	1.5	e
	3123.99	262	1.1	e
	3124.25	262	0.34	e
	3133.09	0	0.28	e
	3135.03	262	0.60	e
	3331.38	0	2.7	f
	3336.18	0	2.1	f
	3345.98	0	1.1	f,g
	3358.62	262	8.6	g
	3360.71	262	1.6	g
Ge I	1954.49	557	4.1	a
	2019.05	557	3.8	a
	2497.96	0	2.4	c
	2533.23	557	1.9	c

Table B.2. (Continued)

Element	Wavelength (Å)	Lower Level (cm^{-1})	gA (10^8 sec^{-1})	Laser (See Table B.1)
Hf I	2482.65	0	0.57	c
	2487.16	0	0.56	c
	2517.86	0	0.66	c
	2730.71	0	0.37	d
	2758.78	0	0.34	d
	2819.74	0	0.61	d
	2833.28	0	0.53	d
	2860.56	0	0.49	d
	2866.37	0	5.8	d
	2889.62	0	2.0	d
	2980.81	0	2.1	e
	3016.78	0	0.93	e
	3018.31	0	1.7	e
	3072.88	0	3.2	e
	3128.76	0	0.11	e
	3129.58	0	0.092	e
	3332.73	0	0.70	f
	3360.06	0	0.13	f
	3400.21	0	0.12	f
	3472.40	0	0.42	g
	3497.49	0	0.55	g
	3536.62	0	0.39	g
	3564.31	0	0.074	g
Hf II	2277.16	0	1.6	b
	2393.83	0	3.7	c
	2467.97	0	1.1	c
	2861.01	0	1.4	d
	2909.91	0	0.22	d
	3012.90	0	1.3	e
	3016.94	0	1.2	e
	3145.32	0	0.18	e
	3399.80	0	1.1	f
	3428.37	0	0.084	f,g
	3561.61	0	0.44	g
Hg I	2536.52	0	3.5	c
In I	2460.08	0	0.38	c
	2560.15	0	4.7	c
	2753.88	0	1.5	d
	2775.37	0	0.079	d

Table B.2. (Continued)

Element	Wavelength (Å)	Lower Level (cm^{-1})	gA (10^8 sec^{-1})	Laser (See Table B.1)
In I	2858.14	0	0.045	d
	3039.36	0	7.1	e
Ir I	2010.65	0	2.1	a
	2127.94	0	2.1	b
	2155.81	0	1.5	b
	2162.88	0	1.2	b
	2175.24	0	2.7	b
	2178.17	0	1.6	b
	2315.38	0	0.65	b
	2431.24	0	1.7	c
	2455.61	0	4.5	c
	2475.12	0	10.0	c
	2481.18	0	6.2	c
	2502.98	0	11.0	c
	2823.18	0	0.89	d
	2849.72	0	4.6	d
	2951.22	0	1.0	e
	3513.64	0	0.99	g
La I	3574.43	0	2.6	g
La II	2187.87	0	0.46	b
	3104.59	0	0.29	e
	3108.46	0	0.097	e
	3550.82	0	0.027	g
Li I	3232.61	0	0.34	d
Lu I	2728.95	0	0.64	d
	2903.05	0	0.23	d
	2989.27	0	1.1	e
	3080.11	0	0.18	e
	3278.97	0	0.93	f
	3312.11	0	1.4	f
	3376.50	0	1.2	f
	3567.84	0	0.64	g
Lu II	2195.54	0	0.22	b
	3507.39	0	0.20	g
Mg I	2852.13	0	9.4	d

Table B.2. (Continued)

Element	Wavelength (Å)	Lower Level (cm^{-1})	gA (10^8 sec^{-1})	Laser (See Table B.1)
Mg II	2795.53	0	9.0	d
	2802.70	0	5.3	d
Mn I	1995.40	0	2.1	a
	1998.86	0	3.0	a
	2003.82	0	4.0	a
	2208.81	0	0.24	b
	2213.85	0	0.46	b
	2221.83	0	0.67	b
	2794.82	0	8.3	d
	2798.27	0	6.7	d
	2801.06	0	4.9	d
Mn II	2576.10	0	80.0	c
Mo I	3002.21	0	0.19	e
	3112.12	0	0.98	e
	3132.59	0	9.8	e
	3456.39	0	0.31	f,g
	3446.83	0	0.10	f,g
Mo II	2015.11	0	11.0	a
	2020.30	0	24.0	a
Na I	3302.32	0	0.65	f
	3302.99	0	0.33	f
Nb I	3497.81	392	0.24	g
	3507.96	154	0.51	g
	3533.66	154	0.11	g
	3535.30	0	2.0	g
	3537.48	392	1.4	g
	3544.02	0	0.49	g
	3550.45	392	0.33	g
	3554.66	154	1.0	g
	3563.50	154	0.62	g
	3563.50	392	0.66	g
	3575.85	695	1.7	g
	3584.97	392	0.51	g
	3589.11	695	0.82	g
	3593.97	392	0.50	g
	3598.35	0	0.044	g

Table B.2. (Continued)

Element	Wavelength (Å)	Lower Level (cm^{-1})	gA (10^8 sec^{-1})	Laser (See Table B.1)
Nb I	3602.56	695	0.54	g
	3604.08	695	0.053	g
Nb II	2302.08	801	4.1	b
	2574.84	159	0.84	c
	2721.63	0	0.35	d
	2721.98	801	5.2	d
	2733.26	801	3.3	d
	2733.46	159	0.71	d
	2737.09	438	1.0	d
	2754.52	438	0.60	d
	2764.56	801	0.51	d
	2768.13	438	2.0	d
	2827.08	159	1.2	d
	2849.56	438	0.48	d
	2865.61	0	0.55	d
	2878.74	159	0.37	d
	2879.36	801	0.31	d
Nd II	3282.78	0	0.066	f
	3328.28	0	0.48	f
	3339.07	513	0.38	f
Ni I	2289.98	0	5.0	b
	2300.78	205	2.2	b
	2310.96	0	7.6	b
	2320.03	0	11.0	b
	2798.65	880	0.56	d
	2821.95	205	0.72	d
	2981.65	880	1.2	e
	2984.13	0	0.41	e
	2992.60	205	0.86	e
	2994.46	205	1.7	e
	3002.49	205	6.7	e
	3003.63	880	4.5	e
	3019.14	0	0.53	e
	3031.87	0	0.18	e
	3037.94	205	2.6	e
	3050.82	205	5.1	e
	3054.32	880	2.6	e
	3064.62	880	0.85	e
	3101.55	880	4.6	e
	3114.12	880	0.47	e

Table B.2. (Continued)

Element	Wavelength (Å)	Lower Level (cm^{-1})	gA (10^8 sec^{-1})	Laser (See Table B.1)
Ni I	3271.12	880	0.11	f
	3315.66	880	0.69	f
	3361.56	880	0.31	f
	3367.89	205	0.051	f
	3369.57	0	2.1	f
	3374.22	205	0.20	f
	3391.05	0	0.91	f
	3392.99	205	2.4	f
	3409.58	0	0.087	f
	3413.94	880	0.28	f,g
	3414.76	205	5.7	f,g
	3433.56	205	1.8	f,g
	3437.28	0	0.62	f,g
	3446.26	880	3.8	f,g
	3452.89	880	1.0	f,g
	3461.65	205	3.2	f,g
	3472.54	880	1.2	g
	3492.96	880	3.9	g
	3502.60	0	0.036	g
	3515.05	880	4.5	g
	3524.54	205	4.6	g
	3561.75	0	0.032	g
	3587.93	205	0.065	g
Os I	2001.45	0	2.9	a
	2018.14	0	10.0	a
	2157.84	0	1.1	b
	2184.68	0	0.94	b
	2202.49	0	0.86	b
	2227.98	0	0.75	b
	2297.31	0	0.79	b
	2395.88	0	4.0	c
	2424.56	0	2.3	c
	2424.97	0	6.9	c
	2476.84	0	4.4	c
	2493.83	0	0.27	c
	2806.91	0	4.5	d
	2872.40	0	0.23	d
	2909.06	0	11.0	d
	3018.04	0	4.3	e
	3058.66	0	7.4	e
	3301.56	0	3.6	f
	3402.51	0	0.094	f

Table B.2. (Continued)

Element	Wavelength (Å)	Lower Level (cm^{-1})	gA (10^8 sec^{-1})	Laser (See Table B.1)
Os I	3523.64	0	0.14	g
	3528.60	0	0.36	g
Os II	2282.26	0	85.0	b
	2538.00	0	98.0	c
Pb I	2022.02	0	0.32	a
	2169.99	0	0.68	b
	2833.06	0	1.8	d
Pd I	2447.91	0	0.83	c
	2476.42	0	1.1	c
	2763.09	0	0.62	d
Pt I	2128.61	776	1.0	b
	2144.23	0	1.8	b
	2165.17	0	0.69	b
	2202.22	776	0.70	b
	2249.30	0	0.27	b
	2274.38	776	0.75	b
	2289.27	776	0.43	b
	2292.40	824	0.43	b
	2308.04	824	0.76	b
	2436.69	776	1.3	c
	2440.06	0	4.2	c
	2450.97	0	0.40	c
	2467.44	0	2.7	c
	2487.17	0	5.7	c
	2490.12	824	1.4	c
	2498.50	776	1.6	c
	2515.58	776	1.5	c
	2539.20	824	0.93	c
	2705.89	824	5.0	d
	2719.04	824	3.9	d
	2733.96	776	5.0	d
	2771.67	776	1.2	d
	2818.25	824	0.11	d
	2830.30	0	2.3	d
	2893.86	776	1.0	d
	2897.87	824	0.50	d
	2997.97	776	2.2	e
	3002.27	824	0.27	e
	3042.64	824	0.89	e

Table B.2. (Continued)

Element	Wavelength (Å)	Lower Level (cm^{-1})	gA (10^8 sec^{-1})	Laser (See Table B.1)
Pt I	3064.71	0	2.6	e
	3139.39	776	0.27	e
	3315.05	0	0.027	f
	3408.13	824	0.16	f
Re I	2003.53	0	2.9	a
	2017.87	0	2.1	a
	2156.67	0	1.2	b
	2167.94	0	1.7	b
	2176.21	0	1.2	b
	2226.42	0	0.87	b
	2235.44	0	0.49	b
	2256.19	0	0.50	b
	2264.39	0	1.2	b
	2274.62	0	1.4	b
	2281.62	0	1.1	b
	2287.51	0	2.1	b
	2294.49	0	2.1	b
	2302.99	0	0.49	b
	2306.54	0	0.53	b
	2405.60	0	1.1	c
	2419.81	0	2.0	c
	2428.58	0	4.4	c
	2441.47	0	0.65	c
	2449.71	0	1.3	c
	2508.99	0	3.0	c
	2520.01	0	0.87	c
	2559.08	0	0.32	c
	2896.01	0	0.22	d
	2976.29	0	0.11	e
	2992.36	0	0.61	e
	3067.40	0	0.50	e
	3451.88	0	2.0	f,g
	3460.56	0	6.8	f,g
	3464.73	0	4.9	f,g
Re II	2214.26	0	15.0	b
	2275.25	0	28.0	b
Rh I	3123.70	0	0.24	e
	3396.85	0	3.1	f
	3434.89	0	4.1	f,g
	3502.52	0	2.6	g

Table B.2. (Continued)

Element	Wavelength (Å)	Lower Level (cm^{-1})	gA (10^8 sec^{-1})	Laser (See Table B.1)
Ru I	2255.52	0	3.5	b
	2259.53	0	1.5	b
	2272.09	0	4.3	b
	2285.38	0	1.0	b
	2735.72	0	11.0	d
	2818.36	0	1.5	d
	2874.98	0	6.7	d
	2988.95	0	3.6	e
	3294.11	0	0.55	f
	3301.59	0	0.41	f
	3344.53	0	0.059	f
	3378.02	0	0.11	f
	3392.54	0	0.34	f
	3428.31	0	4.1	f,g
	3498.94	0	6.0	g
Sb I	2127.39	0	0.43	b
	2175.81	0	2.5	b
	2311.47	0	1.5	b
Sc I	2965.86	0	1.4	e
	2974.01	0	4.9	e
	2980.75	168	6.0	e
	2988.95	168	1.4	e
	3015.36	0	7.8	e
	3019.34	168	9.9	e
	3030.76	168	1.3	e
	3273.63	168	12.0	f
Sc II	2545.22	68	3.4	c
	2552.37	178	18.0	c
	2555.82	0	3.2	c
	2560.25	68	13.0	c
	2563.21	0	6.4	c
	3352.05	0	0.18	f
	3359.68	68	1.3	f
	3361.21	0	1.1	f
	3361.94	0	1.1	f
	3368.95	68	2.6	f
	3372.15	178	4.4	f
	3558.55	68	2.9	g
	3567.70	0	2.6	g
	3572.53	178	5.9	g

Table B.2. (Continued)

Element	Wavelength (Å)	Lower Level (cm^{-1})	gA (10^8 sec^{-1})	Laser (See Table B.1)
Sc II	3576.35	68	4.3	g
	3580.94	0	3.2	g
	3589.64	68	1.7	g
	3590.48	178	1.7	g
Se I	1960.26	0	10.0	a
Si I	2207.97	0	0.30	b
	2210.88	77	0.30	b
	2216.67	223	0.53	b
	2506.90	77	6.3	c
	2514.32	0	5.7	c
	2516.11	223	13.0	c
	2519.21	77	4.3	c
	2524.11	77	8.4	c
	2528.51	223	7.1	c
Sm II	3065.78	327	0.16	e
	3295.81	838	0.64	f
	3304.52	0	0.39	f
	3309.52	838	0.49	f
	3340.58	327	0.98	f
	3341.43	838	0.11	f
	3370.59	327	0.18	f
	3429.75	838	0.11	f,g
	3511.23	838	0.32	g
	3552.30	0	0.082	g
	3557.38	327	0.12	g
	3577.79	0	0.17	g
	3584.26	838	0.14	g
	3591.74	838	0.067	g
Sn I	2246.05	0	2.6	b
	2546.55	0	3.8	c
	2863.33	0	5.3	d
Sr I	2428.10	0	0.20	c
	2569.47	0	0.11	c
Ta I	2427.64	0	2.0	c
	2437.67	0	0.54	c
	2447.17	0	0.65	c
	2478.22	0	0.85	c

Table B.2. (Continued)

Element	Wavelength (Å)	Lower Level (cm^{-1})	gA (10^8 sec^{-1})	Laser (See Table B.1)
Ta I	2484.95	0	2.8	c
	2512.65	0	1.2	c
	2546.80	0	1.0	c
	2559.43	0	4.9	c
	2563.70	0	0.56	c
	2573.54	0	1.9	c
	2579.62	0	0.46	c
	2732.92	0	0.17	d
	2775.88	0	1.7	d
	2836.62	0	0.062	d
	2873.36	0	0.44	d
	3103.25	0	0.54	e
	3406.94	0	0.21	f
	3463.97	0	0.097	f,g
	3484.62	0	0.018	g
	3553.42	0	0.018	g
Ta II	2165.01	0	5.5	b
	2199.67	0	16.0	b
	2210.03	0	15.0	b
	2249.79	0	6.8	b
	2258.71	0	7.8	b
	2261.42	0	13.0	b
	2292.54	0	3.3	b
	2417.33	0	3.1	c
	2429.71	0	16.0	c
	2484.72	0	3.7	c
	2497.77	0	2.2	c
	2763.37	0	2.1	d
	2965.13	0	7.8	e
	2965.92	0	0.96	e
	3417.03	0	0.17	f,g
Te I	2142.75	0	3.8	b
	2259.04	0	0.33	b
Th I	3060.44	0	0.66	e
	3136.83	0	0.32	e
	3145.63	0	0.31	e
	3171.26	0	0.33	e
	3232.31	0	0.22	f
	3244.46	0	0.56	f

Table B.2. (Continued)

Element	Wavelength (Å)	Lower Level (cm^{-1})	gA (10^8 sec^{-1})	Laser (See Table B.1)
Th I	3249.87	0	0.48	f
	3272.05	0	0.52	f
	3304.24	0	2.1	f
	3309.36	0	0.54	f
	3330.48	0	1.0	f
	3348.77	0	1.2	f
	3423.99	0	0.89	f,g
	3461.02	0	0.60	f,g
	3496.81	0	0.20	g
	3526.64	0	0.19	g
	3567.26	0	0.42	g
	3598.12	0	0.62	g
Th II	2459.01	0	0.29	c
	2507.91	0	0.47	c
	2724.89	0	0.25	d
	2732.82	0	0.89	d
	2743.07	0	0.63	d
	2747.16	0	1.8	d
	2840.15	0	0.17	d
	2912.01	0	0.18	d
	2997.19	0	0.045	e
	3009.76	0	0.086	e
	3035.53	0	0.048	e
	3131.07	0	0.14	e
	3270.83	0	0.071	f
	3363.70	0	0.065	f
	3435.98	0	0.34	f,g
	3539.59	0	0.24	g
Ti I	2272.61	387	2.3	b
	2273.28	0	2.5	b
	2276.70	170	2.1	b
	2279.96	387	3.3	b
	2299.85	0	2.7	b
	2302.73	170	2.7	b
	2305.67	387	3.8	b
	2418.36	0	2.0	c
	2421.30	170	3.2	c
	2424.24	387	4.4	c
	2428.23	0	1.5	c
	2433.22	170	1.5	c
	2434.10	387	0.85	c

Table B.2. (Continued)

Element	Wavelength (Å)	Lower Level (cm^{-1})	gA (10^8 sec^{-1})	Laser (See Table B.1)
Ti I	2440.98	387	3.1	c
	2519.04	0	1.3	c
	2520.54	0	5.0	c
	2527.98	170	1.0	c
	2529.85	170	7.4	c
	2541.92	387	6.8	c
	2956.13	387	13.0	e
	2956.80	170	1.3	e
	2967.22	387	1.5	e
	2968.23	0	0.18	e
	2970.38	0	0.50	e
	2983.31	170	1.2	e
	3000.87	387	0.22	e
	3341.88	0	13.0	f
	3342.15	0	0.28	f
	3352.94	170	0.29	f
	3354.64	170	9.7	f
	3358.28	0	0.65	f
	3360.99	170	0.68	f
	3361.84	170	0.28	f
	3370.44	0	2.5	f
	3371.45	387	11.0	f
	3377.48	387	7.0	f
	3379.22	387	0.69	f
	3385.66	387	0.40	f
	3385.95	387	3.4	f
	3506.64	387	0.22	g
Ti II	2524.64	984	2.6	c
	2534.62	984	6.2	c
	2535.87	908	4.2	c
	2909.92	393	0.21	d
	3057.40	0	0.46	e
	3066.22	94	4.6	e
	3072.11	225	2.2	e
	3072.97	0	3.8	e
	3075.22	94	5.4	e
	3078.64	225	8.0	e
	3088.02	393	13.0	e
	3130.80	94	0.71	e
	3143.76	225	0.64	e
	3148.04	0	0.66	e

Table B.2. (Continued)

Element	Wavelength (Å)	Lower Level (cm^{-1})	gA (10^8 sec^{-1})	Laser (See Table B.1)
Ti II	3318.02	984	0.82	f
	3326.76	908	0.90	f
	3335.20	984	4.2	f
	3340.34	908	2.6	f
	3349.41	393	23.0	f
	3361.21	225	13.0	f
	3372.80	94	9.6	f
	3380.28	383	2.6	f
	3383.76	0	9.2	f
	3387.84	225	2.4	f
	3394.58	94	1.8	f
	3407.20	393	0.10	f
	3409.81	225	0.15	f
	3477.18	984	1.0	g
	3491.05	908	0.79	g
Tl I	2315.98	0	0.17	b
	2580.14	0	1.3	c
	2767.87	0	4.1	d
Tm I	2914.83	0	1.4	d
	2973.22	0	3.4	e
	3081.12	0	1.7	e
	3349.99	0	0.58	f
	3410.05	0	1.9	f,g
	3412.59	0	0.74	f,g
	3416.59	0	0.73	f,g
	3429.33	0	0.71	f,g
	3487.38	0	0.79	g
	3499.95	0	62.0	g
	3514.12	0	15.0	g
	3517.60	0	0.45	g
	3563.88	0	0.68	g
	3567.36	0	0.67	g
Tm II	2480.13	237	5.0	c
	2505.89	0	0.15	c
	2509.08	0	6.9	c
	2524.09	237	0.99	c
	2527.42	0	0.55	c
	2542.66	237	0.60	c
	2565.98	237	0.29	c

Table B.2. (Continued)

Element	Wavelength (Å)	Lower Level (cm^{-1})	gA (10^8 sec^{-1})	Laser (See Table B.1)
Tm II	2729.04	237	0.35	d
	2735.33	0	0.11	d
	2753.18	237	0.23	d
	2766.81	0	0.13	d
	2773.80	0	0.17	d
	2779.55	0	0.51	d
	2785.07	237	0.69	d
	2792.15	237	0.34	d
	2796.09	0	0.17	d
	2797.98	237	0.11	d
	2808.42	237	0.30	d
	2814.74	237	0.052	d
	2844.66	237	0.51	d
	2853.25	237	0.046	d
	2860.55	237	0.11	d
	2863.35	0	0.14	d
	2886.46	237	0.19	d
	2913.96	0	0.16	d
	2969.50	0	0.12	e
	2976.42	0	0.15	e
	2985.08	0	0.068	e
	2990.54	237	0.67	e
	2993.26	0	0.19	e
	2993.90	0	0.11	e
	2999.60	237	0.13	e
	3006.36	237	0.059	e
	3014.65	237	0.42	e
	3015.30	237	1.4	e
	3042.35	237	0.23	e
	3046.76	237	0.28	e
	3098.60	237	0.53	e
	3131.26	0	4.6	e
	3133.89	0	1.4	e
	3149.15	0	0.044	e
	3276.81	0	0.46	f
	3283.40	237	0.53	f
	3291.00	0	0.98	f
	3302.45	237	0.88	f
	3316.88	237	0.17	f
	3362.62	237	1.5	f
	3397.50	0	0.56	f
	3425.08	237	2.1	f,g
	3425.63	0	0.30	f,g

Table B.2. (Continued)

Element	Wavelength (Å)	Lower Level (cm^{-1})	gA (10^8 sec^{-1})	Laser (See Table B.1)
Tm II	3441.50	237	1.6	f,g
	3453.67	237	1.5	f,g
	3462.20	0	2.5	f,g
	3536.58	0	0.21	g
	3566.47	237	0.32	g
	3608.77	0	0.46	g
U I	3027.66	620	3.6	e
	3048.64	620	4.0	e
	3114.54	0	1.7	e
	3345.89	620	0.98	f
	3368.98	620	0.46	f
	3418.39	620	0.42	f,g
	3435.49	620	3.2	f,g
	3462.21	0	1.4	f,g
	3489.37	0	6.5	g
	3493.99	620	1.7	g
	3500.07	0	2.6	g
	3507.05	620	1.2	g
	3507.34	0	3.1	g
	3511.44	0	0.96	g
	3514.61	0	6.2	g
	3534.33	0	1.2	g
	3538.23	620	0.54	g
	3555.32	0	2.5	g
	3557.84	0	1.4	g
	3563.66	0	1.4	g
	3566.60	620	9.8	g
	3574.76	0	1.1	g
	3572.92	0	1.3	g
	3580.25	620	0.80	g
	3584.88	0	11.0	g
	3589.66	620	0.99	g
	3591.74	620	1.6	g
	3592.97	620	0.49	g
	3603.36	0	0.48	g
U II	2556.19	0	2.9	c
	2739.39	289	1.0	d
	2815.98	289	0.55	d
	2824.37	289	1.2	d
	2838.62	915	0.26	d

Table B.2. (Continued)

Element	Wavelength (Å)	Lower Level (cm^{-1})	gA (10^8 sec^{-1})	Laser (See Table B.1)
U II	2865.68	0	2.5	d
	2875.20	915	0.70	d
	2886.45	289	0.50	d
	2889.63	289	3.1	d
	2902.81	0	0.22	d
	2904.51	289	0.60	d
	2914.25	289	0.75	d
	2968.40	915	0.41	e
	2987.80	289	0.33	e
	3012.45	289	0.17	e
	3046.46	289	0.32	e
	3055.59	0	0.36	e
	3098.01	915	0.54	e
	3270.12	289	0.41	f
	3303.60	289	0.25	f
	3305.93	0	0.85	f
	3325.66	0	0.11	f
	3337.79	289	0.31	f
	3338.48	915	0.14	f
	3355.11	289	0.056	f
	3357.93	289	0.20	f
	3372.01	289	0.16	f
	3382.68	915	0.063	f
	3384.45	289	0.16	f
	3406.28	915	0.18	f
	3433.71	289	0.047	f,g
	3433.90	289	0.095	f,g
	3511.58	289	0.081	g
	3533.57	915	0.40	g
	3550.82	0	0.55	g
	3590.50	915	0.18	g
V I	2390.87	137	3.3	c
	2397.78	553	3.6	c
	2398.27	553	3.6	c
	2399.96	0	3.1	c
	2406.75	323	6.6	c
	2407.90	137	5.6	c
	2412.69	323	5.1	c
	2413.03	0	3.5	c
	2415.33	0	6.3	c
	2416.75	553	7.4	c
	2417.35	137	4.7	c

Table B.2. (Continued)

Element	Wavelength (Å)	Lower Level (cm^{-1})	gA (10^8 sec^{-1})	Laser (See Table B.1)
V I	2420.12	553	5.9	c
	2421.06	137	5.3	c
	2421.98	323	5.5	c
	2423.38	137	2.3	c
	2428.28	323	6.6	c
	2432.02	323	4.7	c
	2435.52	553	7.4	c
	2439.10	553	3.6	c
	2441.89	553	2.4	c
	2501.61	0	7.2	c
	2503.30	0	4.0	c
	2506.90	0	7.8	c
	2507.78	137	13.0	c
	2511.65	323	10.0	c
	2511.95	137	9.5	c
	2515.15	137	3.5	c
	2517.14	323	9.8	c
	2519.62	323	13.0	c
	2526.22	553	23.0	c
	2530.18	553	13.0	c
	2545.98	0	2.7	c
	2552.65	137	5.4	c
	2554.86	137	2.3	c
	2558.90	323	1.7	c
	2562.13	323	9.6	c
	2564.82	323	5.1	c
	2574.02	553	10.0	c
	2577.29	553	2.1	c
	2838.06	0	0.48	d
	2848.77	0	1.0	d
	2849.18	137	1.1	d
	2855.22	0	2.9	d
	2859.97	137	2.8	d
	2864.36	323	3.8	d
	2870.55	553	3.5	d
	2894.58	0	0.80	d
	2899.20	137	1.2	d
	2899.60	0	1.5	d
	2903.70	0	0.78	d
	2904.13	323	1.2	d
	2906.13	137	2.0	d
	2914.93	323	5.2	d
	2915.33	137	0.78	d

Table B.2. (Continued)

Element	Wavelength (Å)	Lower Level (cm^{-1})	gA (10^8 sec^{-1})	Laser (See Table B.1)
V I	2954.33	137	1.4	e
	2955.80	553	1.2	e
	2957.33	323	1.0	e
	2962.77	323	4.9	e
	2977.54	553	2.9	e
	3043.12	137	2.0	e
	3043.56	0	2.0	e
	3044.94	323	2.1	e
	3050.89	0	1.4	e
	3052.19	137	0.60	e
	3053.65	0	3.8	e
	3056.33	137	10.0	e
	3060.46	323	13.0	e
	3066.38	553	23.0	e
	3069.64	523	1.2	e
	3073.82	323	1.4	e
	3082.11	553	1.4	e
	3271.64	137	0.46	f
	3283.31	323	0.47	f
	3298.14	553	0.77	f
V II	2723.22	209	0.45	d
	2728.68	36	3.4	d
	2733.40	107	0.53	d
	2739.71	0	1.3	d
	2742.41	36	1.2	d
W I	2277.58	0	0.59	b
	2313.19	0	0.66	b
	2452.00	0	4.0	c
	2551.35	0	8.2	c
	2762.34	0	0.68	d
	2879.39	0	0.70	d
	2911.00	0	0.29	d
	3545.23	0	0.15	e
W II	2194.52	0	3.1	b
	2248.75	0	4.7	b
	2554.86	0	12.0	c
	2764.27	0	6.9	d

Table B.2. (Continued)

Element	Wavelength (Å)	Lower Level (cm^{-1})	gA (10^8 sec^{-1})	Laser (See Table B.1)
Y I	2490.42	530	0.66	c
	2723.00	530	1.2	d
	2730.08	0	0.23	d
	2742.53	0	0.71	d
	2760.10	530	1.6	d
	2791.20	0	0.11	d
	2813.64	530	0.25	d
	2919.05	0	0.92	d
	2964.96	530	2.1	e
	2974.59	0	2.4	e
	2984.26	530	4.2	e
	2995.26	530	0.38	e
	2996.94	0	0.65	e
	3005.26	0	0.32	e
	3021.73	530	0.66	e
	3022.28	530	0.44	e
	3045.37	530	0.91	e
	3552.69	0	0.77	g
	3592.92	0	3.7	g
Y II	2243.06	0	0.68	b
	3112.04	0	0.048	d
Yb I	2464.49	0	2.7	c
Yb II	2126.72	0	0.41	b
	2185.70	0	0.16	b
	2224.45	0	0.15	b
	2398.01	0	0.013	c
	2538.67	0	0.19	c
	2891.38	0	0.75	d
	2970.56	0	0.33	e
	3031.11	0	0.13	e
	3289.37	0	1.4	f
	3476.31	0	0.024	g
Zn I	2138.56	0	19.0	b
	3075.90	0	0.013	c
Zn II	2025.51	0	21.0	a

Table B.2. (Continued)

Element	Wavelength (Å)	Lower Level (cm^{-1})	gA (10^8 sec^{-1})	Laser (See Table B.1)
Zr I	2388.01	570	1.0	c
	2539.65	570	1.7	c
	2550.51	570	0.84	c
	2589.65	570	0.36	c
	2727.02	570	1.0	d
	2774.04	570	2.4	d
	2792.04	0	1.4	d
	2795.13	570	0.41	d
	2814.90	0	6.5	d
	2821.56	570	0.64	d
	2837.23	570	8.1	d
	2860.85	570	1.0	d
	2916.25	570	0.24	d
	2960.87	0	3.0	e
	2969.19	570	1.3	e
	2985.39	0	7.2	e
	3011.75	570	7.9	e
	3014.44	0	0.51	e
	3043.25	570	0.28	e
	3085.34	570	0.84	e
	3368.64	0	0.085	f
	3414.66	570	1.4	f,g
	3440.45	0	0.51	f,g
	3447.36	0	1.7	f,g
	3471.19	0	1.6	g
	3482.81	570	0.59	g
	3501.35	570	0.38	g
	3509.32	570	3.0	g
	3519.60	0	5.0	g
	3547.68	570	4.8	g
	3550.46	0	1.5	g
	3575.79	570	2.8	g
	3586.29	0	1.9	g
	3591.72	570	0.17	g
Zr II	2532.46	763	2.9	c
	2542.10	315	3.1	c
	2550.74	0	2.8	c
	2567.64	0	6.5	c
	2571.39	763	29.0	c

Table B.2. (Continued)

Element	Wavelength (Å)	Lower Level (cm^{-1})	gA (10^8 sec^{-1})	Laser (See Table B.1)
Zr II	2726.49	763	11.0	d
	2732.72	763	6.4	d
	2734.86	315	16.0	d
	2742.56	0	11.0	d
	2745.86	763	8.4	d
	2752.21	315	7.2	d
	2758.81	0	5.2	d
	2761.91	0	0.68	d
	2808.16	315	0.32	d
	2991.41	0	0.34	e
	3019.84	315	1.1	e
	3030.92	0	1.1	e
	3060.11	315	0.61	e
	3061.35	763	0.61	e
	3065.21	0	0.28	e
	3095.07	315	1.4	e
	3099.23	0	1.4	e
	3110.88	763	1.3	e
	3125.92	0	1.5	e
	3129.76	315	2.5	e
	3138.68	763	3.9	e
	3272.22	0	1.7	f
	3279.26	763	5.0	f
	3284.71	0	2.8	f
	3288.80	763	0.59	f
	3305.15	315	1.8	f
	3306.28	315	2.9	f
	3319.32	315	0.48	f
	3356.09	763	2.5	f
	3357.26	0	1.4	f
	3388.30	0	1.9	f
	3393.12	315	1.5	f,g
	3424.82	315	0.40	f,g
	3438.23	763	13.0	f,g
	3478.30	763	0.33	g
	3496.21	315	9.0	g
	3551.95	763	3.9	g
	3572.47	0	3.7	g